Random variability or reproducible spatial patterns?
Investigating sulphate dynamics
in forested catchments
with a coupled transport sorption model.

Diplomarbeit

im Studiengang Geoökologie der Universität Bayreuth

vorgelegt von

Heike Büttcher

geboren in Celle

erstellt am

Bayreuther Institut für Terrestrische Ökosystemforschung

Lehrstuhl für Ökologische Modellbildung (Prof. Dr. Michael Hauhs)

Abteilung Hydrogeologie

betreut von Dr. Gunnar Lischeid

Bayreuth, im Juni 2001

Contents

List of Figures

List of Tables

List of Symbols

a: proportion of the fine soil fraction [-]
b: Langmuir sorption maximum [N M^{-1}]
$f(x)$: frequency distribution
h: potential head [L]
i: space counter [-]
j: time counter [-]
k: Langmuir reciprocal of the half saturation point [M^3 N^{-1}]
n: total porosity [-]
q: Darcy velocity [L T^{-1}]
q_{GW}: Darcy velocity of the groundwater [L T^{-1}]
q_{soil}: Darcy velocity of the unsaturated zone [L T^{-1}]
s: distance from the watershed boundary (in direction of slope inclination) [L]
s_{slope}: slope length [L]
s_0: slope at the origin of the Langmuir isotherm curve
t: time [T]
v: seepage velocity [L T^{-1}]
v_{GW}: seepage velocity of the groundwater [L T^{-1}]
x: space co-ordinate in flowline direction [L]
z: depth below surface [L]
z_{reg}: regolith depth [L]
z_s: groundwater level below surface at position s [L]

C_a: adsorbed sulphate [N M^{-1}]
C_l: sulphate concentration in solution [N L^{-3}]
$C_{l\,in}$: input sulphate concentration [N L^{-3}]
C_{tot}: total sulphate [N L^{-3}]
D: dispersion coefficient [L^2 T^{-1}]
J_{conv}: convective sulphate flux [N L^{-2} T^{-1}]
J_{disp}: dispersive sulphate flux [N L^{-2} T^{-1}]
K: hydraulic conductivity [L T^{-1}]
K_d: distribution coefficient of the linear isotherm [L^3 M]
N: last point in space [-]
O: error term (Landau symbol)
R: retardation coefficient [-]

α: angle of inclination [°]
θ: water content [-]

λ: dispersivity [L]

μ: arithmetic mean

$\rho_{b\ eff}$: effective bulk density [M L^{-3}]

σ: standard deviation

$\{C_{tot}\}$: vector of total sulphate

$\{C_l\}$: vector of sulphate concentrations in solution

$[A]$: matrix of coefficients

List of Files on CD-ROM.....X:\Contents.doc

Thesis.....X:\Thesis\...

Cover sheet.doc
Lists.doc
Chap1-4.doc
Chap5.doc
Chap6_part1.doc
Chap6_part2.doc
Chap7.doc
Chap8-12.doc
AppendixA.doc

Results of the Field Sampling in the Lysina Catchment.....X:\Field Sampling\...

water_samples.xls
soil_samples.xls
surveying.xls

Digitised Map of the Lysina Catchment (Auto CAD).....X:\Map\...
(base map: Hrdlička, 1989)

contour_lines.dxf
streams.dxf
watershed_boundary.dxf

Analysis of Flowpath Lengths.....X:\Analysis of Flowpath Lengths\...

Programme.....X:\Analysis of Flowpath Lengths\Programme\...

flowpath.cpp (source code)
flowpath.exe (executable)
catchm.txt (exemplary input files: Lysina main catchment)
grid.txt
isolines.txt
streams.txt

Input Files.....X:\Analysis of Flowpath Lengths\Input Files\...

Lehstenbach.xls
Lysina_main_catchment.xls
Lysina_side_catchment.xls
readme.txt

Output Files.....X:\Analysis of Flowpath Lengths\Output Files\...

Lehstenbach.xls
Lysina_main_catchment.xls
Lysina_side_catchment.xls
readme.txt

Sulphate Model.....X:\Sulphate Model\...

Programme.....X:\Sulphate Model\Programme\...

SulphateModel.cpp (source code)
SulphateModel.exe (executable)
flowl.txt (exemplary input files for a 500 m flowpath in
param.txt the Lehstenbach catchment)
info.txt

Input Files.....X:\Sulphate Model\Input Files\...

Lehstenbach.xls
Lysina.xls
readme.txt

Output Files.....X:\Sulphate Model\Output Files\...

Lehstenbach_stream_water.xls
Lehstenbach_GW04.xls
Lehstenbach_GW05.xls
Lysina_weir1.xls
Lysina_weir2.xls
Lysina_Lenka.xls
readme.txt

X:\ denotes the CD-ROM drive on the computer.

1 Introduction

Anthropogenic atmospheric acid depositions in Central Europe strongly decreased during the last two decades. Forested catchments, however, are still substantially impacted by acidification (Alewell *et al.*, 2000b). Several catchment studies are conducted throughout Europe, which investigate this subject. The Lehstenbach catchment in the Fichtelgebirge region in south-eastern Germany as well as the Lysina catchment in the Slavkovský les region in the western part of the Czech Republic represent two sites which have been intensively monitored for more then a decade.

With respect to sulphate, observed short-term (days) and middle-term (years) dynamics of groundwater and stream water concentration exhibit considerable spatial variability. In the Lysina catchment, in the middle-term trend clearly decreasing concentration in the catchment runoff stands beside markedly less decreasing concentration at the outlet of a side catchment and even a high level stable concentration at a spring exhibiting groundwater from deeper layers (Hruška & Krám, unpublished data). In the Lehstenbach catchment, the middle-term trend of sulphate concentration in the catchment runoff is much less clear, whereas decreasing concentration similar to the Lysina side catchment runoff can be observed in a low order stream. In contrast, concentrations at two wells representing groundwater from deeper layers are still increasing (Lischeid *et al.*, 2000).

So far, these patterns are only understood in a qualitative sense. For the Lehstenbach catchment the varying contribution of waters from different origins is assumed to be the main cause of variability. Recovery thereby seems to be restricted to the topsoil layers, whereas sulphate accumulation still continues in the deeper layers of the aquifer. The dynamics of this process can be described by sorption isotherms (Lischeid *et al.*, 2000). For the Lysina catchment, it is assumed that the spatial variability of sulphate patterns is controlled by the same processes.

The objective of this study is the quantitative investigation of the observed middle- and short-term dynamics of sulphate concentration at different sites in the Lehstenbach catchment and the Lysina catchment. To examine the extent to which the spatial variability can be explained by single processes, a model is developed, which simulates sulphate concentration in soil solution, groundwater, stream water, and on the solid phase. The model considers sulphate transport and equilibrium sorption processes along one-dimensional flowpaths. Different locations are characterised by the contribution of flowpaths of different lengths. Parameterisation is based on experimental data from the catchments determined in preceding studies, whereas particular importance is attached to spatial heterogeneity and uncertainty of input parameters and their effects on model results. Additional soil and groundwater sampling is conducted in the Lysina catchment and supplies further data for model parameterisation and evaluation.

2 Fundamentals

2.1 Anthropogenic Acidification in Focus

During the last century, intensified combustion of fossil fuels led to a great increase of acidifying air pollutants such as SO_2 and NO_x in Europe as well as in North America. These were transported over long distances in the atmosphere. Thus, the resulting deposition affected terrestrial and aquatic ecosystems far away from the emission sources. The first alerts were reported from Scandinavia, where freshwater acidification and loss of fisheries occurred. Soon, visible symptoms such as the widespread forest decline were also detected in Central Europe (Steinberg & Wright, 1994).

One of the countries especially impacted by acid rain was the Czech Republic. At the triangle where the Czech Republic, Germany, and Poland meet, the so-called "Black Triangle", the use of lignite containing large amounts of sulphur for industry and home heating purposes led to average SO_2 concentrations in the air exceeding 100 µg m^{-3}. These were among the highest in the world. The effects were visible in soil acidification, local decreases of stream pH, and widespread forest decline (Pačés, 1985; Moldan & Schnoor, 1992).

In Germany as well, acid deposition and forest decline became a major issue. In the Solling region in central Germany annual sulphate deposition fluxes of up to 3 kmol ha^{-1} could be measured in a Norway spruce stand in the late 1970s (Matzner & Meiwes, 1994). This was also when first symptoms of forest decline became apparent. In the Fichtelgebirge region in south-eastern Germany, which is only approximately 100 km apart from the "Black Triangle", the early signs were mainly needle-yellowing and needle-loss of spruce trees as well as reduced stand growth (Schulze *et al.*, 1989).

On the whole, several authors report on a clear empirical relationship between acid depositions and soil, surface water, and groundwater acidification (Ulrich, 1985; Reuss *et al.*, 1987; Karltun, 1994).

On the political level, this threatening development showed that it was necessary to adopt emission control measures on an international basis. Therefore, in 1979 the "Convention on Long-Range Transboundary Air Pollution" was set up by the United Nations Economic Commission for Europe (UN ECE). Subsequently, sulphur protocols (1985 and 1994) were initiated, in which countries committed themselves to concrete reduction of SO_2 emissions (Lückewille, 1994). Thereby, Germany aimed at a reduction of 87 %, the Czech Republic aimed at 72 % with respect to the reference year 1980 (UN ECE, 2000). Applied measures then, such as the desulphurisation of exhaust gases, resulted in strongly decreased emissions and thus greatly reduced deposition in the last decade (Matzner & Meiwes, 1994; Schnoor *et al.*, 1997; Stoddard *et al.*, 1999).

At this point, reversibility became the predominant subject in acidification research. One way to study the topic was the initiation of roof projects. Within these, whole catchments are covered by a roof, then the actual precipitation is collected above the roof, and a purified

one is spread below. This allows to observe the effects of decreased or even no deposition especially within the scope of response times of different catchments. The first project of this kind was conducted in southern Norway (Risdalsheia) (Wright *et al.*, 1988). Further projects followed in south-western Sweden (Gårdsjön) (Hultberg & Skeffington, 1998), in central Germany (Solling) (Bredemeier *et al.*, 1995), in north-western Denmark (Klosterhede) (Beier *et al.*, 1995; Gundersen *et al.*, 1995; Hansen *et al.*, 1995) as well as in the south-eastern Netherlands (Ysselsteyn) and in the central Netherlands (Speuld) (Boxman *et al.*, 1995). These studies as well as the monitoring of other catchments showed that different sites react differently to reduced deposition. In general, shallow soils with a low sulphate storage capacity respond rapidly, whereas soils and regoliths with a high sulphate storage capacity exhibit a marked delay in recovery from acidification (Alewell *et al.*, 2000).

2.2 Sulphate Dynamics

Within the scope of the outlined subject, it is necessary to take a closer look at sulphate cycling in catchments. Beside the direct damage of plants by SO_2, there is the input into the soil in form of wet and dry deposition. Wet deposition is rain, fog, or snow in which SO_2 is solved and then oxidised to form sulphuric acid H_2SO_4. Dry deposition is the absorption of SO_2 by vegetation and soil surfaces. Subsequently, this SO_2 is subject to leaching by rainfall, in which it reacts to sulphuric acid as well. Because dry deposition can account for even more then 50 % of total deposition, forested ecosystems are affected to a great degree. Generally, sulphuric acid is a strong acid, which means that in solution it instantaneously dissociates resulting in free acidity (H^+) on the one hand and sulphate anions (SO_4^{2-}) on the other hand (Reuss & Johnson, 1986; Scheffer & Schachtschabel, 1992).

In the soil, this acidity is largely buffered by different mechanisms, which lead to an alteration of ecologically relevant soil characteristics. Ulrich (1981, 1983) distinguishes between five buffering systems, to which he assigns corresponding pH ranges. At a pH (H_2O) between 6.2 and 8.6 carbonate buffering prevails and acidity is neutralised by decalcification. Between pH 5.0 and 6.2 silicate buffering takes place, which leads to the weathering of silicates and the formation of clay minerals. At further decreasing pH values (4.2 to 5.0), buffering by exchange cations becomes relevant. In this range, aluminium cations are first released from clay minerals and primary silicates. Due to their high charge these cations are now able to displace base cations as well as other cations such as manganese and heavy metals from the exchange sites of the solid phase, and release them to the soil solution. During aluminium buffering, which prevails at pH 2.8 to 4.2, acidity is buffered by the large release of aluminium ions from clay minerals and aluminium hydroxides. This leads to a strong increase of the aluminium concentration in the soil solution. Finally, iron buffering predominates at pH 2.4 to 3.8. Thereby, iron hydroxides and oxides dissolve, and iron is released into solution.

During the 1970s and 1980s sulphate was the predominant anion in precipitation in many parts of Europe and North America, and it therefore also became a major anion in the soil solution (Galloway *et al.*, 1976; Reuss *et al.*, 1987). The principle of electroneutrality

requires a balance of positive and negative charges. Therefore, high sulphate concentrations in the soil solution lead to further changes. These are generally increased levels of base cations, resulting in the acceleration of base cation depletion, furthermore increased concentrations of aluminium ion species, particularly Al^{3+}, which is potentially toxic to soil organisms and plant roots, and to a lesser degree the increase of free acidity (H^+). Such solutions may be released to surface waters. Due to the mobilised toxic aluminium and heavy metals as well as the low pH, they may lead to fatal consequences on biota within streams and may represent a thread for the drinking water supply (Reuss & Johnson, 1986; Scheffer & Schachtschabel, 1992).

In Central Europe SO_2 concentrations in the air decreased by 63 %, and sulphate in precipitation decreased by 40 % between 1985 and 1996 (Stoddard *et al.*, 1999). The problem however is still relevant. Sulphate retention on the solid phase is one major reason. It leads to a substantial retardation of sulphate transport within catchments and thus a delay from the recovery of acidification. Inorganic sulphate contents (H_2O extractable (extr.)) of up to 0.3 µmol g^{-1} are common in soil (Scheffer & Schachtschabel, 1992). Malessa (1993) investigated solid bound sulphate ($NaHCO_3$ extr.) in soil profiles of up to 3 m depth and reports on an accumulation wave of inorganic sulphate with maximum values of up to 7 µmol g^{-1}. All profiles exhibited the same shape with low concentrations in the upper and lower part and a sulphate peak in between. For different profiles it was located in different depths. From this, he concluded that sulphate may slowly migrate through the soil into deeper layers. Meiwes *et al.* (1994) examined profiles of up to 30 m depth in northern Germany. In some cases they found high sulphate concentrations in the soil solution as well as on the solid phase (up to 4 µmol g^{-1}, Na_2CO_3 extr.) in the upper part of the profiles, whereas measured concentrations in the lower part decreased to a tenth of these values. Besides, a clear delay of recovery can be observed at some places in the deep groundwater, where sulphate concentration is still increasing (Armbruster, 1998; Lehstenbach catchment, cf. Section 3.2).

Generally, sulphate retention on the solid phase can be governed by two processes. These are sorption and precipitation. Sorption refers to adsorption and desorption. Adsorption describes the adhesion of molecules or ions to the grain surface. The release from the solid phase is called desorption (Spitz & Moreno, 1996). Considering the precise mechanism, as for anions such as sulphate, reactive minerals are mainly hydroxides and oxides of iron and aluminium as well as clay minerals with numerous hydroxide groups on the surface. Thereby, it has to be distinguished between unspecific and specific adsorption (Fig. 2.1). With regard to unspecific adsorption, positive charge on the surface of the adsorbent is created by the addition of a H^+ ion to the hydroxyl group. Thus, adsorption of the sulphate anion takes place by isostatic forces. In case of specific adsorption, the sulphate anion substitutes the hydroxyl group. Subsequently, an oxygen bridge is created to the aluminium or iron atom of the adsorbent (Scheffer & Schachtschabel, 1992). The essential aspect of these reactions, both the unspecific and the specific adsorption, is this: Adsorption consumes acidity, whereas desorption releases the previously stored acidity again. Experimentally this could be

Non-specific adsorption:

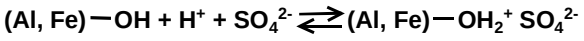

Specific adsorption:

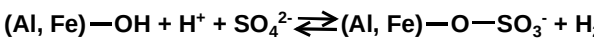

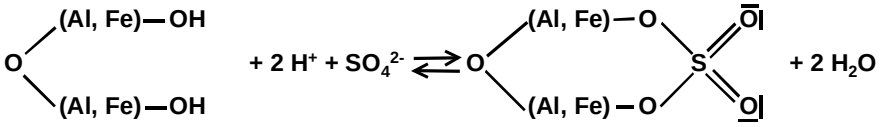

Fig. 2.1 Mechanisms of unspecific and specific sulphate adsorption (modified according to Scheffer & Schachtschabel, 1992).

established by several authors (Meiwes *et al.*, 1980; Hodges & Johnson, 1987; Zhang & Sparks, 1990).

In forested soils the main part of total adsorbed sulphate is H_2O extractable, thus reversibly bound. Harrison *et al.* (1989) report on an average value of 64 %, which could be desorbed by H_2O, whereas Alewell (1995) even found more than 70 % of total sulphate (= $NaHPO_4$ extr.) to be reversibly bound.

Mathematically, the process of sorption is described by isotherms. Assuming equilibrium conditions, the amount of solid bound sulphate is a function of the sulphate concentration in solution. However, these functions may have a variety of shapes depending on the characteristics of the solid phase as well as on the composition of the solution. There are several approaches for a mathematical formulation. The most common ones are addressed in the following. The simplest approach is the linear isotherm, for which the ratio of sorbed sulphate to sulphate in solution is given by a constant distribution coefficient. The Langmuir isotherm represents another description, which is based on the assumption of a finite number of identical adsorption sites per unit mass. Starting therefore at the origin of the isotherm curve, the quantity of adsorbed sulphate increases for increasing solute concentration and finally asymptotically approximates a sorption maximum. In contrast to the linear isotherm, in this case the rate of adsorption is not only proportional to the concentration in solution, but also to the number of unfilled sites on the surface. The Freundlich isotherm, on the other hand, does not exhibit a sorption maximum. Hence, it is suitable for substances which act as though the surface contained different sorption sites. Mathematically, this curve is described by a power function with the exponent being smaller than one (Jury *et al.*, 1991).

The kinetics of the sorption process were not found to play a role for middle and long-term time scales. In laboratory experiments Houle & Carignan (1995), for instance, found equilibrium conditions for adsorption to be reached after 3 hours. For desorption, Courchesne

& Hendershot (1990) even found 50 % of previously adsorbed sulphate to be in solution after only 5 minutes. This is in line with isotopic studies conducted at the field scale, which showed that sulphur isotope fractionation is negligible during sorption processes in soils. It suggests that there is a rapid exchange between dissolved and adsorbed sulphate (Torssander & Mörth, 1998).

The second process which may be responsible for the sulphate retention on the solid phase is the precipitation of aluminium sulphates. Böttcher (1992) could identify mineral phases in acidified soils which in their chemical composition were similar to alunite-jarosite, zaherite, basaluminite, and hydrobasaluminite. However, Matzner *et al.* (2001) report on a laboratory study in which gibbsite was exposed to varying solutions of sulphate and aluminium. Sulphate precipitation did not occur over large surface areas, but was restricted to certain sites characterised by steps and edges of the minerals. In addition, modelling of sulphate dynamics on the basis of precipitating aluminium sulphates resulted in steep increases and decreases of sulphate concentrations in the soil solution and the stream water. This effect was due to spontaneous precipitation and dissolution reactions of the mineral phases. However, this has not been observed in on site measurements. Therefore, it is unlikely that this process accounts for the major proportion of sulphate storage in soils. Observed gradual changes instead point to the fact that sorption is the governing process (Lückewille, 1995).

Within the scope of sulphate dynamics the organic sulphur pool cannot be neglected, as the sulphur contained in soil organic matter represents the largest part of the sulphur pool in most forested ecosystems (Reuss & Johnson, 1986). Furthermore, isotope studies conducted in several catchments (Torrsander & Mörth, 1998; Alewell & Gehre, 1999; Novák *et al.*, 2000) clearly show that the cycling of sulphur through the organic pool takes place. During assimilation sulphate is incorporated into organic matter, whereas it is released again by mineralisation. However, a quantification of the process is still difficult. Consequently, it is unknown to which extent this process contributes to sulphate retention within catchments. Reuss & Johnson (1986) point to the fact that biological sulphur requirements for forests are modest, generally less than 0.15 kmol ha^{-1} yr^{-1}, which is still less compared to the actual input by throughfall. In addition, they present data from different catchments in the United States which give evidence that sulphate adsorption is the more important accumulation process compared to biological immobilisation. Catchments exhibiting podzolic soils with a high adsorption maximum generally show a net accumulation of sulphur, whereas catchments with soils much richer in organic matter but poor sulphate adsorption capacities are rather balanced with respect to sulphate input and output.

One further process needs to be taken into account in the context of sulphate dynamics. Bacterial dissimilatory sulphate reduction can act as a net sulphur retention process, especially in bogs and fens (Urban *et al.*, 1989; Novák & Wieder, 1992). It occurs in aqueous systems containing organic matter at low redox potentials (E_H) of smaller than –0.2 V (Stumm & Morgan, 1996). Reduced sulphur species can either degas in form of hydrogen sulphide or they can be fixed in the catchment in form of reduced sulphur compounds, e.g. metal sul-

phides or elemental sulphur. Dissimilatory sulphate reduction leads to a large fractionation of sulphur isotopes (Thode, 1991). Therefore, isotope studies provide an important tool for the investigation of its role in the sulphur cycling of forested ecosystems (Mörth *et al*., 1999; Alewell & Novák, 2001). Within the scope of recovery from acidification, the significance of sulphate reduction is rooted in a proton consumption, which results in an alkalinity gain for the soil solution. Vice versa however, the re-oxidation of reduced inorganic sulphur releases protons and leads to a renewed acidification (Giblin & Wieder, 1992).

2.3 Acidification Models

Models are used to investigate sulphate dynamics in a quantitative way. There are two primary purposes: Firstly, a model can act as a tool for the better understanding of observed patterns. Thus, insights into the predominant relationships of the system are gained. Secondly, a model might be able to predict future behaviour of a system (Ball & Trudgill, 1995). Due to the numerous processes and interactions within ecosystems however, models can never be "white boxes", but at the most "grey" ones. This leads to predictions which are highly uncertain. However, especially in the context of policy making predictive models are extremely useful, and with a fair estimation of uncertainty they are justifiable to a given degree as well.

Acidification models can be classified into two groups, process-oriented and empirical. Well-known process-oriented models are PROFILE (Sverdrup *et al.*, 1987), SMART (De Vries *et al.*, 1989), MAGIC (Cosby *et al.*, 1985a, 1985b), and the Birkenes model (Christophersen & Wright, 1981). Basically, all of them are highly lumped models representing a continuously stirred reactor. They lump together the hydrology of a catchment within a small number of boxes and do not offer any further spatial resolution. The chemistry is simply determined by mass balance equations. Hence, it is implied that each box is chemically and hydrologically homogeneous. For most of these models, a number of chemical processes is incorporated such as cation exchange, weathering, sulphate sorption, carbon dioxide and gibbsite dissolution (Ball & Trudgill, 1995).

There are two main problems which arise in the context of these modelling approaches. Firstly, even if models fit observed runoff data fairly well and in a way produce reasonable future scenarios, the addition of new field data, e.g. on soil solution chemistry and water residence times, often reveals great inconsistencies between model assumptions and observations. Models assume simple processes like mineral equilibrium formulations, which have not been observed in on site measurements. Furthermore, soil parameters are modelled homogenous by "representative" parameter values. Observed values however, exhibit a large heterogeneity (Christophersen *et al.*, 1993). Secondly, models are often overparameterised. In these cases, there may be no "optimum" set of parameter values, but a number of "best" fits with parameters which are distributed throughout the parameter space. Predictions with such models would therefore be useless, because the range of future scenarios would be extremely large (Beven, 1993).

Empirical models are “black boxes”. They describe statistical relationships between different parameters in a catchment. They do not account for the internal mechanisms of the system and they are not transferable to different catchments (Ball & Trudgill, 1995). There are several types of empirical models such as e.g. mixing model relationships (Eshleman, 1988), multiple regression models (Lynch *et al.*, 1986), or artificial neural networks (Lischeid, 2001a). All of them have the purpose of identifying relationships at short-term time scales. As they are not transferable to different catchments, empirical models are also not transferable to longer time scales, because boundary conditions might change and other relationships might become the predominant ones.

3 Study Sites

3.1 General Characteristics

Both the Lehstenbach and the Lysina catchment belong to the low mountain range of Central Europe. They are approximately 60 km apart from each other (Fig. 3.1).

The Lehstenbach catchment (Fig. 3.2) is located in south-eastern Germany (north-eastern Bavaria) in the Fichtelgebirge mountains. The highest peaks of the Fichtelgebirge region are Mount Schneeberg (1051 m a.s.l.) and Mount Ochsenkopf (1024 m a.s.l.). The Waldstein massif, in which the study catchment is situated, is in the northern part of that region. The catchment is 4.2 km^2 in size and exhibits an elevation range of 694 to 877 m a.s.l.. It is drained in south-easterly direction through the Lehstenbach stream, which flows into the Eger river and finally into the Elbe river.

The Lysina catchment (Fig. 3.3) is located in the western part of the Czech Republic in a mountainous region called the Slavkovský les. Its highest peaks are Mount Lesný (983 m a.s.l.) and Mount Lysina (982 m a.s.l.). The study catchment is situated at the north-east facing slope of Mount Lysina. It is 0.27 km^2 in size and its elevation ranges from 829 to 942 m a.s.l.. A stream drains the catchment towards east into the Eger river and finally into the Elbe river as well. Approximately 10 km north of the catchment near the city of Sokolov there is an industrial area with several lignite surface mines as well as the Tisová power plant, where the high sulphur lignite (2 to 12 % of sulphur by mass) is burned (Krám *et al.*, 1997).

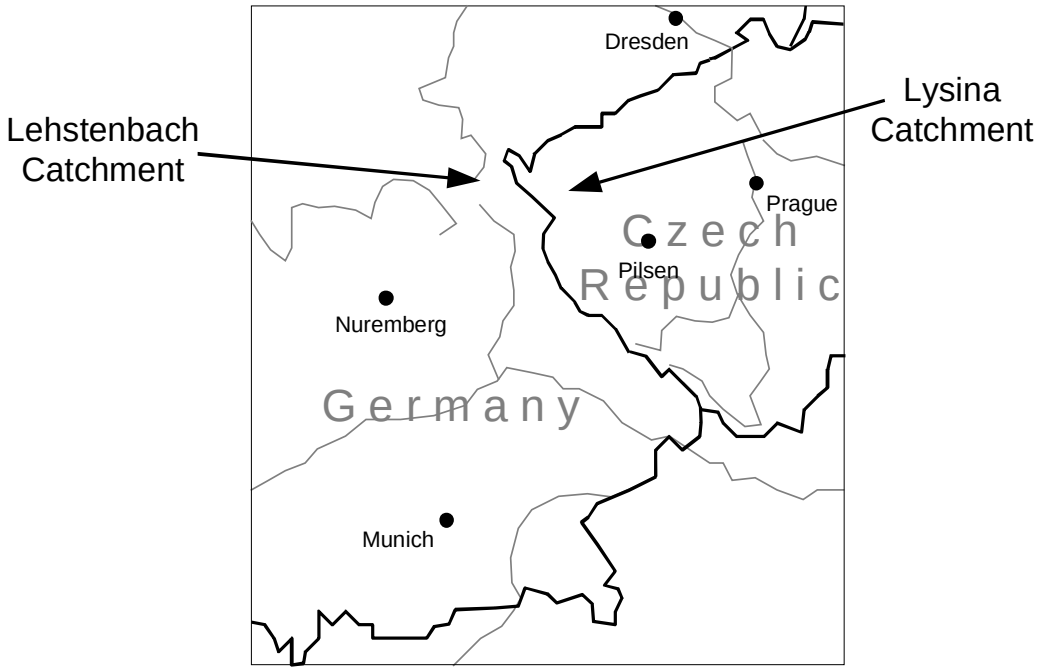

Fig. 3.1 Location of the study catchments.

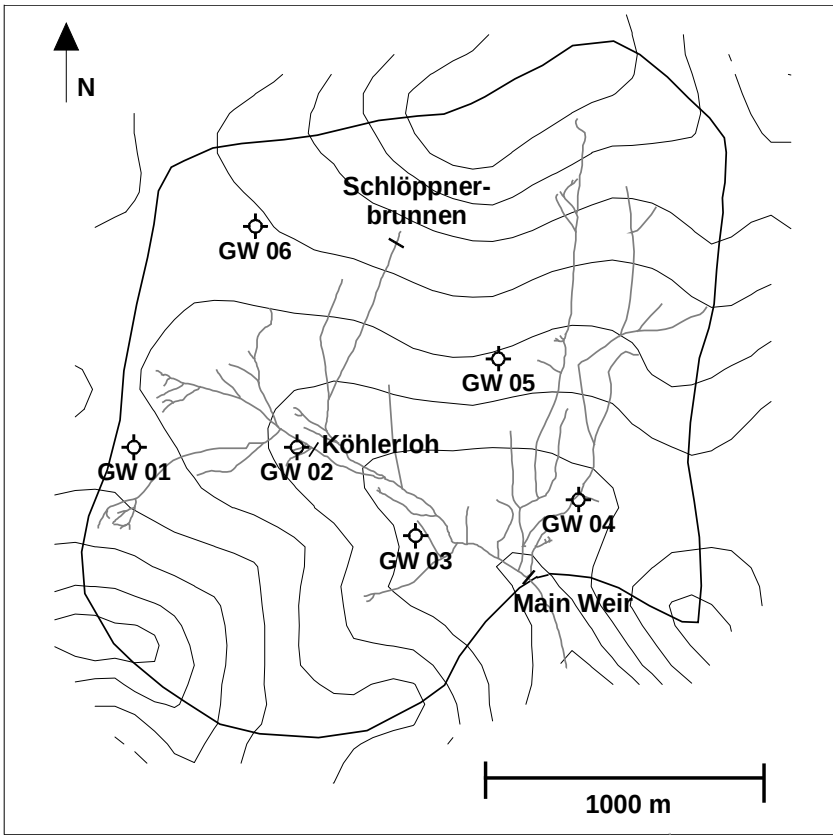

Fig. 3.2 Map of the Lehstenbach catchment with the main weir at the catchment's outlet, the stream water sampling sites Schlöppnerbrunnen and Köhlerloh, the groundwater wells GW 01 to GW 06, the stream system, the watershed boundary, and the 20 m contour lines.

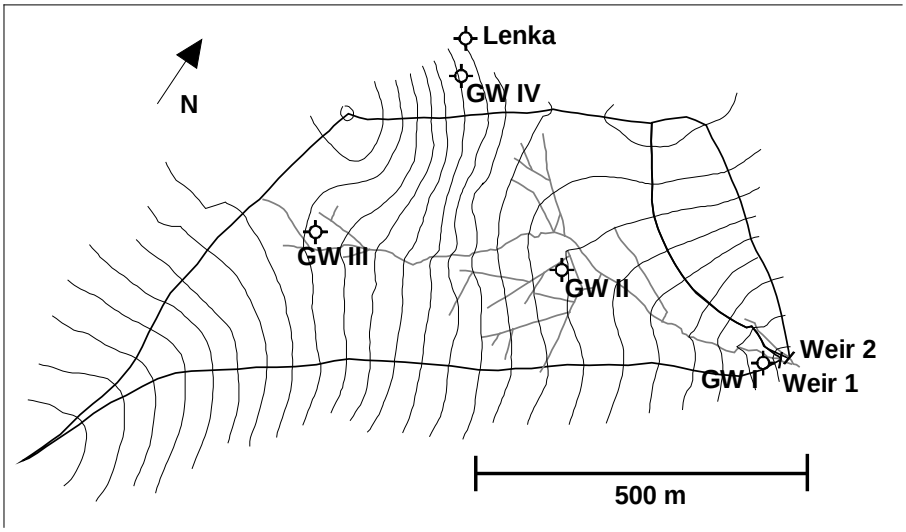

Fig. 3.3 Map of the Lysina catchment with the main catchment and its outlet weir 1, the side catchment and its outlet weir 2, the spring Lenka, the four sites GW I to GW IV, at which piezometers were installed in this study, the stream system, the watershed boundary, and the 5 m contour lines (modified according to Hrdlička, 1989).

Geologically, both catchments are underlain by younger variscan granites (Haunschild & Jerz, 1981). The variscan orogenesis took place from the Devonian to the Permian era (380 to 320 million years) and the mountain folding was accompanied by granite intrusions from greater depth (Stettner, 1981). In the Lehstenbach catchment, granite mainly consists of a porphyric type with a fine-grained matrix (Stettner, 1964). Lysina granite on the other hand is coarse-grained (Krám *et al.*, 1995). Both granites contain only a very small amount of base cations with quartz and feldspar being the primary minerals. At Lysina the oxides of silicon and aluminium (SiO_2 and Al_2O_3) comprise 87 % of the rock by weight (Krám *et al.*, 1997). For the Lehstenbach catchment no such analysis was performed. However, it was done for the same type of granite at two sites close to the catchment exhibiting very similar results compared to the Lysina analysis. Here, the average weight % of silicon and aluminium oxides was determined to be 88 % (Stettner, 1964). Thus, both granites may be referred to as leucocratic granites.

In the Tertiary (65 to 2.4 million years) tropical to subtropical climatic conditions prevailed in the area. That led to a deep weathering of the granitic bedrock. Today however, entire tertiary weathering profiles can hardly be found, because they were cut by erosion in the younger Tertiary as well as in the Quaternary, but there are still residuals (Stettner, 1964). Thus, for the Lehstenbach catchment, the average regolith depth was determined to be 32 m (Rüdiger, 1993a). In contrast, the Lysina catchment exhibits only a shallow regolith with an average depth of 2.5 m (Gurtler & Nikl, 1999).

Within the Lehstenbach catchment, humid-continental climate prevails. Mean annual bulk precipitation is 985 mm, whereas mean annual discharge measured at the main weir is 470 mm (Moritz *et al.*, 1994; Moritz, unpublished data). Water residence times were determined at different sites in the catchment and varied between 2 and more than 4 years, with a value of 3.6 years at the main weir (Zahn, 1995). More than 95 % of the catchment is covered with forest, of which approximately 90 % is Norway spruce (*Picea abies*) (Heindl *et al.*, 1995). In the upper parts of the catchment, predominant soils are dystric cambisols and podzols. However, in the hollows, which account for one third of the area, gleysols and histosols prevail (Moritz *et al.*, 1994).

For the Lysina catchment, mean annual bulk precipitation is 933 mm and mean annual discharge measured at weir 1 is 432 mm (Krám *et al.*, 1997; Hruška & Krám, unpublished data). Water residence time in the main catchment was estimated to be between 1.1 and 1.5 years (Buzek *et al.*, 1995). 70 % of the main catchment's area is covered with Norway spruce forest (*Picea abies)*. The remaining area was clear-cut in the 1980s and is now covered with young forest and grass. Dystric cambisols are the predominant soils which developed from the granitic bedrock and characterise about half of the main catchment, the side catchment, and the catchment of the spring Lenka. For the remaining half of the main catchment however, soils are influenced by shallow groundwater, which led to the formation of peaty gleys (Hruška & Krám, 1994). Within this area, a system of small ditches was laid out to provide for better drainage.

On the whole, both catchments are sensitive to acid deposition. This is due to the low neutralising ability of the substratum, which is caused by the small amount of base cations in the bedrock as well as by the low weathering rate of granites in general (Chadwick *et al.*, 1991). In the Lysina catchment the situation is exacerbated by the shallow regolith depth, which further reduces the overall buffering potential. Thus, in the early 1990s, critical loads of acid deposition were exceeded by a factor of 27, resulting in average aluminium concentrations of 68 µmol l^{-1} in the runoff of the catchment, which were higher than that of reported stream waters from small catchments in any other part of the world (Hruška & Krám, 1994). For the Lehstenbach catchment, the situation does not appear to be as dramatic. However, in the early 1990s as well, 44 % of raw waters for the drinking water supply in the whole Fichtelgebirge region exceeded the European Union reference value of 0.05 mg l^{-1} (= 1.9 µmol l^{-1}) for aluminium, thus making deacidification treatment necessary (Moritz *et al.*, 1994).

3.2 Preceding Measurements

In the Lehstenbach catchment measurements were initiated in 1987 by the Bavarian State Office for Water Management (LfW). In 1995 the majority of measurements were taken over by the newly established Bayreuth Institute of Terrestrial Ecosystem Research (BITÖK). Bulk precipitation, throughfall, and soil solution up to three meters depth are sampled biweekly on several plots within the catchment. Besides, stream water sampling is performed at biweekly intervals at different sites, including the main weir, the Köhlerloh site, and the Schlöppnerbrunnen spring. Depth-integrated groundwater sampling is conducted bimonthly at 13 observation wells. Six of them, which are shown in Fig. 3.2, were already established in 1987, whereas the remaining seven were established 10 years later in 1997. In addition, the amount of bulk precipitation at one site as well as discharge at the main weir are recorded continuously. If not stated differently, the data presented in the following refer to these measurements (Moritz *et al.*, 1994; Moritz, unpublished data; BITÖK, unpublished data).

Sulphate concentration in throughfall decreased by 80 % between 1992 and 1999. In the soil solution of 20 cm depth a decrease of 75 % could be observed with respect to the same time interval, whereas concentrations in 90 cm depths decreased by 43 % (Alewell *et al.*, 2000a).

Stream water concentrations do not show such a clear trend. Sulphate concentration at the main weir exhibits a great range with minimum values of about 0.1 mmol l^{-1} during baseflow conditions and maximum values of up to 0.35 mmol l^{-1} during stormflow conditions (Fig. 3.4A). Thereby peak concentrations, which may mainly represent water from the topsoil (Lischeid, 2001a), show a clear decrease, whereas for baseflow, which is derived from the deeper aquifer, concentrations remain stable. The time series of the Köhlerloh subcatchment is very similar to the one observed at the main weir. The Schlöppnerbrunnen subcatchment

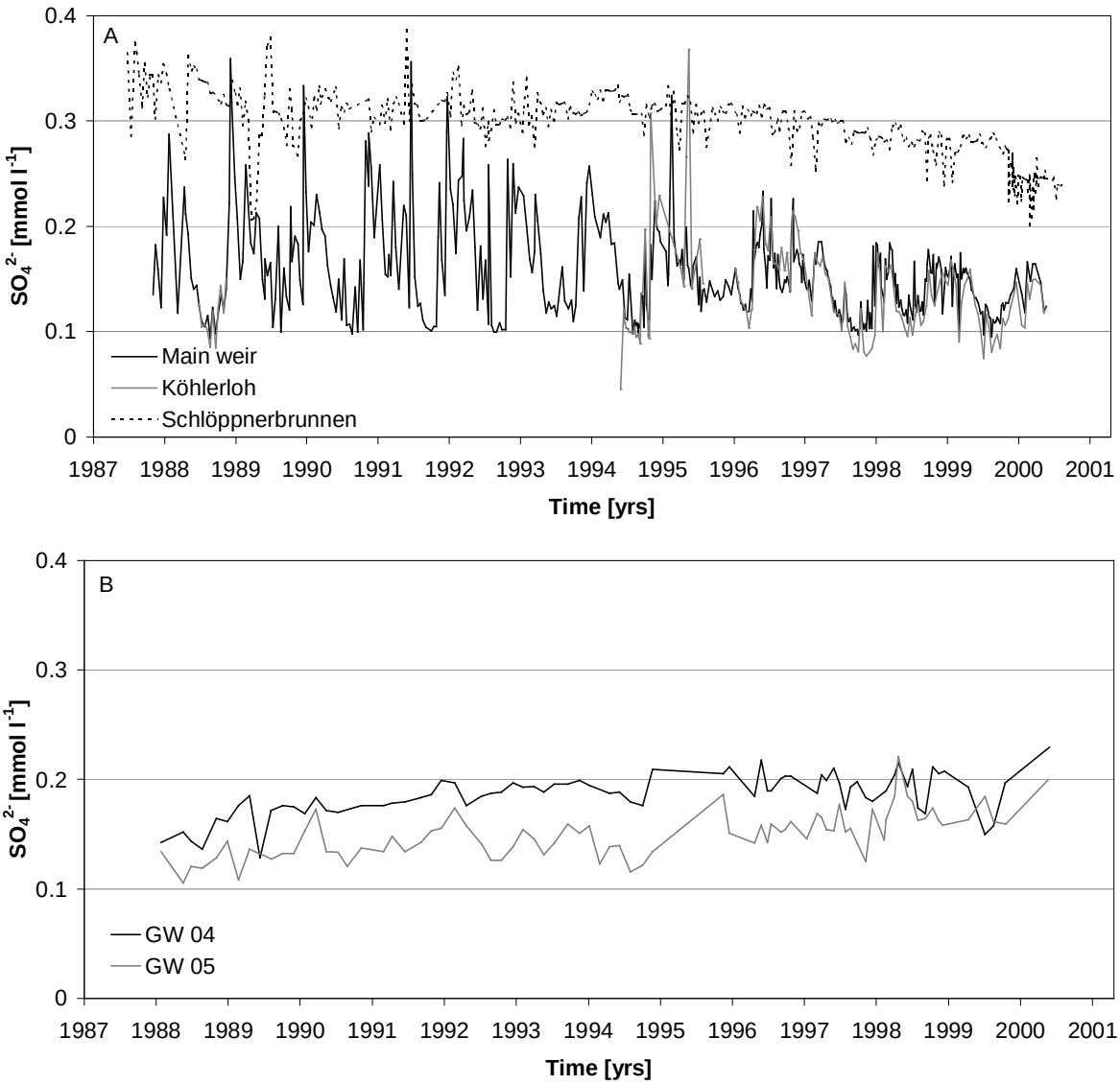

Fig. 3.4 Time series of sulphate concentration at different locations in the Lehstenbach catchment. **A**. Stream water at the main weir, Köhlerloh, and Schlöppnerbrunnen. **B**. Groundwater at the wells GW 04 and GW 05.

however shows a markedly different pattern. Here, the overall range of concentrations is smaller and with about 0.3 mmol l^{-1} the base level is higher. Furthermore, since 1995 a decrease is observed on the whole scale.

For groundwater sulphate concentration, long time series are available for the six wells established in 1987. Fig 3.4B shows two of them, GW 04 and GW 05, which are modelled in this study. Despite of the extremely decreased input concentrations in throughfall, at GW 05 as well as at GW 06 (not shown) an increasing sulphate concentration can still be observed. With average groundwater levels of 13.5 m (GW 05) and 6.5 m (GW 06) below surface (b.s.) respectively, both of them represent the deeper groundwater component. At the well GW 04 values increase in the late 1980s, but in the 1990s this trend is not visible anymore. Instead values are stable at around 0.2 mmol l^{-1}. In addition, there is another remarkable observation.

At six out of the 13 wells, sulphate concentration and groundwater level are significantly correlated: The closer the groundwater level to the surface, the higher is the sulphate concentration and vice versa, thus indicating decreasing sulphate concentrations with depth (Lischeid, pers. comm.).

Altogether, the picture appears as follows: decreasing deposition, decreasing sulphate concentration in soil solution and during stormflow events in runoff, stable low level baseflow, still increasing values at two groundwater wells, and decreasing concentrations with depth indicated at some groundwater wells. These patterns clearly point towards a slow movement of sulphate through the regolith, for which sorption on the solid phase may be responsible. Thus, at present recovery is only visible in the top layers, whereas sulphate is further accumulated in the deeper aquifer.

Further investigations support these findings. For different places in the catchment inorganic solid bound sulphate as well as adsorption and desorption isotherms were determined by laboratory analyses for the topsoil and for the samples of up to 10 m depth. Firstly, on average 2.28 µmol g^{-1} of inorganic solid bound sulphate (NaH_2PO_4 extr.) are stored in the topsoil and still 1.14 µmol g^{-1} in greater depth, whereas sulphur mineral phases were not detected. Secondly, sorption and desorption curves, to which Langmuir isotherms could well be fitted, show a considerable spatial heterogeneity. Thirdly, there is a high capacity to store further sulphate in greater depth as indicated by Langmuir sorption maximums of the determined isotherms. Fourthly, an equilibrium with the desorption isotherms can be observed between groundwater sulphate and solid bound sulphate (Jungnickel, 1996; Schweisser, 1998; Manderscheid *et al.*, 2000a; Manderscheid *et al.*, 2000b).

There is one study which slightly stands apart from the picture. Rötting (2000) took depth-specific groundwater samples at the six wells GW 01 to GW 06. In contrast to the correlation of sulphate concentration and groundwater level, which is observed for the integrated samples he could not find any clear gradients.

Besides, it always has to be kept in mind that there are other processes operating which are able to shape sulphate dynamics. Alewell & Gehre (1999) conducted stable sulphur isotope studies on water samples of the Lehstenbach catchment. From the observed signals, they concluded firstly that in the upland soils sulphur mineralisation from the organic pool would be an important process. Secondly, data showed that wetland soils in the catchment represent a sink for sulphate due to dissimilatory reduction.

In the Lysina catchment sampling was first initiated in 1988 by the Czech Geological Survey (ČGÚ). Regular monitoring has been conducted since 1990. Bulk precipitation is sampled biweekly. Throughfall and soil solution are sampled monthly. Surface water samples from weir 1 are taken on a weekly basis, whereas the water level is recorded continuously. Weir 2 is sampled monthly. Additionally, the spring Lenka, which is assumed to represent deeper groundwater is sampled on a monthly basis (Krám, 1997). If not stated differently, the

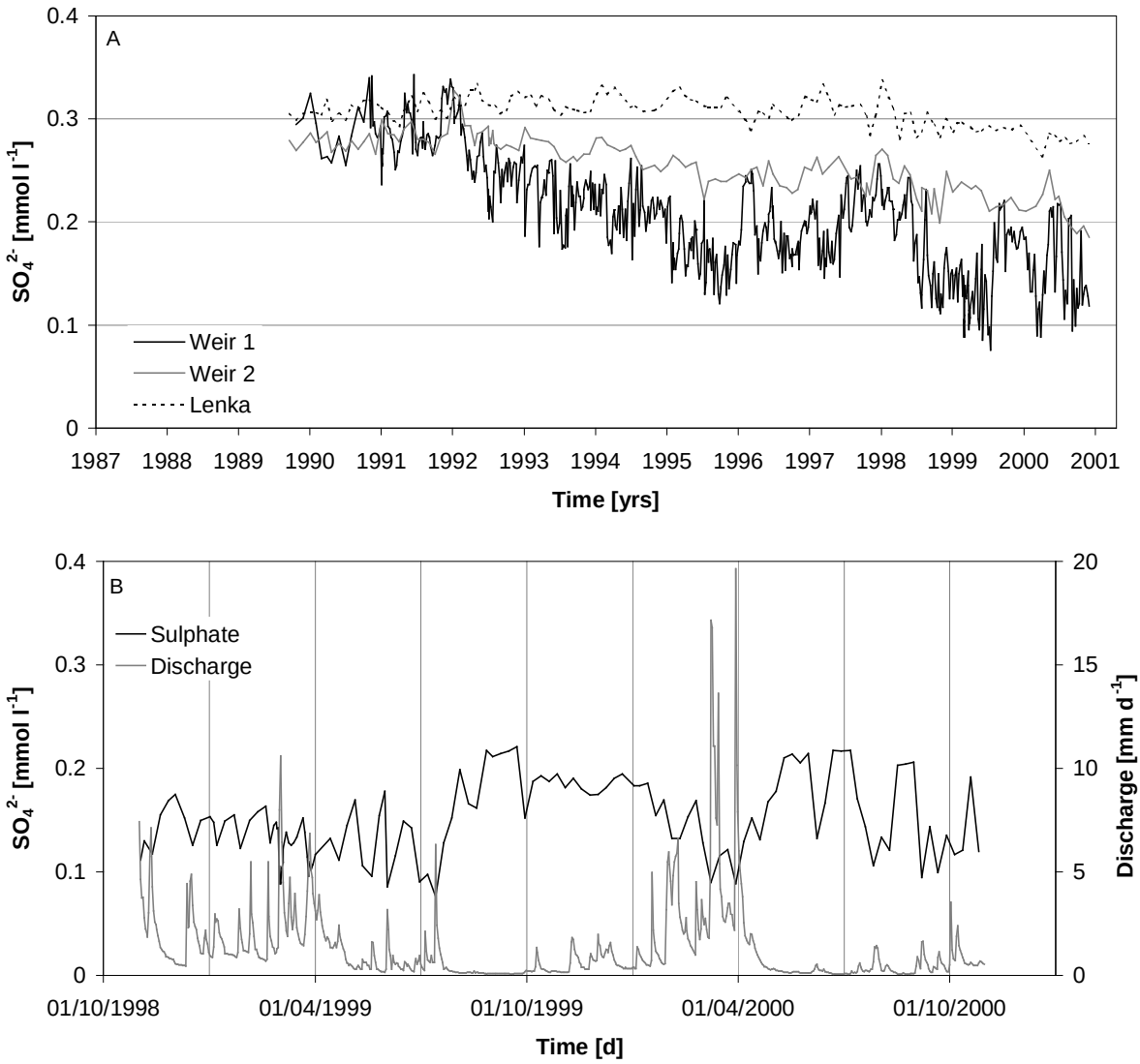

Fig. 3.5 Time series of sulphate concentration at different locations in the Lysina catchment. **A**. Weir 1, weir 2, and Lenka. **B**. Sulphate concentration and discharge at weir 1 for the hydrologic years 1999 and 2000.

data presented in the following refer to these measurements (Hruška & Krám, unpublished data).

Sulphate fluxes in throughfall decreased by 70 % between 1991 and 2000 (cf. Appendix D). This is reflected in the soil solution of 15 to 20 cm depth, in which the annual volume weighted sulphate concentration decreased by approximately 50 % between 1995 and 2000.

Here, sulphate patterns of stream water and groundwater look differently compared to the Lehstenbach catchment (Fig. 3.5A). For the outlet of the main catchment, weir 1, concentrations exhibit a clear decrease from values of about 0.3 mmol l^{-1} in the late 1980s to values ranging from 0.1 to 0.2 mmol l^{-1} at present. Like at the Lehstenbach main weir, short-term variability is considerable, but the dynamic is reverse (Fig. 3.5B). High sulphate concentrations are obtained during baseflow conditions, in which water is mainly derived from the deeper groundwater. Stormflow on the other hand, which contains a great proportion of top-

soil water (Buzek *et al.*, 1995), is characterised by low concentrations. Time series of weir 2 and the spring Lenka are different compared to weir 1. Even though in the late 1980s values of all three sites are very similar, differences become evident in the 1990s. The decrease at weir 2 is much less pronounced than at weir 1, and Lenka does not even show any decline until recently.

In summary, for the Lysina catchment the picture is this: decreasing deposition, decreasing sulphate concentration in the soil solution in shallow depth and during stormflow events in runoff, higher but still decreasing concentrations in baseflow and finally stable high level concentrations in the deeper groundwater at Lenka. Thus, even if at first sight patterns look differently compared to the Lehstenbach catchment, a closer look reveals the similarities. These are the recovery in the topsoil as well as the delayed reaction to reduced deposition in layers, which are not so close to the surface. A deep groundwater component with still increasing sulphate concentration such as in the Lehstenbach catchment does not exist for the Lysina catchment, as regolith depth is only shallow (cf. Section 3.1).

Furthermore, soil samples were taken at nine locations in the catchment and were analysed with respect to various parameters, of which inorganic sulphate was one. They give evidence that there is a considerable amount of inorganic sulphate which is bound to the solid phase in the Lysina catchment as well (Krám, 1997), even if it is less compared to average values from the topsoil of the Lehstenbach catchment (Jungnickel, 1996).

In addition, sulphur isotopes were studied in the catchment. Soil samples from vertical profiles indicated that part of the incoming sulphate by precipitation is cycled through the organic sulphur pool (Novák *et al.*, 1996). Isotopic signals of water samples from bulk precipitation, throughfall, and runoff however did not reveal a shift (Hruška, pers. comm.). This gives evidence that large isotope fractionation processes such as the dissimilatory reduction of sulphate do not play a role at the catchment scale.

4 Materials and Methods

4.1 Drilling

In the Lysina catchment knowledge about sulphate dynamics in the deeper aquifer is rare. Additional data were needed for model parameterisation and evaluation. Therefore, seven new boreholes were drilled. On the one hand, they provided soil samples from different depths of the regolith. On the other hand, the installation of piezometers allowed depth specific groundwater sampling.

Drilling was performed in August 2000. Four locations, GW I, GW II, GW III, and GW IV were chosen (Fig. 3.3), which represent the different characteristics of the area. At each location except for GW IV two piezometers with different screen depths were installed in order to gain information on depth specific sulphate variability in the groundwater. Label "a" always refers to the shallower piezometer and "b" denotes the deeper one.

The screen position as well as the median of the groundwater level of the piezometers are given in Tab. 4.1. Sampling locations GW I, GW II, and GW III are situated in the main catchment. GW I is close to weir 1, the outlet of the catchment. The site is forested and the water table is deep. With a screen position between three and five meters below surface, piezometers at this site exhibit the greatest depths and therefore represent groundwater from the deeper aquifer. GW II and GW III are situated in the boggy part of the catchment. Site GW II is forested, whereas GW III is located at a clearing. In contrast to GW I, the groundwater level of these sites is close to the surface, except for GW IIb, where a second deeper aquifer was encountered. Screen positions range from less than a meter to three meters below surface and thus water sampled from these piezometers exhibits a shallower component of groundwater compared to GW I. GW IV is not located in the main catchment, but uphill of the spring Lenka. Therefore it is assumed to represent the same aquifer as the spring. The site is forested. The screen position of the piezometer is about three meters below surface. However, as the water table was still below that depth in August 2000, a second drilling was not performed at

Tab. 4.1 Median of the groundwater level and screen position of the piezometers installed in the Lysina catchment.

	Median of the groundwater level [m b.s.]	**Screen position [m b.s.]**
GW Ia	1.76	3.40 – 3.60
GW Ib	1.72	4.23 – 4.43
GW IIa	0.52	1.25 – 1.45
GW IIb	1.48	2.57 – 2.77
GW IIIa	0.15	0.82 – 1.02
GW IIIb	0.06	0.99 – 1.19
GW IV	> 3.00	2.80 – 3.00

this site.

Drilling was conducted using a pneumatic percussion drill (Cobra 148, Atlas Copco) with a diameter of 36 mm. Directly after drilling, PVC tubes were inserted into the boreholes, of which the lower 20 cm were perforated with holes of 5 mm in diameter. Several difficulties arose in connection with drilling. Firstly, at GW III the substratum did not allow deep drilling, as probably the bedrock or a granitic woolsack was encountered. Secondly, at GW III as well, deeper parts of the boreholes collapsed immediately after drilling, so that tubes could only be inserted in shallow depth. Thirdly, first groundwater samplings revealed that most of the piezometers were locked by fine-grained particles. In order to clean the screen, stream water was added from above, and was then flushed through the screen into the aquifer by means of a pump. Certainly, this procedure resulted in a short-term contamination of the aquifer. However, afterwards piezometers worked well and samples exhibited reasonable solute concentrations.

4.2 Water Samples

Weekly groundwater sampling at the newly installed piezometers in the Lysina catchment took place from August to November 2000. Every two weeks the full sampling procedure was conducted. First, the standing groundwater level was recorded. Then old water was pumped out of the piezometers by a hand pump and subsequently new water from the aquifer was sampled. Within this, the parameters pH, electrical conductivity, temperature, redox potential, oxygen, and hydrogen sulphide were directly measured by means of electrodes (Tab.

Tab. 4.2 In situ measured parameters and their devices for Lysina groundwater sampling.

	Device
pH	WTW SenTix 41
Electrical conductivity	TetraCon 325
Temperature	Temperature probe of the conductivity electrode
Oxygen	CellOx 325
Hydrogen sulphide	Ingold Typ H_2S 245-85
Redox potential	WTW SenTix ORP

Tab. 4.3 Chemical analysis methods for the Lysina water samples.

	Method
Al, Ca, Fe, K, Mg, Mn, Na, S, Si	Atomic emission spectrometry with an inductively coupled argon plasma, ICP-AES GBC Integra XMP
Cl^-, NO_3^-, PO_4^{3-}, SO_4^{2-}	Ion chromatography, Dionex DX 100
NH_4^+, NO_2^-	Flow injection (photometrically), Lachat FIA QuickChem AE 100
DN	Chemoluminescence after oxidative pyrolysis, Abimed TN 05
DOC, DIC	IR spectrometry after digestion to carbon dioxide, Elementar high-TOC

4.2). Calibration of the hydrogen sulphide electrode was performed according to a method of Peters *et al.* (1984). Additional samples were taken from the side catchment's outlet weir 2, the spring Lenka, and a ditch in the boggy area, which is close to the sampling location GW II. In the weeks between these samplings, only the groundwater level was recorded and old water was sampled from the piezometers. Samples were transported in PE bottles and were stored in the dark at 2 °C until further analysis.
Samples were analysed with respect to their main constituents as well as dissolved organic carbon (DOC), dissolved inorganic carbon (DIC), and dissolved nitrogen (DN). After filtration (Sartorius Cellulose Acetate Filter 0.45 µm), chemical analyses were performed in the Central Analytical Department of BITÖK. Analytical methods are given in Tab. 4.3 (for identification limits and coefficients of variation see Appendix A).

4.3 Soil Samples

4.3.1 Field Sampling and Preparation

During drilling soil samples were taken from the drill stem at intervals of less than a meter. For each sample, texture as well as colour were determined. For texture, this was done manually according to the German soil classification scheme (Finnern *et al.*, 1994), whereas colour determination took place without a classification scheme. Samples were transported in PE-bottles. Subsequently, corresponding to Schweisser (1998) they were sieved to 5 mm in field moist condition. Until further analysis they were stored at 2 °C.

Samples from one drilling core of each site were analysed. In addition, one sample from the second core was analysed. It represents the one obtained from the depth at which the piezometer screen is located. That was to enable the direct comparison of the groundwater and the respective solid phase. Appendix B informs about the samples which were chosen in particular.

4.3.2 Sulphate Contents, Desorption Isotherms, and Adsorption Experiments

The analysis of Lysina soil samples with respect to their inorganic sulphate content (H_2O and NaH_2PO_4 extr.) as well as their adsorption and desorption behaviour was based on batch experiments which were developed by Alewell (1995). In order to allow a direct comparison, methods in this study were mainly adopted from Schweisser (1998), who performed similar analyses in the Lehstenbach catchment. Tab. 4.4 states the general procedure of the batch method. For different analyses only the quantity of added soil as well as the chemical composition and the volume of the solution were altered.

For the determination of inorganic sulphate contents, sulphate which had previously been bound to the solid phase was transferred into solution by means of the batch method, where it could subsequently be quantified. In case of the water extraction, 10 g of soil were mixed with 50 ml of aqua bidest.. The shaking procedure was repeated five times, and after each step the solution was decanted and analysed with respect to sulphate. In case of the

Tab. 4.4 Analytical procedure of the batch shaking method, as performed on the Lysina soil samples.

- Weighing of the specified quantity of field moist soil
- Addition of the defined volume of solution
- Shaking with an end-over-end shaker for 18 h at 5°C
- Centrifugation for 10 min. at 3000 rpm
- Decanting and filtration (Sartorius Cellulose Acetate Filter 0.45 µm) of the supernatant solution
- Analysis with respect to sulphate (ion chromatography, see Tab. 4.3)

phosphate extraction, 10 g of soil were mixed with 50 ml of a 0.02 M NaH_2PO_4 solution. The shaking procedure was repeated twice. The decanted solution was diluted with a ratio of 1:6, in order to ensure the separation of the sulphate peak from the phosphate peak during the subsequent analysis by ion chromatography.

The determination of desorption isotherms was performed similarly. Sulphate of the solid phase was dissolved step by step in small quantities. 20 g of soil were mixed with different volumes of aqua bidest.. The shaking procedure was repeated ten times and solute volumes increased from one step to the next. For steps one and two 12.5 ml of aqua bidest. were added, steps three to five were conducted with 25 ml, steps six to eight with 100 ml, and finally steps nine and ten with 200 ml.

Adsorption experiments were conducted by adding solutions of high sulphate concentration (Na_2SO_4) to the soil. 5 g of soil were mixed with 40 ml of solution. Two different sulphate solutions were chosen, one of 100 mg l^{-1} (= 1.04 mmol l^{-1}) and the other one of 250 mg l^{-1} (= 2.60 mmol l^{-1}). The shaking procedure was applied once for each of these solutions.

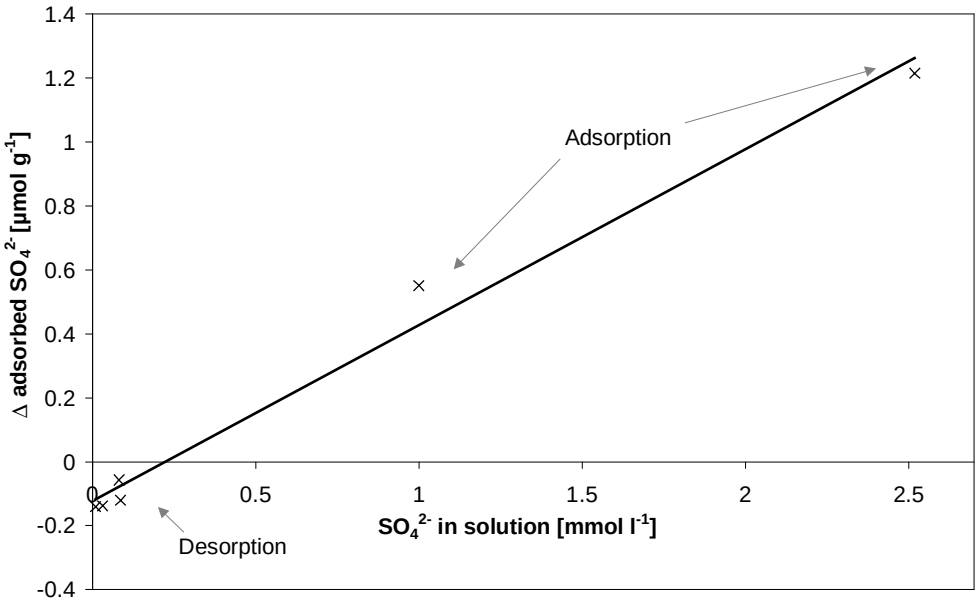

Fig. 4.1 Linear isotherm fit for the experimentally determined adsorption and desorption points (sample GW Ia2 from the Lysina catchment).

For the calculation of water and phosphate extractable sulphate contents, desorbed quantities of sulphate from the five or two extraction steps respectively were added up. Considering desorption isotherms, the total released sulphate until a particular extraction step is derived and set in relation to the concentration in solution which was measured at this step (Fig. 4.1). During the experimental procedure it was not possible to completely decant the supernatant solution. The residue was determined by weighing and considered in the calculations. Derived values were related to the dry weight of the employed soil.

For the desorption isotherms no sulphate could be measured in solution anymore after at maximum five extraction steps. Concentrations were below the identification limit. Therefore, only few points were available for the isotherm fit. Langmuir isotherms could not be fitted with the Levenberg-Marquardt algorithm. The results were unreasonable. Hence, the only possibility to have an estimate of the sorption behaviour was to fit linear isotherms. For each sample this was done by considering adsorption and desorption points together (Fig. 4.1).

4.3.3 Elemental Analyses and pH-Measurements

Total quantities of carbon, nitrogen, and sulphur of the Lysina soil samples were measured. The soil was dried in an oven at 105 °C for three days and was subsequently ground. Chemical analyses were performed in the Central Analytical Department of BITÖK. Total carbon and total nitrogen were measured using a CHN-Analyser (Foss Heraeus CHN-O-Rapid). Total sulphur was determined by means of the Seiff pressure digestion method with nitric acid. Afterwards sulphur was measured with the ICP-AES (Tab. 4.3).

Soil pH was determined in aqua bidest. as well as in a 0.01M solution of $CaCl_2$ with a standard mass ratio of soil to solution of 1:2.5. Measurements were conducted using the WTW SenTix 41 pH electrode.

4.4 Surveying and Map Processing

The Lysina catchment was surveyed in September 2000. The aim was to determine the position of the newly installed piezometers as well as to derive local groundwater contour maps. These maps were based on the median of the groundwater level recorded at the piezometers and the position of adjacent stream points.

Map processing was based on a detailed map of the catchment area given in a local coordinate system (Hrdlička, 1989). It was digitised using AutoCAD 12.0. Further processing was done with Surfer 6.04.

4.5 Statistical Methods

Statistical tests can be divided into parametric and non-parametric. Parametric tests generally require normally distributed data sources. Many processes in nature such as the conversion of substances however lead to parameters which are not normally distributed. This problem can be avoided by applying non-parametric tests, which do not pose such require-

ments on data. The disadvantage of these tests however is their smaller power compared to the parametric tests, which is due to the fact that only the ordinal information of the data is used (Bortz *et al.*, 1990; Sachs, 1997).

In this study mainly non-parametric methods were utilised. Only for modelling, where Monte-Carlo simulations were conducted, parametric methods were applied, as the specification of distributions was explicitly required. In the following all tests which were utilised will briefly be stated. The information is taken from Bortz *et al*. (1990) and Sachs (1997).

Significant monotonous relationships between two parameters were tested by means of the Spearman correlation coefficient. The test was conducted two-sided. The H-Test of Kruskal-Wallis was applied in order to test significant differences between the medians of several independent samples. It is the non-parametric analogue of the parametric analysis of variance. The Kolmogoroff-Smirnov-Test served to examine the extent to which a sample was normally distributed. In this case, Lillefors limits had to be applied, because the parameters describing the normal distribution, which are the arithmetic mean and the standard deviation, were estimated from the sample itself.

Two parametric methods were applied. The Pearson correlation coefficient was used to test relationships between two parameters. In contrast to the Spearman coefficient, the linearity of the relationship is tested rather than just the monotony. The test was conducted two-sided. Furthermore, two arithmetic means of connected samples were examined by a T-Test.

In all cases the level of significance was chosen to be 5 %. The analyses were done using SPSS 10.0.5.

5 Model Design

5.1 Model Objectives

Sulphate dynamics in the Lysina and the Lehstenbach catchment exhibit a great spatial variability (cf. Section 3.2). Well-known process-oriented acidification models such as MAGIC (Cosby *et al.*, 1985a, 1985b) however are unable to simulate this. They lump the hydrology of a catchment into a small number of boxes, which means that they are zero-dimensional (cf. Section 2.3).

Therefore, another long-term modelling approach is developed, which offers further spatial resolution. It simulates the development of sulphate concentration from the beginning of the industrialisation in the middle of the 19th century until present. The approach is one-dimensional and sulphate transport in the unsaturated zone and the groundwater is modelled along flowpaths. The processes included are convection, dispersion, and equilibrium sorption. Additionally, Monte-Carlo simulations allow for spatial heterogeneity of sorption isotherms. Both slope cross-sections and catchment runoff can be simulated in a simple way by considering the contribution of flowpaths of different lengths. Consequently, the approach is also quasi-two-dimensional (slope) as well as quasi-three-dimensional (runoff).

The main objective is to examine, if the model is able to reproduce the different sulphate dynamics which are observed in the middle- and short-term trend at different sites in the stream water and the groundwater in the Lehstenbach and the Lysina catchment, thus if the considered processes together with the parameterisation are appropriate to describe the system. In order to guarantee the independence of model parameterisation and model results, no calibration by inverse modelling is performed. Instead, model parameters are entirely based on field measurements and literature values in cases where no field data are available. The uncertainty of the parameters is taken into account by a sensitivity analysis.

5.2 Conceptual Model

5.2.1 Slope Concept of Water Flow

In the model, the natural water flow regime of a catchment is represented in an idealised slope (Fig. 5.1). This slope represents a parallelogram, which ranges from the watershed boundary to the stream. Thus, the inclination of the slope and the regolith depth are considered to be constant. The slope is divided into two parts: the unsaturated zone, in which water movement is purely vertically and where the water content is given by field capacity, and the groundwater, where the flow direction is parallel to the inclination of the slope. Thereby, water flow is limited to the regolith and groundwater movement in the bedrock is neglected. Assuming an unconfined aquifer, its thickness increases from the watershed boundary to the stream. This is due to the increasing water volume which has to be transported. Finally,

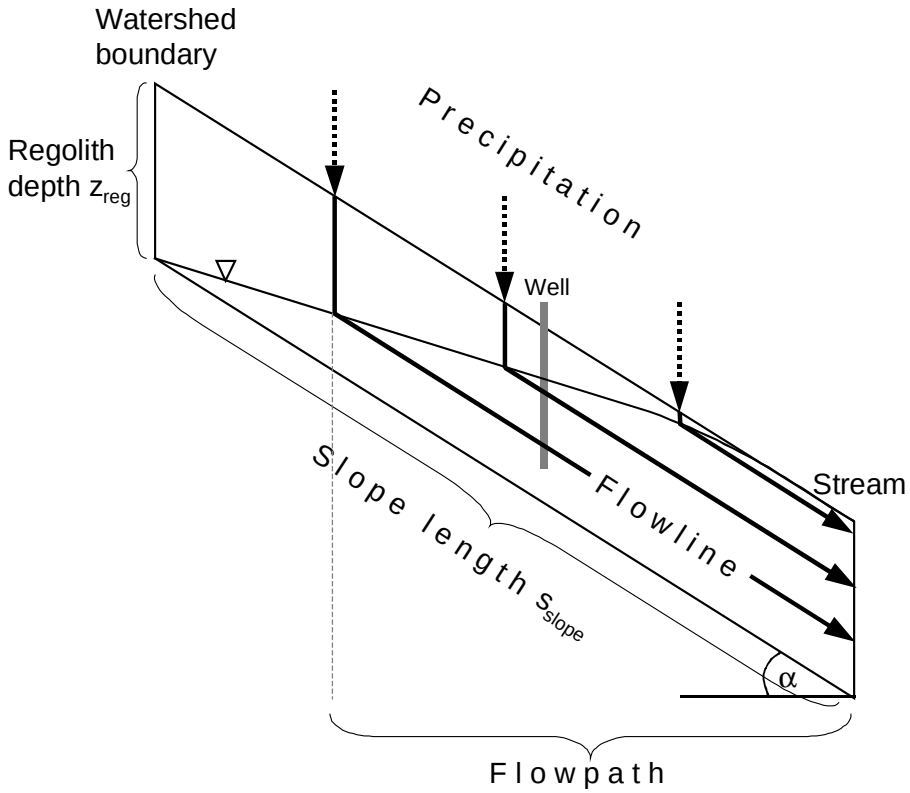

Fig. 5.1 Idealised slope cross-section with flow regime.

groundwater discharges to the stream. The last part, in which water movement is directed upwards, plays a minor role within the scope of the whole slope and is neglected in this approach.

Steady state Darcian water flow is assumed. Precipitation infiltrates uniformly in space and time. Since evapotranspiration is neglected, the quantity of precipitation is given by mean annual discharge per unit area of the catchment. This value also specifies the Darcy velocity in the unsaturated zone, in which water moves downwards vertically until the water table is reached. At this point the flow direction changes and the flow velocity increases, as the flow's cross-section decreases. The Darcy velocity in the aquifer results from the restriction of mass conservation. Considering the whole slope, water input per unit time (precipitation) has to equal water output (discharge to the stream). This is given by:

$$q_{soil} \cdot s_{slope} \cdot \cos\alpha = \int_0^{z_{reg}} q_{GW}(z)\, dz \qquad (5.1)$$

where q_{soil}: Darcy velocity of the unsaturated zone [L T^{-1}]

s_{slope}: slope length [L]

α: angle of inclination [°]

z_{reg}: regolith depth [L]

q_{GW}: Darcy velocity of the groundwater [L T^{-1}]

z: depth below surface [L]

The groundwater Darcy velocity is equal the product of the seepage velocity and the total porosity.

$$q_{GW}(z) = v_{GW} \cdot n(z) \tag{5.2}$$

where v_{GW}: seepage velocity of the groundwater [L T^{-1}]

n: total porosity [-]

Thereby, it is simplistically assumed that all water is both mobile and in equilibrium with the solid phase. Thus, effective porosity equals total porosity. Furthermore, seepage velocity of the groundwater is assumed to be constant over depth. Therefore, substitution of the Darcy velocity in equation (5.1) by the right-hand side term of equation (5.2) results in:

$$v_{GW} = \frac{q_{soil} \cdot s_{slope} \cdot \cos\alpha}{\int_0^{z_{reg}} n(z)\, dz} \tag{5.3}$$

Finally, resubstitution of v_{GW} according to equation (5.2) leads to the demanded Darcy velocity for the specified depth z:

$$q_{GW}(z) = n(z) \frac{q_{soil} \cdot s_{slope} \cdot \cos\alpha}{\int_0^{z_{reg}} n(z)\, dz} \tag{5.4}$$

The hydraulic conductivity of groundwater flow can be derived from Darcy's law (Jury *et al.*, 1991).

$$q_{GW}(z) = -K(z) \frac{dh}{dx} \tag{5.5}$$

where K: hydraulic conductivity [L T^{-1}]

h: potential head [L]

x: space co-ordinate in flowline direction [L]

Generally, the gradient of the gravitational potential drives groundwater flow. That means that the potential head gradient is only determined by the steepness of the slope. Thus, the hydraulic conductivity arises to:

$$q_{GW}(z) = K(z) \cdot \sin\alpha \Leftrightarrow K(z) = \frac{q_{GW}(z)}{\sin\alpha} \tag{5.6}$$

The position of the water table below surface can be calculated from the mass conservation approach as given in equation (5.1). Now, only a part of the slope is considered. Water infiltrating within a certain distance s from the watershed boundary flows through the lower part of the aquifer between the bottom of the regolith and the depth z_s, which represents the groundwater level at the position s. The formulation of equation (5.3) for that part of the slope is given by replacing s_{slope} by s and 0 in the integral by z_s:

$$v_{GW} = \frac{q_{soil} \cdot s \cdot \cos\alpha}{\int_{z_s}^{z_{reg}} n(z)\, dz} \tag{5.7}$$

where s: distance from the watershed boundary (in direction of slope inclination) [L]

z_s: groundwater level below surface at the position s [L]

As the seepage velocity in the groundwater is constant, equation (5.7) may be equated with equation (5.3) to form:

$$\int_{z_s}^{z_{reg}} n(z)\, dz = \frac{s}{s_{slope}} \int_{0}^{z_{reg}} n(z)\, dz \tag{5.8}$$

The groundwater level results from the solution to z_s. From the equation it becomes clear that the shape of the groundwater level is only dependent on the porosity function. For decreasing porosity values with increasing depth the shape is convex.

Within the catchments there are slopes of different lengths and regolith depths. However, seepage velocity of the groundwater (equation (5.3)) is set constant everywhere. Therefore, maximum slope length as well as maximum regolith depth of the catchment are chosen to form a basic slope. When considering shorter slopes, the regolith depth is changed accordingly.

5.2.2 Analysis of Flowpath Lengths and Runoff Generation

A flowline characterises the way of a water molecule from precipitation through the unsaturated zone and downhill through the groundwater into the stream (Fig. 5.1). The corresponding flowpath is defined by the projection of the flowline on the horizontal plane.

Groundwater wells are located at the slope between the watershed boundary and the stream. The distance from the watershed boundary and the distance from the stream determine their position (Fig. 5.1). These distances are given by the lengths of the groundwater flowpath from the watershed boundary to the well and from the well to the stream. Now, it is possible to derive flowlines, which terminate in different depths at the well, thus simulating a vertical profile of the sampling site. For observation wells, this two-dimensional approach of a slope cross-section is appropriate, as flowpaths run mainly parallel to each other in the vicinity of the wells.

Simulating runoff however is more complicated. In this case, flowpaths are not anymore parallel to each other, but converge in the vicinity of the stream. This problem is approached by deriving a distribution of flowpath lengths for each catchment. For that, the catchment area is overlain by a grid of 25 x 25 m in size. Subsequently, for each of these grid points the flowpath to the stream is derived. Fig. 5.2 depicts the method of flowpath generation, which was realised in a computer programme. For that, the catchment's stream system, the topographic contour lines, and the watershed boundary need to be available in a digitised form. It is then assumed that groundwater flowpaths run downhill perpendicular to the con-

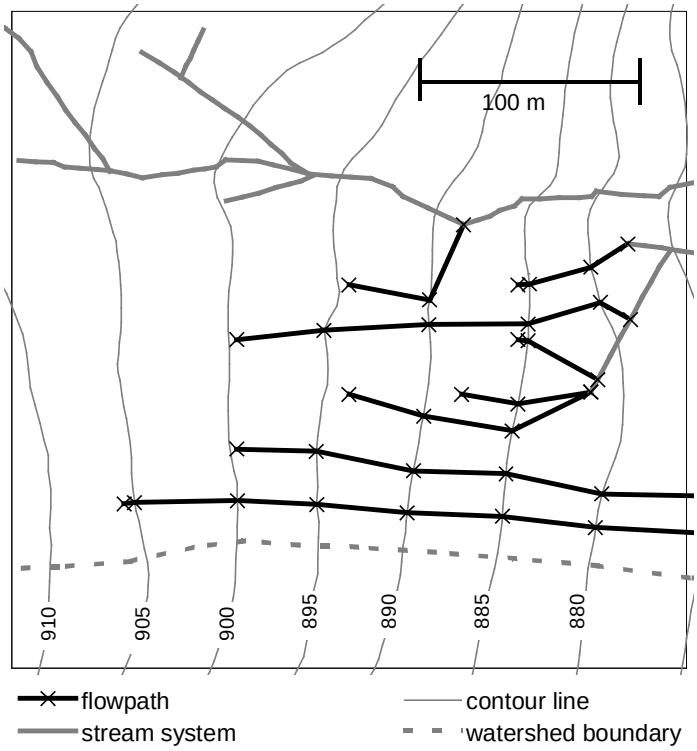

Fig. 5.2 Method of determining flowpath lengths. A detail of the Lysina main catchment is shown with selected flowpaths.

tour lines and finally terminate at the nearest section of the stream system. Starting at one particular grid point, first of all the perpendicular to the lower adjacent contour line is derived. Then, taking the intercept with this contour line, the intercept of the perpendicular to the next lower contour line is determined. This is continued until the distance to the next stream section is less than the distance to the next contour line. In this case, the flowpath terminates at that stream.

The distribution of flowpath lengths arises from the flowpath lengths of all the grid points of a catchment. Considering subcatchments, as required for the Schlöppnerbrunnen and the Köhlerloh sampling sites in the Lehstenbach catchment, their flowpaths form a subset of the total set of flowpaths of the main catchment. This subset is given by these flowpaths which terminate in the stream section located uphill of the sampling site.

The distribution of flowpath lengths specifies the extent to which different flowpath lengths contribute to runoff generation. These are now grouped into classes with a width of 50 m. Only the mean flowpath of each class is modelled, thus the 25 m, 75 m, 125 m etc. flowpaths. For that, the corresponding flowline has to be determined, which arises by the projection of the flowpath on the basic slope (Fig. 5.1). The length of the groundwater part of that flowline is given by the length of the flowpath corrected by the angle of the slope. The length of the unsaturated zone is given by the depth of the groundwater level in that respective distance from the stream. Finally, modelled concentrations at the ends of representative flowlines are mixed conservatively weighted by the number of flowpaths in the respective class.

5.2.3 Solute Transport Equations

Sulphate transport in the regolith is modelled one-dimensionally in flowline direction (cf. Fig. 5.1). Thereby, the processes of convection, hydrodynamic dispersion, and equilibrium sorption are considered. The basic equations of the following exposition are taken from Jury *et al.* (1991) and Spitz & Moreno (1996).

The convective flux, which is the bulk transport of dissolved sulphate moving with flowing water, is given by the product of the Darcy velocity and the solute concentration.

$$J_{conv} = q \cdot C_l \tag{5.9}$$

where J_{conv}: convective sulphate flux [N L^{-2} T^{-1}]

q: Darcy velocity [L T^{-1}]

C_l: sulphate concentration in solution [N L^{-3}]

Dispersive spreading of the solute is due to aquifer heterogeneities. Mathematically, it can be approximated by a Fickian process, which is described by Fick's law of diffusion.

$$J_{disp} = -D \cdot \theta \frac{\partial C_l}{\partial x} \tag{5.10}$$

where J_{disp}: dispersive sulphate flux [N L^{-2} T^{-1}]

D: dispersion coefficient [L^2 T^{-1}]

θ: water content [-]

Molecular diffusion itself is neglected, as field scale dispersion coefficients are several orders of magnitude higher. The dispersion coefficient can be expressed as the product of the dispersivity and the seepage velocity, which leads to the following equation:

$$J_{disp} = -v \cdot \theta \cdot \lambda \frac{\partial C_l}{\partial x} = -q \cdot \lambda \frac{\partial C_l}{\partial x} \tag{5.11}$$

where v: seepage velocity [L T^{-1}]

λ: dispersivity [L]

For equilibrium sorption processes to be included in the model, the solid phase becomes relevant in addition to the dissolved phase. Thus, the total sulphate pool needs to be divided into two parts.

$$C_{tot} = \rho_{b\,eff} \cdot C_a + \theta \cdot C_l \tag{5.12}$$

where C_{tot}: total sulphate [N L^{-3}]

$\rho_{b\,eff}$: effective bulk density [M L^{-3}]

C_a: adsorbed sulphate [N M^{-1}]

The effective bulk density characterises that proportion of the bulk density which is made up by the fine soil fraction. This is the effective part with respect to sorption processes. It is calculated from the porosity, the mineral density of quartz, which is given by 2.65 g cm^{-3} (Scheffer & Schachtschabel, 1992), and a dimensionless factor representing the proportion of the fine soil fraction.

$$\rho_{b\,eff} = a \cdot (1-n) \cdot 2.65\ \mathrm{g\ cm^{-3}} \tag{5.13}$$

where a: proportion of the fine soil fraction [-]

Two different sorption isotherm functions are implemented. By their means the quantity of adsorbed sulphate in equation (5.12) can be expressed in terms of the concentration of sulphate in solution. According to the available data sources, the linear isotherm is applied for the Lysina catchment and the Langmuir isotherm for the Lehstenbach catchment. In case of the linear isotherm, the quantity of adsorbed sulphate is a linear function of the concentration in solution.

$$C_a(C_l) = K_d \cdot C_l \tag{5.14}$$

where K_d: distribution coefficient of the linear isotherm [L^3 M]

For the Langmuir isotherm, the mathematical expression is the following:

$$C_a(C_l) = \frac{b \cdot k \cdot C_l}{1 + k \cdot C_l} \tag{5.15}$$

where b: Langmuir sorption maximum [N M^{-1}]

k: Langmuir reciprocal of the half saturation point [M^3 N^{-1}]

Equations (5.9), (5.11) and (5.12) are then combined by the restriction of solute conservation leading to the well-known convection-dispersion equation.

$$\frac{\partial C_{tot}}{\partial t} + \frac{\partial (J_{conv} + J_{disp})}{\partial x} = 0 \tag{5.16}$$

$$\Rightarrow \frac{\partial (\rho_{b\,eff} \cdot C_a(C_l) + \theta \cdot C_l)}{\partial t} = -q \frac{\partial C_l}{\partial x} + q \cdot \lambda \frac{\partial^2 C_l}{\partial x^2} \tag{5.17}$$

where t: time [T]

Each part of the flowline, the part in the unsaturated zone and the part in the aquifer (cf. Fig. 5.1), is modelled separately. Within each of these the Darcy velocity q and the dispersivity λ are constant. Consequently, they can be extracted from the space derivatives, which is done on the right-hand side of equation (5.17).

In the context of sorption often the retardation coefficient is introduced. For that, the terms of the sum on the left-hand side of equation (5.17) are differentiated separately with respect to the time t. The differentiation of $C_a(C_l)$ is done using the chain rule. The effective bulk density $\rho_{b\,eff}$ and the water content θ are constant with time and can therefore be extracted from the derivatives. This results in the following equations:

$$\underbrace{\left(\rho_{b\,eff} \frac{\partial C_a(C_l)}{\partial C_l} + \theta \right)}_{\theta \cdot R} \frac{\partial C_l}{\partial t} = -q \frac{\partial C_l}{\partial x} + q \cdot \lambda \frac{\partial^2 C_l}{\partial x^2} \tag{5.18}$$

$$\Rightarrow \frac{\partial C_l}{\partial t} = -\frac{q}{\theta \cdot R} \frac{\partial C_l}{\partial x} + \frac{q \cdot \lambda}{\theta \cdot R} \frac{\partial^2 C_l}{\partial x^2} \tag{5.19}$$

where R: retardation coefficient [-]

Thus, for the linear isotherm the retardation coefficient is given by:

$$R_{linear} = \frac{\rho_{b\,eff} \cdot K_d}{\theta} + 1 \tag{5.20}$$

For the Langmuir isotherm, it amounts to:

$$R_{Langmuir} = \frac{\rho_{b\,eff} \cdot b \cdot k}{\theta \cdot (1 + k \cdot C_l)^2} + 1 \tag{5.21}$$

Equation (5.19) clearly shows the effects of sorption. The solute transport velocity, which is the coefficient in front of the first derivative of C_l in space is divided by the retardation coefficient. As this parameter is always greater or in case of no sorption equal to one, it effectively leads to a reduction of the transport velocity, thus a retardation.

For the Lehstenbach catchment, laboratory experiments on sulphate sorption behaviour in the topsoil and up to 10 m depth revealed a clear discrepancy between sulphate adsorption and sulphate desorption (Alewell, 1995; Schweisser, 1998). The adsorption isotherm runs flat and large amounts of sulphate can only be adsorbed for high sulphate concentrations in solution. Desorption however takes place only at small concentrations in solution, but then in large quantities (Fig. 5.3). This behaviour is referred to as hysteresis. Based on this, a schematic hysteresis loop is set up in the model. It is only applied for the Lehstenbach catchment. In the case of increasing total sulphate at a given point in space and time, adsorption parameters are chosen for isotherm equilibration. In the case of decreasing total sulphate, desorption parameters are chosen. At the transition from one isotherm to the other, the loop becomes operative. It guarantees the continuity of dissolved sulphate as well as of sorbed sulphate. So, for the transition from adsorption to desorption, sorbed sulphate remains constant

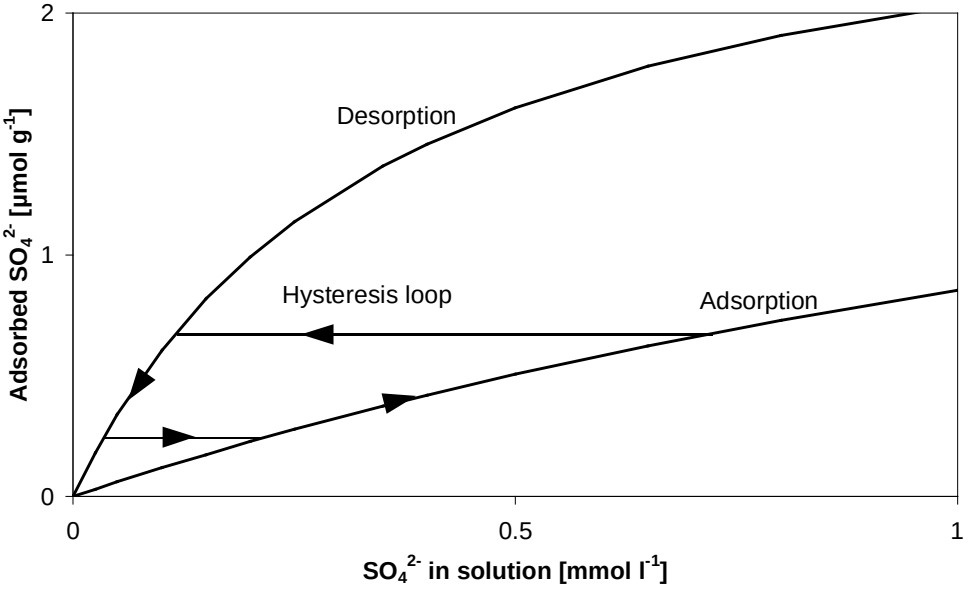

Fig. 5.3 Hysteresis loop of the isotherms. Isotherm curves shown are derived by log-averaging of parameters determined by Schweisser (1998).

until the desorption isotherm is reached. That means that during transition periods the solid phase becomes inactive and as a consequence the solute is not retarded anymore.

With respect to initial conditions, the sulphate inventory of the regolith is set to zero for the pre-industrial time. Thus, bedrock sulphur sources, pre-industrial sulphate depositions, and the influence of the organic sulphur pool on sulphate dynamics are neglected.

The upper boundary condition of the model is given by the annual sulphate flux in precipitation, from which a normalised input concentration arises according to the following equation.

$$Input\ \ flux = q_{soil} \cdot C_{l\ in} \tag{5.22}$$

where $C_{l\,in}$: input sulphate concentration [N L^{-3}]

It is a Dirichlet condition, as the input concentration is given as a function of time. In practice, values are not given continuously, but only at distinct points in time. Interpolation is conducted by means of a linear spline. The lower boundary condition is a Neumann condition, as it specifies the first derivative in space at the lower end of the flowline. This is equal to zero.

$$q \cdot \lambda \frac{\partial C_l}{\partial x} = 0 \tag{5.23}$$

With this, both boundary conditions state that no dispersion is allowed to take place across the boundaries. Sulphate is only convected to and from the system. There is a third boundary in the model. The Darcy velocity as well as the dispersivity change at the transition from the unsaturated zone to the groundwater. The easiest way to model that is by separating the two parts and by treating them each alone. The upper boundary of the groundwater part is then given by the modelled concentration at the lower end of the unsaturated zone part. The only difference from a continuous system is that dispersion is neglected in the transition zone between the unsaturated zone and the groundwater.

5.3 Model Realisation

5.3.1 Numerical Solutions

The convection-dispersion equation (5.17) is solved numerically by a finite differencing scheme. For easier handling it may be rewritten to:

$$\frac{\partial C_{tot}(C_l)}{\partial t} = -q \frac{\partial C_l}{\partial x} + q \cdot \lambda \frac{\partial^2 C_l}{\partial x^2} \tag{5.24}$$

As regards the Langmuir isotherm, C_{tot} within the derivative in time is a non-linear function of C_l. In this case equation (5.24) therefore represents a non-linear parabolic partial differential equation.

The following finite differencing approximations for the derivatives in the partial differential equation are taken from Strikwerda (1997) and Bronstein *et al.* (1999). For the time derivative, the explicit Euler scheme is selected, which is a forward differencing scheme.

$$\left.\frac{\partial C_{tot}(C_l)}{\partial t}\right|_{i,j} = \frac{C_{tot}(C_l)_i^{j+1} - C_{tot}(C_l)_i^{j}}{\Delta t} + O(\Delta t) \tag{5.25}$$

where *i*: space counter [-]

j: time counter [-]

O: error term (Landau symbol)

With respect to the first derivative in space, the Upwind scheme, which is a backward differencing scheme, is applied.

$$\left.\frac{\partial C_l}{\partial x}\right|_{i,j} = \frac{C_{l\,i}^{\,j} - C_{l\,i-1}^{\,j}}{\Delta x} + O(\Delta x) \tag{5.26}$$

Finally, the second derivative in space is expressed by centred differences.

$$\left.\frac{\partial^2 C_l}{\partial x^2}\right|_{i,j} = \frac{C_{l\,i+1}^{\,j} - 2C_{l\,i}^{\,j} + C_{l\,i-1}^{\,j}}{\Delta x^2} + O(\Delta x^2) \tag{5.27}$$

Substitution of the finite differencing approximations given in equation (5.25), (5.26) and (5.27) into the partial differential equation (5.24) leads to the core of the sulphate model: **the finite differencing scheme**.

$$C_{tot}(C_l)_i^{j+1} = \frac{q \cdot \Delta t}{\Delta x}\left((1+\frac{\lambda}{\Delta x})C_{l\,i-1}^{\,j} - (1+2\frac{\lambda}{\Delta x})C_{l\,i}^{\,j} + \frac{\lambda}{\Delta x}C_{l\,i+1}^{\,j}\right) + C_{tot}(C_l)_i^{j} \tag{5.28}$$

Thus, total sulphate at a given point in space *i* and a given point in time *j*+1 arises from quantities at that point in space *i* as well as the two adjacent points *i*+1 and *i*-1 at the precedent point in time *j*. For the boundaries however, adjacent points are not available. Therefore, the scheme needs to be modified, whereby the boundary conditions replace the missing information. In case of the given conditions (Section 5.2.3) the equations for the first and the last point in space become (according to Anlauf & Liu, 1990):

$$C_{tot}(C_l)_1^{j+1} = \frac{q \cdot \Delta t}{\Delta x}\left(C_{l\,in}^{\,j} - (1+\frac{\lambda}{\Delta x})C_{l\,1}^{\,j} + \frac{\lambda}{\Delta x}C_{l\,2}^{\,j}\right) + C_{tot}(C_l)_1^{j} \tag{5.29}$$

$$C_{tot}(C_l)_N^{j+1} = \frac{q \cdot \Delta t}{\Delta x}\left((1+\frac{\lambda}{\Delta x})C_{l\,N-1}^{\,j} - (1+\frac{\lambda}{\Delta x})C_{l\,N}^{\,j}\right) + C_{tot}(C_l)_N^{j} \tag{5.30}$$

where *N*: last point in space [-]

These three equations, the general finite differencing scheme (equation (5.28)) and the boundary schemes (equation (5.29) and (5.30)) may be integrated into one matrix equation. Thereby, quantities occurring at the same point in time are represented as an array of points in space.

$$\{C_{tot}\}^{j+1} = [A]\{C_l\}^{j} + \{C_{tot}\}^{j} \tag{5.31}$$

where $\{C_{tot}\}$: vector of total sulphate

$\{C_l\}$: vector of sulphate concentrations in solution

$[A]$: matrix of coefficients

Until now, only total sulphate at the step in time *j*+1 is known. This, however, consists of adsorbed sulphate and dissolved sulphate (equation (5.12)). Adsorbed sulphate again is a

function of dissolved sulphate (isotherm equations (5.14) and (5.15)). Consequently, total sulphate is basically only a function of dissolved sulphate. For the linear isotherm the concentration of dissolved sulphate is therefore:

$$C_l = \frac{C_{tot}}{\rho_{b\,eff} \cdot K_d + \theta} \tag{5.32}$$

For the Langmuir isotherm the solution is more complicated, as a quadratic equation needs to be solved. The following term gives the demanded concentration.

$$C_l = -\frac{1}{2\theta \cdot k}\Big(-C_{tot} \cdot k + \rho_{b\,eff} \cdot b \cdot k + \theta - \sqrt{{C_{tot}}^2 \cdot k^2 - 2C_{tot} \cdot k^2 \cdot \rho_{b\,eff} \cdot b + 2\theta \cdot k \cdot C_{tot} + {\rho_{b\,eff}}^2 \cdot b^2 \cdot k^2 + 2\rho_{b\,eff} \cdot b \cdot k \cdot \theta + \theta^2}\Big) \tag{5.33}$$

The great advantage of the explicit Euler scheme applied for the time derivative (equation (5.25)) is demonstrated in equation (5.31). In order to calculate quantities at the point in time j+1 the scheme only requires quantities at the point in time j. Therefore, it is possible to calculate concentrations step by step starting at the initial point in time. In contrast, application of an implicit scheme would result in the fact that j+1 would not only appear on the left-hand side of equation (5.31), but also on the right-hand side. In case of the given non-linear partial differential equation, it would then be necessary to solve a non-linear system of equations. This is only possible by iteration methods, which it is refrained from in this approach. However, there is also a disadvantage with the explicit scheme. For stability of the method small timesteps are required. According to Strikwerda (1997) the von Neumann stability analysis reveals the following criterion for the chosen scheme. Thereby, it is simplistically assumed that the retardation coefficient is constant for the transition from the point in time j to j+1 (Marsal, 1976).

$$\Delta t \le \frac{\theta \cdot R \cdot \Delta x}{q\,(2\frac{\lambda}{\Delta x} + 1)} \tag{5.34}$$

During model application this criterion has to be taken into account. A general calculation of the right-hand side term, however, is not possible, as the retardation coefficient in the numerator varies both in space and time. What is known though is that it is always greater or equal to one. Great R values thereby ease the restriction, small ones tighten it. Thus, the calculation is always performed with the smallest value which R takes on and this is one.

The Upwind backward differencing scheme approximates the first derivative in space (equation (5.26)). Compared to central differencing schemes it offers the advantage of having no restriction on resolution in space. However, it is only first order accurate and therefore generates an artificial dispersion term, which is referred to as numerical dispersion (Strikwerda, 1997). The term can be quantified by Taylor expansions (Bronstein *et al.*, 1999), on which finite differencing schemes in general are based. The formulation of equation (5.26) with consideration of the second order error term is given in the following equation.

$$\frac{C_{l\,i}^{\,j} - C_{l\,i-1}^{\,j}}{\Delta x} = \left.\frac{\partial C_l}{\partial x}\right|_{i,j} - \frac{\Delta x}{2}\left.\frac{\partial^2 C_l}{\partial x^2}\right|_{i,j} + O(\Delta x^2) \tag{5.35}$$

It demonstrates that the finite difference actually does not represent the first derivative in space, but the term given on the right-hand side of equation (5.35). Substitution of the first derivative in space in the partial differential equation (5.24) by that term leads to:

$$\frac{\partial C_{tot}(C_l)}{\partial t} = -q\frac{\partial C_l}{\partial x} + q\,(\lambda + \frac{\Delta x}{2})\frac{\partial^2 C_l}{\partial x^2} \tag{5.36}$$

Due to the numerical scheme, the term $\Delta x/2$ is added to the dispersivity λ, which leads to an increase of the dispersion coefficient in front of the second derivative of C_l in space. That numerical dispersion term is taken into consideration during the adjustment of the dispersivity in the model.

The explicit Euler scheme for the time derivative (equation (5.25)) is also only first order accurate. A quantitative estimate of this error in terms of space derivatives however proves to be difficult. For that, the retardation coefficient R would have to be derived in space. This is impossible, as isotherm parameters, which determine R, are generated randomly for every point in space by means of the Monte-Carlo simulation (Section 5.3.2). Generally, it is thus necessary to keep Δt small and therewith to minimise the error or that scheme. A practical estimate of the error at least is given by running the model with different timesteps. This is done in Section 6.3.2.

5.3.2 Monte-Carlo Simulations

Sulphate sorption isotherms of the regolith in the Lehstenbach catchment exhibit a great spatial variability (Jungnickel, 1996; Schweisser, 1998; Manderscheid *et al.*, 2000a; Manderscheid *et al.*, 2000b). Measurements of this study indicate that this is true for the Lysina catchment as well (cf. Section 6.1.2). This variability is taken into account by a Monte-Carlo simulation. For each point of discretisation along a flowline a different set of random isotherm parameters is generated. Thus, it is necessary to assume a suitable distribution function. It needs to be selected according to the statistical properties of measured isotherms, which are investigated in detail in Section 6.3.1. Thereby, the log-normal distribution is chosen to describe the distribution, which amounts to the same as a normal distribution of log-transformed values.

Normally distributed random numbers are generated from equally distributed random numbers. The latter are provided by a random number generator within the standard library of the C++ programming language. A method of von Neumann is applied (Sobol, 1991). It is illustrated in Fig. 5.4. At first, a normal distribution with a given arithmetic mean μ and a given standard deviation σ is taken into consideration. Its mathematical formulation is the following (Bronstein *et al.*, 1999):

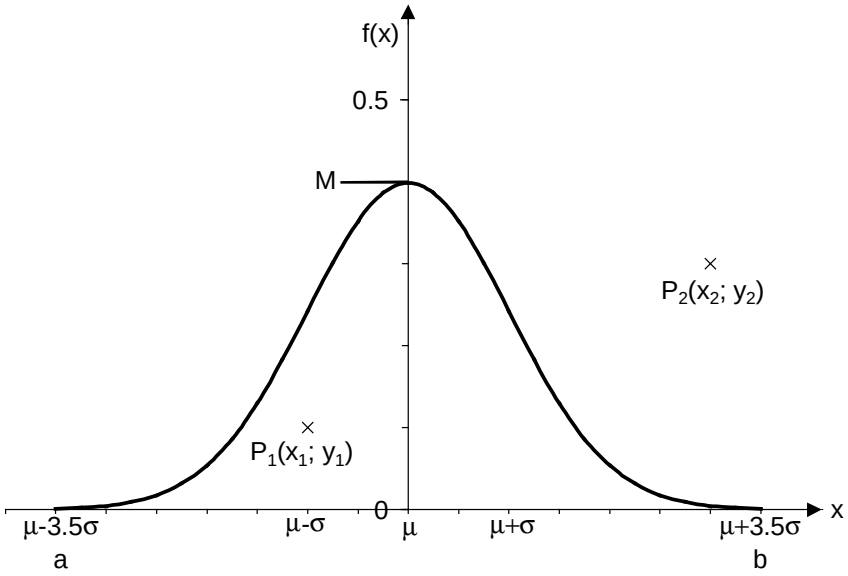

Fig. 5.4 Demonstration of the von Neumann method for the generation of normally distributed random numbers. P_1 is located below the curve and is accepted, P_2 is located above the curve and is thus rejected.

$$f(x) = \frac{1}{\sigma\sqrt{2\pi}} e^{-\frac{1}{2}\left(\frac{x-\mu}{\sigma}\right)^2} \tag{5.37}$$

where $f(x)$: frequency distribution

μ: arithmetic mean

σ: standard deviation

Subsequently, two equally distributed random numbers are generated: x within the interval $[a; b]$ and y within the interval $[0; M]$. In case the point $P(x; y)$ is located below or at the normal distribution curve, the demanded random number is given by x. In case P is located above the curve, the set $(x; y)$ is rejected and a new one is generated. There is only one problematic aspect with this method when applied for the generation of normally distributed random numbers. $[a; b]$ needs to be a finite interval, but the normal distribution is infinite. By selecting an interval of $\mu \pm 3.5\sigma$ for $[a; b]$, it is assured that at least 99.95 % of all cases are included, which is sufficient for the given purpose.

5.3.3 Programming Structure

The source code of the sulphate model as well as that of the analysis of flowpath lengths were written in the C++ programming language. It is an object-oriented language, which means that data as well as the methods which process the data are integrated into objects (Breymann, 1999). This coupling of data with their assigned methods leads to an easy handling and a comprehensible programming style. The code was compiled using the Borland C++ Compiler 5.3. The input and output of data is generally controlled by text files. Input files are prepared in Microsoft Excel 97 and then saved as text files. Output files are constructed in such a way that direct reading by Microsoft Excel 97 is possible.

Tab. 5.1 General data type structuring of the sulphate model. The introduced classes are given with their attributes and methods as well as the objects which are described by these classes.

Class	Attributes	Methods	Objects
Grid Point	- C_{tot}, C_l, and C_a - Soil and flow parameters for the given point - Random realisation for the isotherm parameters	- Finite differencing scheme - Solution of the mass balance	- Every point of the discretisation in space
Parameters	- General parameterisation - Statistical description of isotherm parameters - Discretisation scheme	- Generation of the parameterisation for a given grid point - Generation of a set of random isotherms parameters	- One object containing the parameterisation
Boundary	- Given points of the input scenario	- Spline interpolation	- One object containing the upper boundary condition

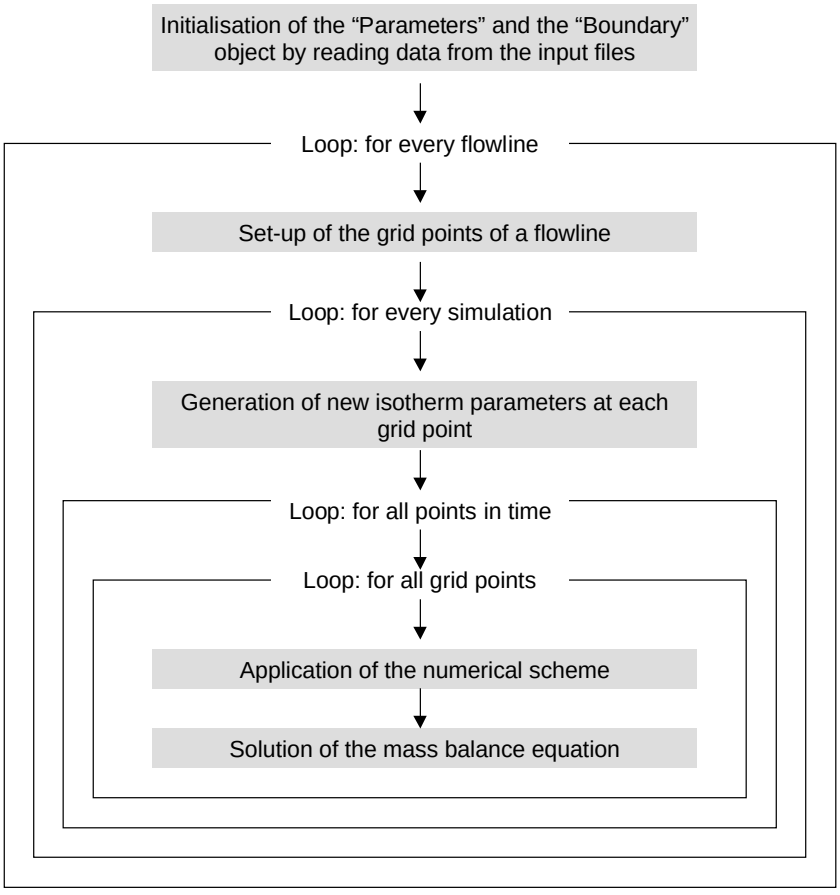

Fig. 5.5 Main features of the programming structure of the sulphate model.

Sulphate Model

In the sulphate model input data are organised by means of two input files. The first one deals with the general parameterisation, in the second one modelled flowlines are specified. Thereby, the length of the unsaturated zone part as well as the length of the groundwater part are already calculated according to the geometry of the basic slope (Section 5.2.1).

Within the programme, data are organised in classes, which describe the objects. There are three of them, whose main features are given in Tab. 5.1. Firstly, there is the "Grid Point" class, of which every point of the discretisation in space along a flowline is a member. Within this, sulphate concentrations as well as the special soil and flow properties that predominate at that point are stored together. Two methods are defined within this class: the finite differencing scheme and the solution of the mass balance equation, which serves to calculate sulphate in solution from total sulphate (cf. Section 5.3.1). Secondly, there is the "Parameters" class, which contains the parameterisation of the model. There is only one object, which is a member of that class. Within this object, general parameters are stored such as the discretisation scheme and the information which is necessary to generate the special parameterisation of a given "Grid Point" object. It is accessed during the construction of a "Grid Point" object and provides the required parameters. Thirdly, there is the "Boundary" class with also only one object. It serves to store the upper boundary condition, which is given by the time series of the normalised sulphate concentration in precipitation (cf. equation (5.22)). As it is only specified at distinct points in time, a method is provided which interpolates the data by means of linear splines.

The structure of the main programme is dominated by nested loops (Fig. 5.5). Starting from inside, the core of the programme is given by the numerical finite differencing scheme and the mass balance equation. A single simulation of one flowline is then the application of these equations to every point in space at every point in time starting with the initial timestep. This is represented by the two inner loops. The second outer loop then allows that such simulations can be executed repeatedly with different sets of random isotherm parameters. Finally, the outer loop offers the possibility to simulate several flowlines successively, which all exhibit different lengths of the unsaturated zone and the groundwater part respectively.

Analysis of Flowpath Lengths

The general features of the analysis of flowpath lengths were already described in Section 5.2.2. With regard to input data, the starting points of the flowpaths need to be specified, which is done by overlying the catchment area with an orthogonal grid of a mesh spacing of 25 m. In addition, contour lines at 5 m intervals, streams, and the watershed boundary need to be given as polylines, i.e. as a set of points with known co-ordinates, which are connected linearly.

Tab. 5.2 General data type structuring and methods of the analysis of flowpath lengths. **A**. Introduced classes with their attributes and the objects which are described by these classes. **B**. Global methods employed.

A

Class	Attributes	Objects
Point	- *X* and *Y* co-ordinate	- Points of the grid overlying the catchment - Every point of a polyline
Polyline	- An array of points	- Every contour line - Every stream as part of the stream system - Watershed boundary

B

Global methods

- Calculation of the distance between two points
- Determination of the intercept of the perpendicular from a given point to a polyline
- Ascertainment of an intersection between a line given by two points and a polyline

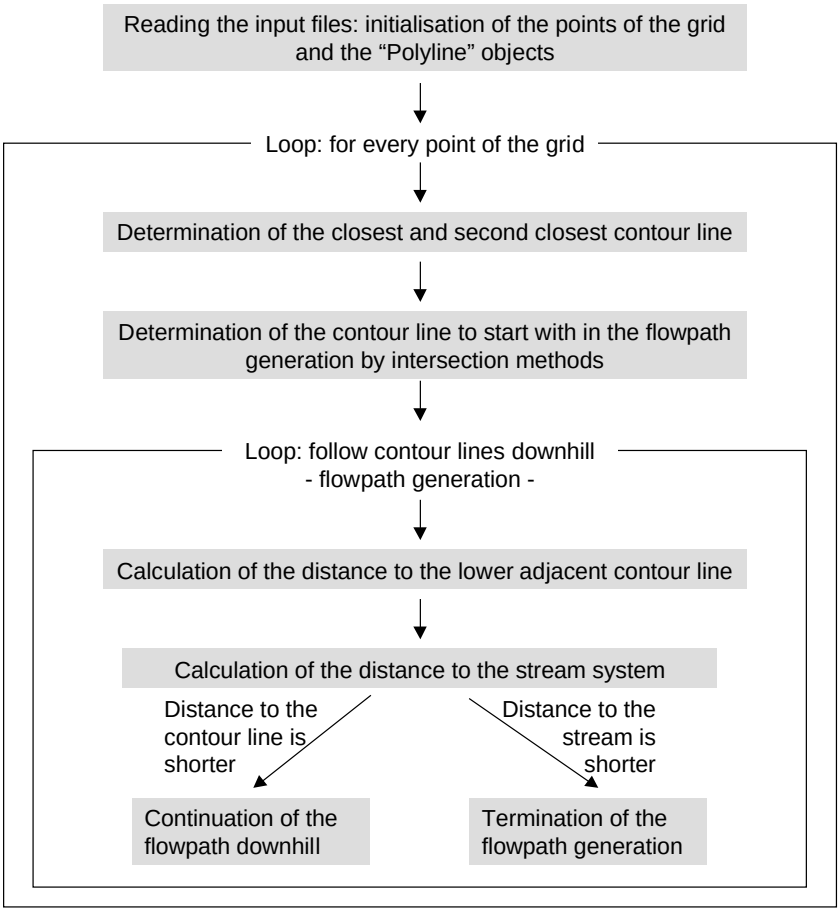

Fig. 5.6 Main features of the programming structure of the analysis of flowpath lengths.

The data type structure of the programme is shown in Tab. 5.2A. There are two classes: the “Point” class, containing the *X* and *Y* co-ordinate of a point and the “Polyline” class, containing an array of points. The contour lines, the stream system, and the watershed boundary are “Polyline” objects, whereas the points of the grid overlying the catchment, which serve as starting points of the flowpaths, are stored as an array of “Points”. Within this programme, methods for data processing do not belong to classes, but are declared globally, which leads to an unrestricted use (Tab. 5.2B). The distance between two points is derived by the Euclidean norm (Bronstein *et al*., 1999). The intercept of the perpendicular from a given point to a polyline is mainly determined by selecting the two closest points of the polyline and dropping the perpendicular to the line connecting these points. Finally, ascertaining if a line of two points intersects a polyline is done by dividing the polyline into single lines. Subsequently, each of them is tested on intersection with the given line by geometrical methods.

The structure of the programme itself is represented in Fig. 5.6. At first, input data are read by the programme. Afterwards, flowpaths in stream direction are generated from each point of the grid overlying the catchment area. Considering such a point, the lower adjacent contour line needs to be determined, as this is the one to start with in the flowpath generation. For this, the closest as well as the second closest contour line are detected. In order to establish if both of these lines are located at the same side of the starting point or at different ones, it is ascertained if the line from the starting point to the second closest contour line is intersected by the closest contour line. Having found the lower adjacent contour line, the flowpath can be derived. This is done by comparing the distance of the starting point to the lower adjacent contour line with that to the closest stream section. If the distance to the contour line is the shorter one, the procedure is repeated by taking the intercept to the contour line as the new starting point. If however the stream is closer than the next contour line, the flowpath terminates at that point of the stream system. Additionally, within each pass of this loop it is ensured that the flowpath does not leave the catchment by examining a possible intersection with the watershed boundary. To minimise calculation effort, a segmentation is carried out. For each step of the algorithm only these points, contour lines, streams, and parts of the watershed boundary are considered which are located within a square of 500 x 500 m in size around the point of interest.

5.4 Parameterisation

5.4.1 Water Flow Parameters

The model presented here minimises the number of required parameters. This section deals with the data sources and methods required to generate numerical estimates for the parameters. These were entirely derived from measurements in the catchments and literature values in the cases where no field data were available. Numbers, however, are not given in this section. This is done in Section 6.3.1. Considering the water flow regime of the basic slope, the required parameters are the following: the mean annual discharge of the catch-

ments, the slope geometry parameters, which are in particular the maximum slope length, the maximum regolith depth, and the mean angle of inclination occurring in the catchments, as well as the total porosity and field capacity in the regolith layer. For this, the Lysina and the Lehstenbach catchment needed to be considered separately. However, no distinction in the parameterisation was made for single sites within the same catchment (apart from different deposition scenarios for the Lysina catchment). Differences in modelled sulphate concentrations were thus entirely based on the different distributions of flowpath lengths at the different locations.

Discharge measurements in the Lehstenbach catchment have been conducted since 1987 (Moritz *et al.*, 1994; Moritz, unpublished data; BITÖK, unpublished data) and in the Lysina catchment since 1989 (Krám *et al.*, 1997; Hruška & Krám, unpublished data). Consequently, mean annual discharge values are based on long time series and are therefore relatively certain.

With respect to the geometry of the slope, values of the maximum slope length and the mean angle of inclination arose from the analysis of flowpath lengths. The maximum slope length was given by the maximum flowpath generated for the catchment and corrected by the angle of inclination. The angle of inclination for a given flowpath resulted from the number of contour lines, which were crossed by the flowpath. The median of these was considered in the parameterisation. Values of the maximum regolith depth were based on geophysical measurements. For the Lehstenbach catchment, Rüdiger (1993a) determined regolith depths at the wells GW 01 to GW 06 by Schlumberger soundings. In the Lysina catchment the regolith depth was determined by seismic methods along three horizontal profiles (Gurtler & Nikl, 1999).

Measurements of total porosity values in the Lehstenbach catchment are only available for the upper meter (Moritz *et al.*, 1994). An estimate of values occurring in deeper layers was obtained by investigating groundwater level fluctuations. The basic idea was adopted from Olsen (1980). Thereby, the increase of groundwater levels resulting from wet periods was taken into consideration. All water entering the system by precipitation, which is throughfall in this case, is assumed to contribute to groundwater recharge. Hence, it fills the effective pore volume of the soil above the old groundwater level, which was previously filled with air. Thus, the effective porosity arises to:

$$\textit{effective porosity [-]} = \frac{\textit{amount of throughfall [m]}}{\textit{change of the groundwater level [m]}} \qquad (5.38)$$

The method presumes a closed system. Thus, only special periods were considered for the calculations: Firstly, they needed to be wet, so that the water table increased. Secondly, they needed to be in winter (between November and February), because in these months evapotranspiration is close to zero. Thirdly, they needed to be shorter than a month, in order to ascertain only a small amount of lateral groundwater discharge. Further, the sulphate model requires total porosity. This method, however, calculates the effective porosity. Therefore,

values needed to be converted. This was done by assuming that the pore volume of the unsaturated zone is already filled with water at field capacity before the increase of the groundwater level. Field capacity thereby is given as a fixed percentage of total porosity. For the method, groundwater level records (Moritz *et al.*, 1994; Moritz, unpublished data, BITÖK, unpublished data) as well as throughfall quantities needed to be specified. The latter were provided by daily bulk precipitation measurements (BITÖK, unpublished data), which were rescaled on throughfall values. Calculations could only be performed for the wells GW 01, GW 03, GW 05, and GW 06, because only for these wells long time series are available with a sufficient number of suitable periods. At GW 02 and GW 04 increases of the groundwater level were difficult to quantify. These wells are located in groundwater discharge zones. Thus, the water table is shallow and increases are limited by the surface. For the Lysina catchment neither porosity measurements nor groundwater level records are available. Thus, literature values had to be considered to provide an estimate for total porosity. Typical values for weathered granite were taken from Morris & Johnson (1967, cit. in Spitz & Moreno, 1996).

Field capacity in the model needed to be specified as a proportion of the total pore volume. Like with total porosity, in the Lehstenbach catchment measurements were only conducted for the upper meter (Moritz *et al.*, 1994). Here, the mean value of C horizons was considered in the parameterisation. Furthermore, this value was adopted for the Lysina catchment, for which no data were available.

5.4.2 Solute Transport Parameters

In order to model solute transport, a number of further parameters has to be specified. These are the sulphate deposition scenario of the last 150 years, which defines the upper boundary of the system, the statistical distribution of isotherm parameters derived from the set of measured parameters for each catchment, an estimate of the proportion of the fine soil fraction, and the specification of common field-scale dispersivity values.

Measurements of bulk precipitation and throughfall are only available since 1988 for the Lehstenbach catchment and since 1991 for the Lysina catchment. An estimated deposition scenario therefore had to be taken into consideration for the time before. For the Lehstenbach catchment, which is nearly entirely forested, the scenario was adopted from Alewell (1995), who referred to general scaling factors implemented in MAGIC (Cosby *et al.*, 1984, cit. in Alewell, 1995). With respect to the time from 1988 to the present, measured annual sulphate fluxes in throughfall were considered in the parameterisation (Moritz *et al.*, 1994; Moritz, unpublished data.). For the Lysina catchment a site specific scenario was developed, which is based on data about coal mining activities in the region (Hruška, unpublished data). It was adopted for this modelling approach and supplemented with measured sulphate fluxes of the period from 1991 to present (Hruška & Krám, unpublished data). Here, different vegetation cover has to be taken into account. The side catchment is completely forested. Similarly, the catchment of the spring Lenka only exhibits a small clearing. However, only 70 % of the main catchment's area is forested, whereas the remaining 30 % were clear-cut in the early 1980s

and are now covered by young forest and grass. Therefore, two scenarios were applied: For the main catchment the scenario of Hruška (unpublished data), who already accounted for the clear-cut, was considered together with a correspondingly weighted mean of sulphate fluxes in bulk precipitation and throughfall for the measuring period. For the side catchment and the catchment of Lenka only throughfall fluxes were considered. Further, the scenario needed to be modified by increased deposition fluxes in the 1980s according to the measured ratio of sulphate in throughfall to sulphate in bulk precipitation.

Isotherm parameters for the Lehstenbach catchment were given by 34 Langmuir sorption isotherms and 44 Langmuir desorption isotherms determined for samples from drilling cores of up to 10 m depth at eight locations in the catchment (Schweisser, 1998). For the Lysina catchment, 18 linear isotherms from drilling cores of up to 4.5 m depth at four locations were determined in this study (cf. Section 4.3.2).

Furthermore, the specification of the proportion of the fine soil fraction is required. For the Lysina catchment data directly resulted from soil sample sieving prior to the laboratory analysis. For the Lehstenbach catchment, no such data were available. In the scope of sulphate modelling however, it is extremely important to have an estimate of that parameter, because only the fine soil fraction effectively contributes to the sorption capacity. Therefore, drilling profiles from the 13 groundwater wells in the catchment (Rüdiger, 1993a; Schweisser, 1998) were considered and each profile was assessed on the proportion of weathered granite with respect to the total drilling depth.

Finally, an estimate of field-scale dispersivity values was taken from literature values presented in a review article of Gelhar *et al*. (1992).

6 Results

6.1 Experimental Findings from the Lysina Catchment

6.1.1 Water Samples

Time series of solute concentration in the Lysina water samples from autumn 2000 are presented for sulphate, calcium, magnesium, aluminium, oxygen, and nitrate (Fig. 6.1). The whole data record is given in Appendix A. Additionally, baseflow and stormflow concentration (median and quartiles) at weir 1 for the hydrologic year 2000 (November 1999 to October 2000) are given as bars for those parameters which are related to discharge. Baseflow refers to dates with a discharge of less than 0.2 mm d^{-1} (25 % percentile). Stormflow is defined by a discharge of more than 3 mm d^{-1} (90 % percentile). Daily discharge at weir 1 is included in the sulphate plot.

Old and new water from the piezometers were sampled alternately (cf. Section 4.2). However, no distinction is made in the plots, as data indicate that this effect is negligible. Only those samples are plotted, which were taken after the piezometers were cleaned (cf. Section 4.1). Concentrations which were below the identification limit are plotted as zero. At GW IV samples could only be taken in November, because the water table was below the piezometer depth before.

Sulphate exhibits a low temporal variability at all sampling sites except for weir 1 (Fig. 6.1A). In contrast, spatial variability is considerable. Values are significantly positively correlated with the electrical conductivity (Spearman correlation coefficient; level of significance < 0.05). Highest concentrations, which are between 0.2 and 0.3 mmol l^{-1}, are observed in the deeper aquifer at the piezometers GW Ia, GW Ib, GW IV, and at the spring Lenka. Concentrations at weir 2 are only slightly less. In contrast, piezometers at the sampling sites GW II and GW III, which represent shallower groundwater in the riparian zone, show markedly lower sulphate concentrations. At GW II sulphate is about 0.1 mmol l^{-1} and at GW III the lowest concentrations are achieved, which range from 0.03 to 0.08 mmol l^{-1}. Sulphate concentrations of the small stream close to GW II are between these of GW II and GW III. The differences between the deep groundwater with high sulphate concentrations and the shallow groundwater with low sulphate concentrations can even be observed on a small scale by comparing the values of the two piezometers of each of the sampling sites GW I, GW II, and GW III. The piezometer with the deeper screen exhibits the higher sulphate concentration for 75 % of the sampling dates at GW I and GW III and for all dates at GW II.

Sulphate concentrations at weir 1, the outlet of the main catchment, show considerable temporal variability. During baseflow conditions, sulphate concentrations are around 0.2 mmol l^{-1}. During stormflow conditions, they are markedly lower and only around

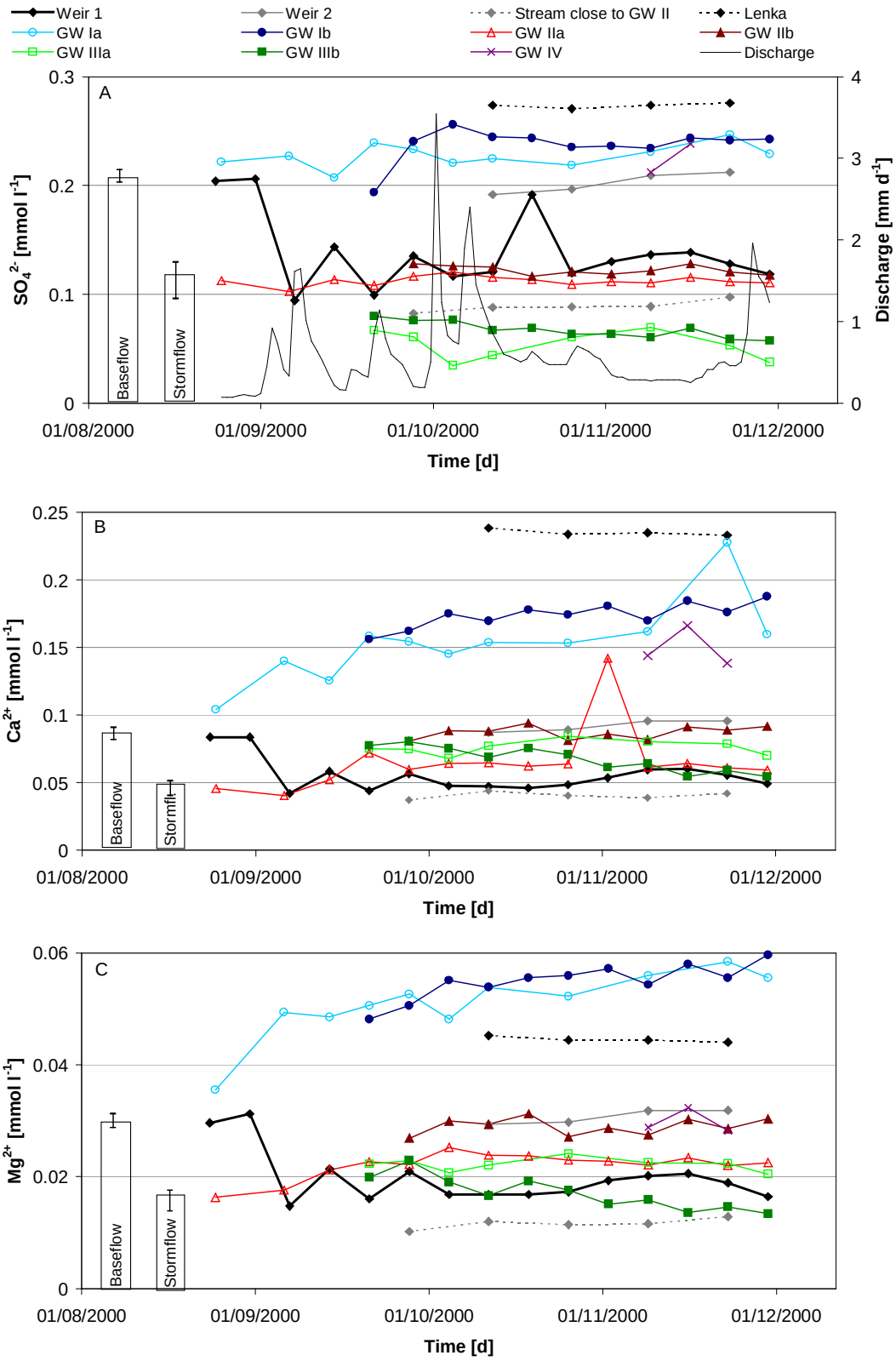

Fig. 6.1 Time series of solute concentration at different sites in the Lysina catchment in autumn 2000 and the median and quartiles of concentrations in baseflow (discharge < 0.2 mm d^{-1}) and stormflow (discharge > 3 mm d^{-1}) at weir 1 for the hydrologic year 2000. See Fig. 3.3 and Tab. 4.1 for location and depth of the piezometers. **A**. Sulphate and discharge. **B**. Calcium. **C.** Magnesium. (chemistry and discharge data from weir 1: Hruška & Krám, unpublished data).

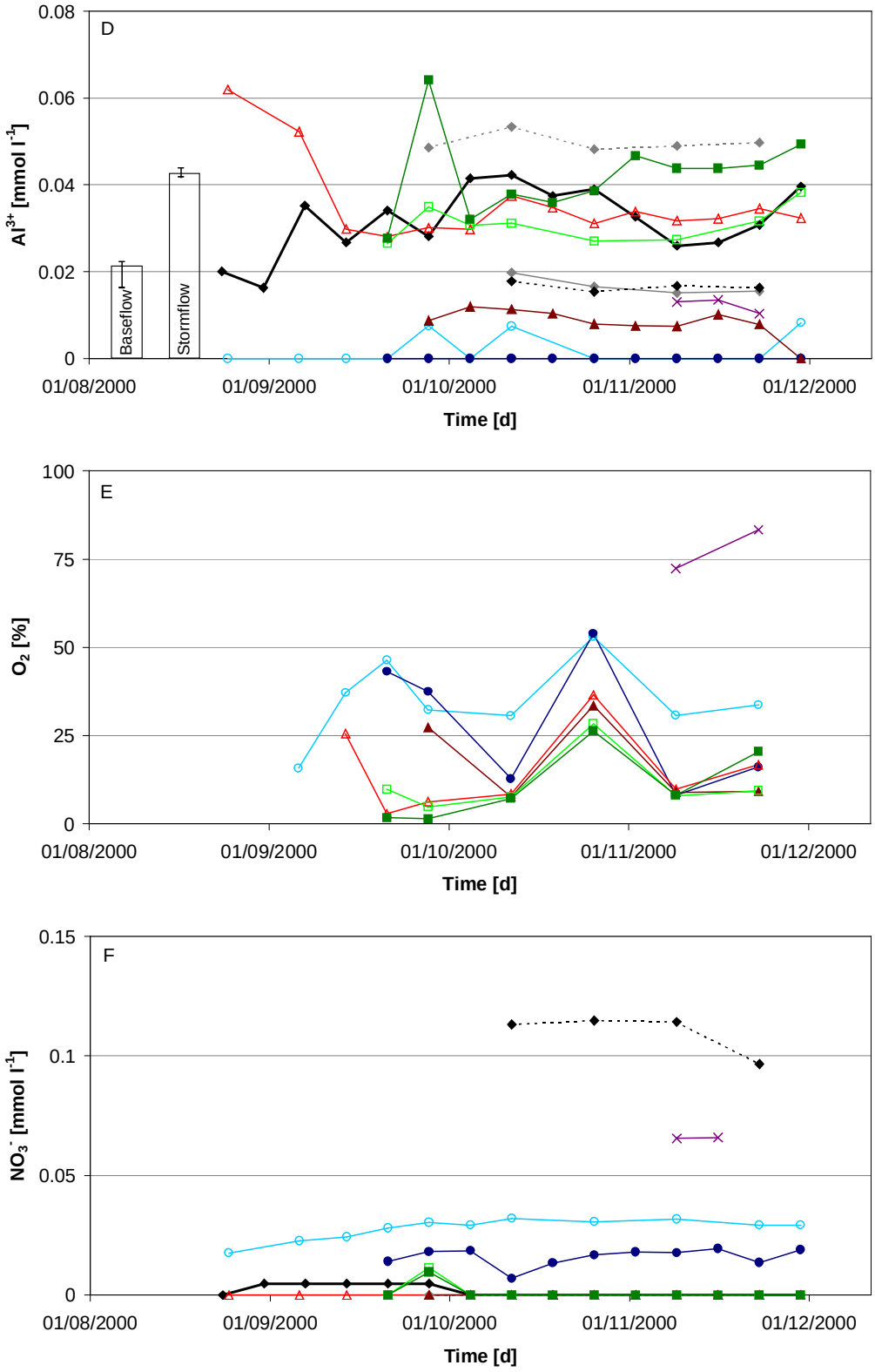

Fig. 6.1 (continued) Time series of solute concentration at different sites in the Lysina catchment in autumn 2000 and the median and quartiles of concentrations in baseflow (discharge < 0.2 mm d^{-1}) and stormflow (discharge > 3 mm d^{-1}) at weir 1 for the hydrologic year 2000. See Fig. 3.3 and Tab. 4.1 for location and depth of the piezometers. **D**. Aluminium. **E**. Oxygen. **F**. Nitrate (chemistry and discharge data from weir 1: Hruška & Krám, unpublished data).

0.1 mmol l^{-1}. This phenomenon was already described in Section 3.2. Groundwater data now indicate, where stormflow and baseflow discharge is generated. Sulphate concentrations in baseflow are in the range of these measured in the deeper aquifer, whereas concentrations in stormflow are similar to these of shallower groundwater such as sampled at the site GW II.

At the beginning of the sampling period in autumn 2000, baseflow conditions prevail. Consequently, sulphate concentrations are high. With the start of the rewetting, discharge increases and thus sulphate concentrations decrease. Minimum concentrations are achieved during single discharge peaks. There is one sampling date in October, where sulphate concentrations are high again. These concentrations cannot be ascribed to baseflow conditions, because discharge peaks on this day as well. However, it is a very small peak compared to the preceding ones. Therefore, it may represent a flushing effect which initiates the mobilisation of deeper groundwater with higher sulphate concentration.

In general, sulphate makes up more than 90 % of total sulphur in the water samples. Only for the piezometers at the site GW III and the small stream close to the site GW II sulphate amounts to less than 90 % of total sulphur. These sites exhibit the highest concentrations of DOC (not shown). Consequently, the residual sulphur may be present in form of organically bound species. The mass ratio of DOC to organic sulphur (total sulphur - inorganic sulphur) is 64 for the piezometer GW IIIa, 69 for GW IIIb, and 46 for the stream close to the site GW II.

The base cations calcium and magnesium show a similar pattern as sulphate (Fig. 6.1B and C). In fact, both are significantly positively correlated with sulphate (Spearman correlation coefficient). High concentrations are observed in the deep groundwater at GW I, GW IV (not for magnesium), and Lenka with 0.1 to 0.25 mmol l^{-1} of calcium and 0.04 to 0.06 mmol l^{-1} of magnesium. Low concentrations of 0.03 to 0.1 mmol l^{-1} for calcium and 0.01 to 0.03 mmol l^{-1} for magnesium occur at the sites GW II and GW III representing the shallower aquifer. Baseflow and stormflow concentrations at weir 1 show the same general tendency as for sulphate with high values during baseflow and low values during stormflow conditions. However, the difference is not as pronounced as for sulphate and baseflow values are considerably lower than those measured in the deeper aquifer. This indicates that baseflow may not only be generated from the deepest groundwater component.

Aluminium exhibits the reverse pattern compared to sulphate and the base cations (Fig. 6.1D). It is significantly negatively correlated with sulphate (Spearman correlation coefficient), whereas the correlation with DOC (not shown) is significantly positive. Aluminium concentrations in the deep groundwater at the sites GW I, GW IV, and Lenka are low with values of less than 0.02 mmol l^{-1}. Concentrations in the shallow groundwater at GW IIa, GW IIIa, and GW IIIb are higher and range from 0.03 to 0.06 mmol l^{-1}. Values measured at weir 1 range from 0.02 to 0.04 mmol l^{-1} and short-term dynamics are reverse compared to sulphate and the base cations. Lower concentrations prevail during baseflow, whereas stormflow is characterised by high aluminium concentrations.

The general trend of low base cation and high aluminium concentrations in the top layers of the aquifer and higher base cation and lower aluminium concentrations in the deeper aquifer is also reflected in the pH of samples. The total range is from 4 to 6.5, and the lowest values are measured in the shallow aquifer at GW IIa, GW IIIa, and GW IIIb (not shown).

During sampling a clearly noticeable rotten smell from the piezometers at the sites GW II and GW III indicated hydrogen sulphide and thus sulphate reduction to occur. Hydrogen sulphide was also detected by the electrode, but only in small quantities. Maximum concentrations measured were 0.45 µmol l^{-1} at GW IIb (cf. Appendix A). Oxygen and nitrate concentrations confirm that reduction processes play a role in the catchment (Fig. 6.1E and F). For oxygen, only the piezometer GW IV exhibits values which are close to saturation. For the sampling sites GW I, GW II, and GW III concentrations are considerably lower with maximum values of 50 % achieved at GW I. Nitrate is similar. High concentrations only prevail in the deep groundwater of GW IV and the spring Lenka. At GW I concentrations are low, but still above the identification limit. At this site nitrite could be measured. Nitrate concentrations at GW II and GW III are below the identification limit.

6.1.2 Soil Samples

The results of the analyses of Lysina soil samples are presented as depth profiles for the parameters sulphate (H_2O extractable (extr.)), total carbon, total sulphur, pH ($CaCl_2$), and pH (H_2O) (Fig. 6.2). Values below the identification limit are plotted as zero. Depth, texture, and colour of the samples are given in Appendix B. At GW IIb a clayey organically rich horizon was sampled in 1 m depth (sample GW IIb1; cf. Appendix B). It exhibits high values of sulphate (H_2O extr.) (1.7 µmol g^{-1}), total carbon (11.1 %), and total sulphur (17.7 µmol g^{-1}). It was refrained from plotting these values, as the remaining patterns would not be visible anymore. Referring to the sample as the "outlier sample" however does not imply that values are unreasonable.

For H_2O extractable sulphate (Fig. 6.2A), values range from 0.05 to 0.4 µmol g^{-1} (without the outlier). Especially the samples from GW Ia and GW IV, where the water table is deep, exhibit a distinct depth gradient. Samples from the boggy part of the catchment do not show such a clear trend. By means of the determined sulphate contents an estimate of the total pool of H_2O extractable sulphate of the regolith layer was derived. With an assumed regolith

Tab. 6.1 Total pool of H_2O extractable sulphate calculated for a 4 m thick regolith layer in the Lysina catchment. Values are derived from the median and the quartiles of measured solid bound sulphate.

	Median	First quartile	Third quartile
SO_4^{2-} (H_2O extr.) [µmol g^{-1}]	0.14	0.08	0.26
SO_4^{2-} (H_2O extr.) pool [kmol ha^{-1}]	6.6	3.7	12.2

depth of 4 m and an effective bulk density of the fine soil fraction of 1.17 g cm^{-3}, which are taken from model parameterisation (cf. Section 5.4 and Section 6.3.1), the mean total sulphate pool arises to 6.6 kmol ha^{-1} (Tab. 6.1).

NaH_2PO_4 extractable sulphate could not be determined. In most cases values were below the identification limit.

The total carbon content (Fig. 6.2B) exhibits a pronounced depth gradient. Values (without the outlier) range from 0.1 mass % for the deep samples to 1 mass % for samples from about 1 m depth. As the existence of carbonates is unlikely for granitic bedrock, values can exclusively be ascribed to organically bound carbon. For total nitrogen values of 0.02 to 0.07 mass % were measured for the bulk of samples and a value of 0.44 mass % for the outlier (not shown).

Total sulphur contents (without the outlier) range from below the identification limit to 3.5 µmol g^{-1} (Fig. 6.2C). The identification limit however is high. For the chosen soil quantities and solution volumes it arises to 0.9 µmol g^{-1}. Some important features can still be observed. In general values decrease with depth. Furthermore, the sample from GW Ib and 4 m depth is interesting (GW Ib7; cf. Appendix B). It is the deepest sample of all. In comparison to all other samples from greater depth of the sites GW I and GW IV, it exhibits a remarkably high total sulphur content. This value can neither be ascribed to sulphate nor to organic matter, as both sulphate and total carbon are low for that sample. Instead, groundwater sampling gives an indication about its origin. For that borehole the piezometer screen is only 20 cm deeper than the position the sample was taken from. In the first groundwater sample increased concentration of iron and manganese (0.06 mmol l^{-1} each; cf. Appendix A) were measured, which point to reduced sulphur minerals, thus metal sulphides. This is in accordance with black mineral phases, which were observed in the drilling core 50 cm above the depth of that sample (GW Ib6; cf. Appendix B).

pH values in $CaCl_2$ are around 4 and pH values in H_2O are between 4.5 and 5.5 (Fig. 6.2D and E). Only the outlier sample shows different values, which are markedly lower compared to the other samples. Generally, highest values are achieved in the deeper part of the profile and lower ones further up.

The ratio of sulphate (H_2O extr.) to total sulphur ranges from 2.2 to 17.3 %. Samples with total sulphur contents below the identification limit were not considered. The C:S ratio varies between 11 and 196. The median is 52.3. Sulphate (H_2O extr.) and total carbon are significantly negatively correlated with depth. pH (H_2O), and pH ($CaCl_2$) are significantly positively correlated with depth (Spearman correlation coefficient). Only total sulphur is not significantly correlated with depth. Thus, except for total sulphur parameters are significantly intercorrelated as well. Further, the texture of samples (Appendix B) and the sulphate content are related. Three out of the four highest sulphate contents are obtained for the three clayey and loamy samples. The sandy samples in general exhibit lower sulphate contents.

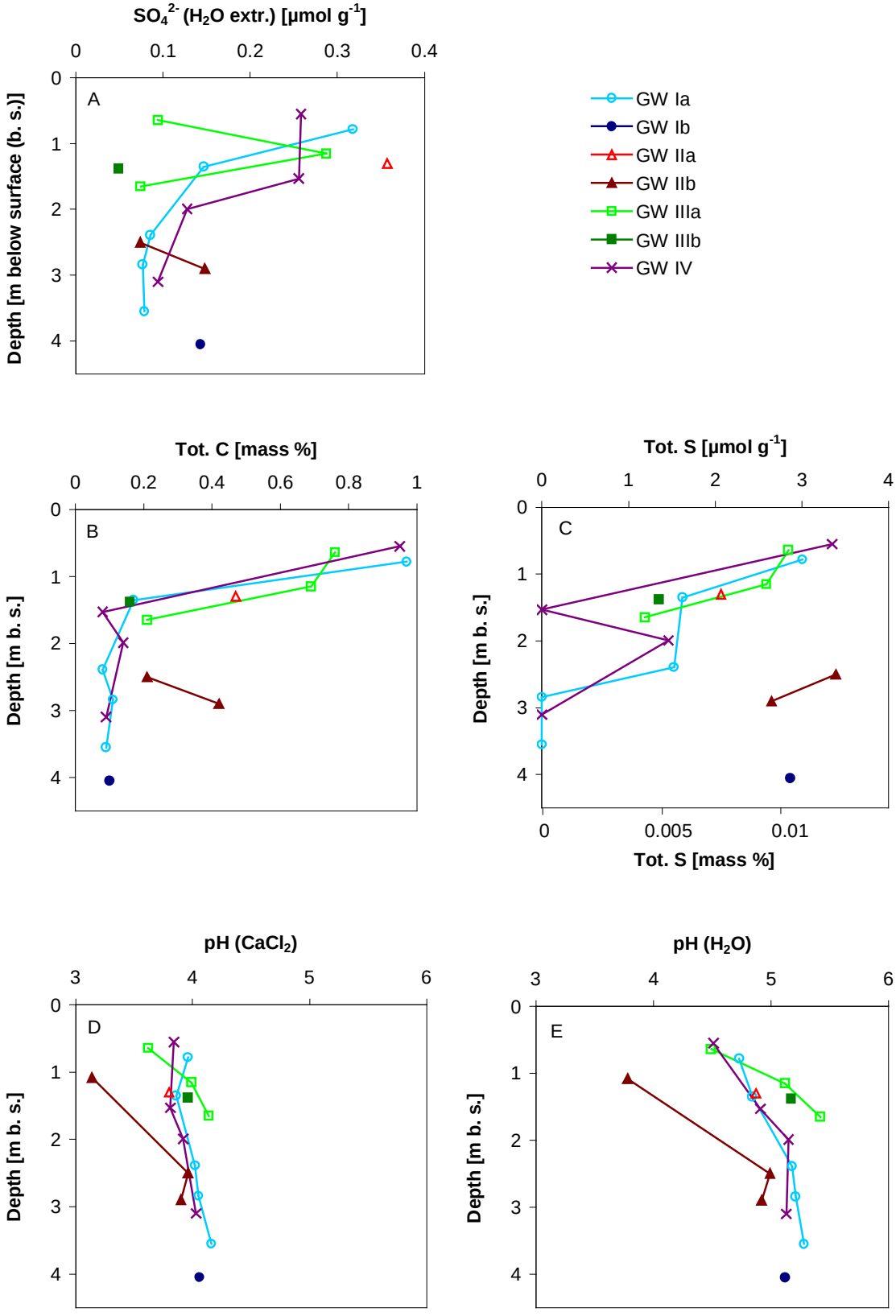

Fig. 6.2 Depth profiles of soil parameters determined for the fine soil fraction (< 5 mm) of samples from the drilling cores the Lysina catchment. The uppermost sample of GW IIb (GW Ib1; cf. Appendix B) is left out in chart A, B, and C. **A**. Sulphate (H_2O extr.). **B.** Total carbon. **C.** Total sulphur. **D**. pH ($CaCl_2$). **E**. pH (H_2O).

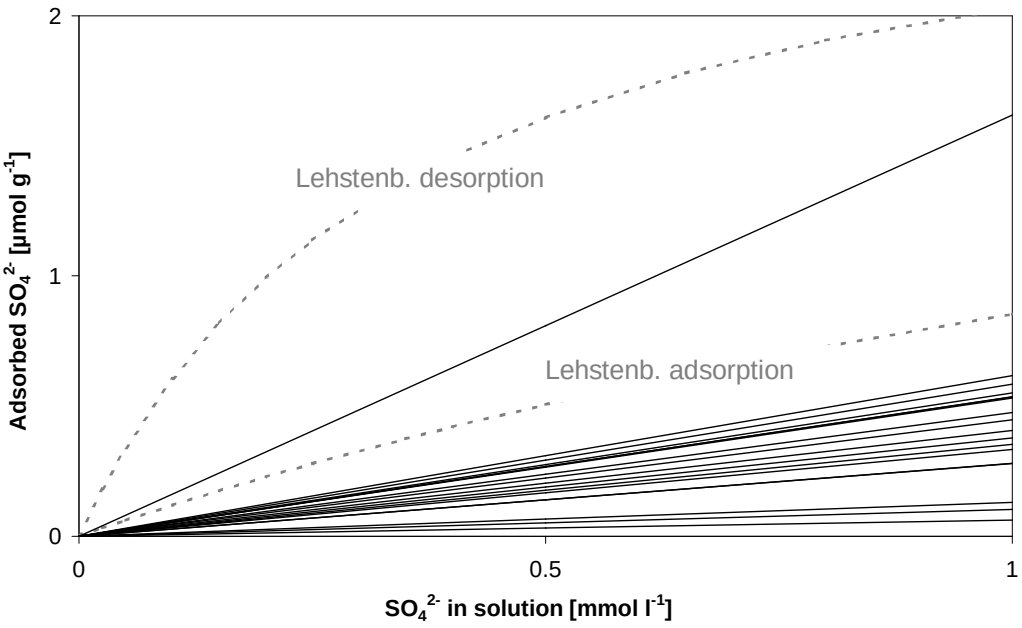

Fig. 6.3 Fitted linear sorption isotherms for the Lysina soil samples (black solid lines) and log-averaged adsorption and desorption Langmuir isotherms from the Lehstenbach catchment (grey dashed line) (Schweisser, 1998).

During sorption experiments, difficulties arose. For the desorption isotherms, sulphate could not be detected anymore in solution after five shaking steps at maximum. Thus, the batch method adopted from Schweisser (1998) proved to be unsuitable for the Lysina soil samples, which is due to the generally low sulphate contents on the solid phase. Since only a few points were available, the Langmuir isotherm fit with the Levenberg-Marquardt algorithm did not lead to reasonable results. An estimate of the sorption behaviour, however, was required for modelling. Thus, linear isotherms were fitted to adsorption and desorption points together for each sample. Adsorption points thereby do not indicate a sorption maximum for the employed solvent concentrations. The slopes of the linear isotherms range from 0.06 to 1.62 ml g^{-1} (Appendix C). Fig. 6.3 illustrates that with one exception curves are clearly flatter than the log-average of Langmuir isotherms Schweisser (1998) determined for the regolith layer in the Lehstenbach catchment. The isotherm slopes (K_d) are significantly positively correlated with sulphate (H_2O extr.) and significantly negatively correlated with pH (H_2O) (Spearman correlation coefficient). A significant difference between the sampling sites is not detected (Kruskal-Wallis test).

For the soil samples from the depth of the piezometer screen, equilibrium sulphate contents were calculated based on the isotherm and the median of measured groundwater sulphate concentrations. Comparison with measured sulphate contents (H_2O extr.) reveals a good agreement for the majority of cases. Only the samples from GW IIa and GW IIIa exhibit too high sulphate contents of 0.36 and 0.29 µmol g^{-1}, which cannot be explained by the determined isotherms.

6.1.3 Groundwater Contour Maps

Groundwater contour maps for the different sampling sites were generated based on the piezometer heads and adjacent stream points (Fig. 6.4). The analysis could not be performed for GW IV, which is not located in the vicinity of a stream.

Maximum groundwater gradients between the piezometers and the adjacent stream are around 8 % (= 4.6°) except for GW IIb (see below). At GW Ia (Fig. 6.4A), groundwater contours run almost perpendicular to the stream. Consequently, at this site groundwater flow occurs parallel to the stream. However, contour lines indicate that groundwater finally discharges to the stream shortly in front of weir 1. The piezometer head of GW Ib is 4 cm lower (median) compared to GW Ia. It therefore belongs to the same aquifer.

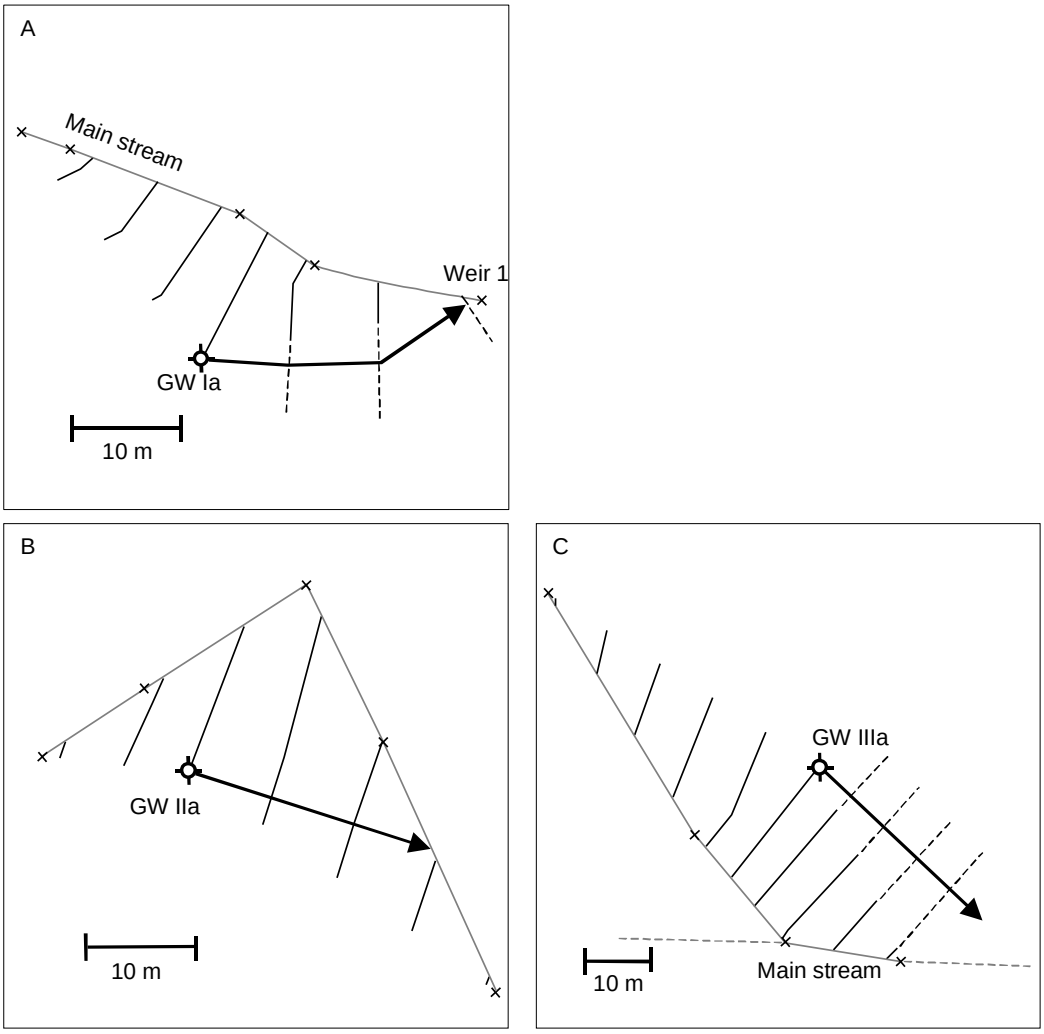

Fig. 6.4 Groundwater contour maps for the vicinity of the piezometers in the Lysina catchment with the interpolated 0.5 m groundwater contours (black solid lines), the linearly extrapolated groundwater contours (black dashed lines), the stream system (grey solid lines) with the surveyed points (x), the hinted further stream system (grey dashed lines), the piezometers (⌖), and the groundwater flowpath from the piezometers (arrow). **A**. GW Ia. **B**. GW IIa **C**. GW IIIa.

At GW II the drainage system is dominated by artificial ditches. Calculated groundwater contours for the piezometer GW IIa (Fig. 6.4B) run diagonal to this system and indicate that water flow occurs out of the left-hand ditch into the right-hand ditch. The piezometer head of GW IIb is 1.09 m lower compared to GW IIa (median). This results in a groundwater gradient of 27 % between the piezometers, whereas the topographic gradient is only 3 %. The deep water table of GW IIb further leads to gradients of up to 14 % to the adjacent ditches. It is unlikely that water flow occurs along such gradients. Hence, it is concluded that groundwater of GW IIb belongs to a second aquifer, which is not directly connected to the one of GW IIa. This is supported by the different chemical composition of the groundwater. For instance, aluminium concentrations at GW IIb are distinctly lower compared to those of GW IIa (Fig. 6.1D). Similarly, iron concentrations at GW IIb (0.008 mmol l^{-1}, median) are only half of values measured at GW IIa (0.017 mmol l^{-1}), and the pH at GW IIb (5.3) is higher than at GW IIa (4.7) (cf. Appendix A).

At site GW III (Fig. 6.4C) the piezometer head (median) differs by only 1.5 cm for the two piezometers. Therefore, they both belong to the same aquifer. At this site the stream system is characterised by a small tributary on the left-hand side of the map, which drains into the main stream of the catchment at the bottom of the map. The interpolated groundwater contours run approximately perpendicular to the tributary. Consequently, groundwater flows parallel to the tributary and discharges into the main stream of the catchment.

The three sites indicate that groundwater discharges to the stream system. Thereby, groundwater flow takes place mainly parallel or at acute angles to the stream. At one piezometer groundwater is not directly connected to the local drainage system, but may occur in a second deeper aquifer.

6.2 Distribution of Flowpath Lengths

The analysis of flowpath lengths was performed for the Lehstenbach catchment with the subcatchments of Köhlerloh and Schlöppnerbrunnen as well as for the Lysina main catchment and side catchment. The lengths of the generated flowpaths are presented as histograms (Fig. 6.5).

In the Lehstenbach catchment (Fig. 6.5A) flowpaths range up to 1550 m. Flowpaths of less than 50 m length account for 14 % of total runoff. For increasing flowpath lengths the proportion to runoff decreases. The distribution for the Köhlerloh subcatchment (Fig. 6.5B) exhibits a very similar shape with maximum lengths of 1300 m. Only the contribution of short flowpaths is slightly less compared to the whole catchment. In the Schlöppnerbrunnen subcatchment (Fig. 6.5C) the distribution is different. Flowpath lengths are approximately equally distributed with each class of 50 m width accounting for about 10 % of total runoff. In contrast to the whole catchment and Köhlerloh, maximum flowpath lengths determined are less than 500 m.

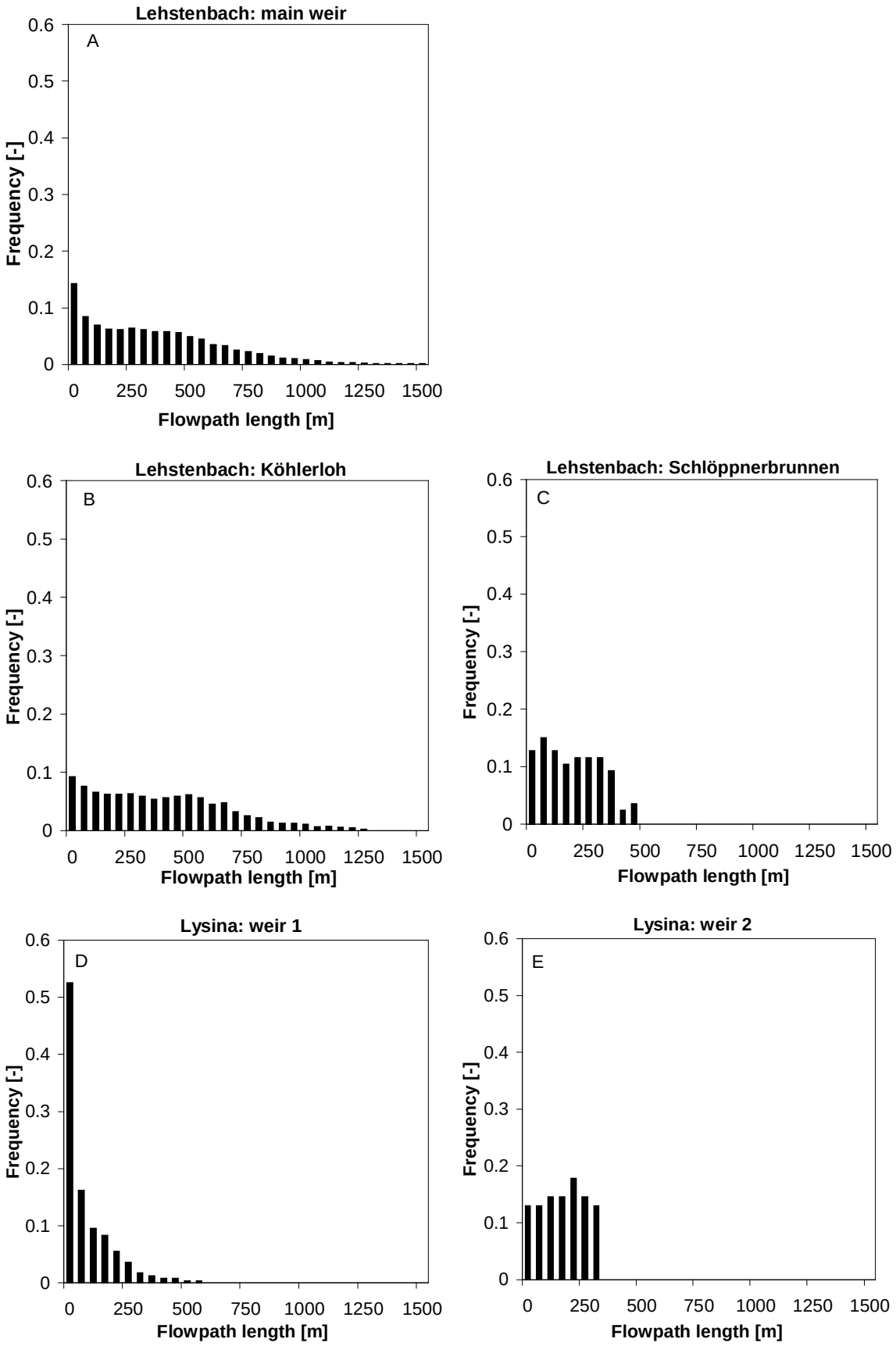

Fig. 6.5 Distribution of flowpath lengths in the catchments and subcatchments of the Lehstenbach and the Lysina catchment. **A**. Lehstenbach main weir. **B**. Köhlerloh. **C**. Schlöppnerbrunnen. **D**. Lysina weir 1. **E**. Lysina weir 2.

Tab. 6.2 Flowpaths for the groundwater wells GW 04 and GW 05 in the Lehstenbach catchment and the Lenka spring in the Lysina catchment.

	Flowpath length [m] from the watershed boundary	**to the stream**
Lehstenbach: GW 04	2028	4
Lehstenbach: GW 05	933	643
Lysina: Lenka	218	0

In the Lysina main catchment with the outlet at weir 1 (Fig. 6.5D) flowpath lengths reach up to 600 m. The distribution is characterised by a strong right skew and 52 % of all flowpaths are shorter than 50 m. Therewith, it reflects the drainage system of ramified ditches in the boggy part of the catchment. The side catchment with the outlet at weir 2 (Fig. 6.5E) exhibits a different distribution, which is similar to the one generated for the Schlöppnerbrunnen subcatchment in the Lehstenbach catchment. Maximum flowpaths achieve a length of 350 m and the shape of the curve is an equal distribution. Each class of 50 m width contributes with approximately 15 % to total runoff.

The flowpaths characterising the modelled groundwater wells GW 04 and GW 05 in the Lehstenbach catchment are represented in Tab. 6.2. Flowpaths to the stream were derived by the programme for the analysis of flowpaths length (cf. Section 5.3.3). Flowpaths from the watershed boundary were read manually from the topographic map. The wells differ in their position at the slope (cf. Fig. 5.1). GW 04 is located in direct vicinity to the stream system. The flowpath length from the watershed boundary is long, whereas the flowpath length to the stream is very short. In contrast, GW 05 is situated in the middle of the slope and flowpath lengths from the watershed boundary and to the stream are in the same range.

At GW 04 the total flowpath from the watershed boundary to the stream is 2032 m. This is distinctly longer than the maximum flowpath lengths generated by the programme for the analysis of flowpath length (cf. Section 5.3.3) when applied to the Lehstenbach catchment (Fig. 6.5A). This is due to the fact that the programme tends to underestimate flowpath lengths, as each generated flowpath terminates at the first stream section appearing in its vicinity.

For the spring Lenka in the Lysina catchment the delimitation of a subcatchment is difficult. The topography indicates diverging flowpaths in its vicinity. Therefore, a distribution of flowpath lengths in the way it is performed for the other catchments and subcatchments cannot be derived for this catchment. It is only possible to determine one flowpath from the watershed boundary. Its length is 218 m (Tab. 6.2). Assuming that water infiltrates uniformly along this flowpath leads to an equal distribution of flowpaths for the Lenka catchment. The maximum length is given by the flowpath lengths from the watershed boundary.

6.3 Model Set-Up

6.3.1 Parameterisation

The data sources and methods of the parameterisation were represented in Section 5.4. This section deals with the numerical values of model parameters. For the standard parameterisation these are represented in Tab. 6.3. Sulphate deposition fluxes are given in Appendix D. In the following, the results of the porosity determination for the Lehstenbach catchment and the statistical analysis of isotherm parameters for both catchments required for the Monte-Carlo simulations are taken into consideration.

The effective porosity values determined from groundwater level fluctuations at the groundwater wells GW 01, GW 03, GW 05, and GW 06 in the Lehstenbach catchment (cf. Section 5.4.1) are represented in the form of a depth profile (Fig. 6.6). For every considered time interval a porosity value arises, which is plotted against the mean groundwater level in that period. Values exhibit a great variability and range from 0.03 to 0.27. The median is 0.09. A significant difference between the sampling sites cannot be observed, since values are highly variable at each site (Kruskal-Wallis-Test). Thus, on the basis of these data a depth

Tab. 6.3 Standard parameterisation. **A**. General parameters. **B**. Statistical description of the distribution of the isotherm parameters.

A

	Lehstenbach catchment	**Lysina catchment**
Mean annual discharge [mm yr^{-1}]	470	432
Maximum slope length [m]	2039	567
Angle of inclination [°]	4.6	4.9
Maximum regolith depth [m]	42	4
Total porosity [-]	-0.607z + 0.797 (topsoil)* 0.17 (deeper regolith)	0.46
Field capacity [prop. of tot. poros.]	0.45	0.45
Sulphate deposition fluxes	→ Appendix D	
Fine soil fraction [prop. of tot.]	0.34	0.82
Dispersivity [m]	1.5 (unsaturated zone) 2.5 (groundwater)	1.5 (unsaturated zone) 2.5 (groundwater)

*z: depth below surface [m]

B

	Arithmetic mean	**Standard deviation**
Lehstenbach catchment		
ln *b* (adsorption and desorption)	1.01	0.75
ln *bk* (adsorption)	0.21	0.57
ln *bk* (desorption)	2.05	1.12
Lysina catchment		
ln K_d	-1.01	0.75

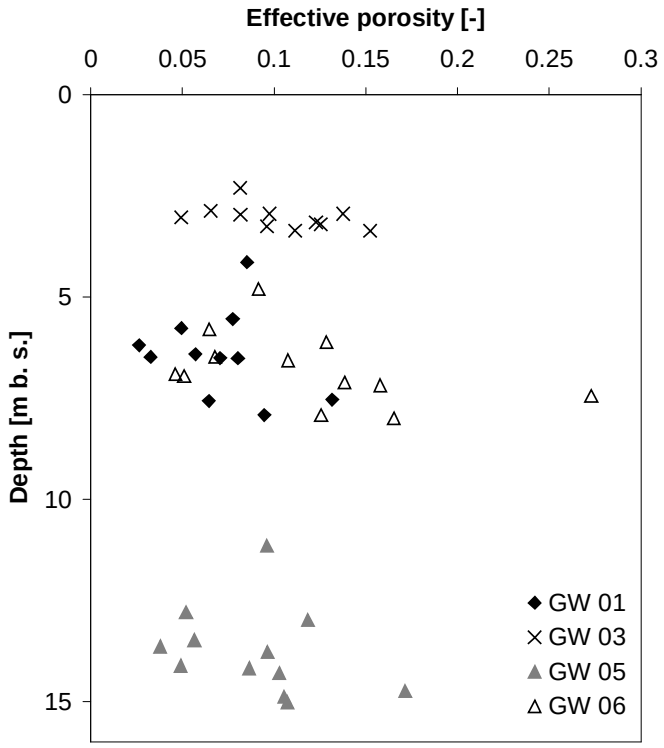

Fig. 6.6 Effective porosity values determined by groundwater level fluctuations at the wells GW 01, GW 03, GW 05, and GW 06 in the Lehstenbach catchment.

gradient cannot be ascertained. Therefore, in the model porosity is assumed to be constant over depth. For the standard parameterisation the median of values was considered and converted into total porosity according to the procedure stated in Section 5.4.1. For the topsoil, where values are distinctly higher, a linearly decreasing function with depth was implemented as given in Tab. 6.3A. It is based on mean total porosity values of the different soil horizons. The depth of transition between the linear function in the topsoil and the constant function in the deeper regolith is given by their point of intersection. It varies for different parameterisations of the porosity. For the standard parameterisation it is 1.03 m.

For the statistical analysis of sorption isotherm parameters the following data sets are given: For the Lehstenbach catchment Langmuir isotherms are available. Mathematically, these are defined by the sorption maximum b and the reciprocal of the half saturation point k. They are given in two sets as adsorption and desorption isotherms (Schweisser, 1998). For the Lysina catchment linear isotherms are available. They do not distinguish between adsorption and desorption and are defined by the distribution coefficient K_d. The objective of the following investigation is to find an appropriate statistical description of the parameter distribution in order to enable the Monte-Carlo simulation. Firstly, the distribution of individual parameters is tested. Secondly, their correlation with depth is examined. Thirdly, the statistical connection between the parameters b and k describing the Langmuir isotherm is analysed. Finally, the differences between adsorption and desorption parameters are investigated. The last two points only apply to the Lehstenbach isotherms.

The distributions of Lehstenbach and Lysina isotherm parameters are characterised by a right skew. They are bounded below by zero, to the other direction, however, they exhibit several outliers. Distributions of this kind may be best described by a log-normal distribution, which cannot take on negative values and shows a tailing to the right. Therefore, data were log-transformed and subsequently tested on normal distribution (Kolmogoroff-Smirnov-Test with Lillefors limits). Considering the 5 % level of significance, the linear coefficient of Lysina isotherms and the *b* and *k* parameters of Lehstenbach adsorption isotherms pass the test and can thus be considered as log-normally distributed. However, Lehstenbach desorption parameters fail. Nevertheless, for the Monte-Carlo simulations a distribution has to be specified. The log-normal distribution was chosen, because other distributions such as the normal distribution or the equal distribution fit even less.

The test on depth dependency of isotherm parameters revealed for only one parameter, the *k* of Lehstenbach adsorption isotherms, a significant correlation (Spearman correlation coefficient). For the remaining parameters no trend was observed. Consequently, no depth gradient was implemented in the model. Instead, the same distributions are valid for the whole regolith.

For Lehstenbach parameters the connection between *b* and *k* (log-transformed values) was tested. The test revealed a highly significant negative correlation with a Pearson coefficient of -0.74 for adsorption parameters and -0.48 for desorption parameters. Instead of *b* and *k* however, the Langmuir isotherm may also be described by the sorption maximum *b* and its slope at the origin, which is given by:

$$s_0 = b \cdot k \tag{6.1}$$

where s_0: slope at the origin of the Langmuir isotherm curve

Expression of *k* in the Langmuir equation (5.15) in terms of *b* and s_0 leads to the following modified Langmuir isotherm equation.

$$C_a(C_l) = \frac{s_0 \cdot C_l}{1 + \frac{s_0}{b} C_l} \tag{6.2}$$

s_0 is assumed to be log-normally distributed, even if the Kolmogoroff-Smirnov-Test with Lillefors limits is again only passed for adsorption parameters. The correlation between *b* and s_0 (log-transformed values) is not significant anymore for either adsorption or desorption (Pearson correlation coefficient). Thus, the Langmuir isotherm function is described by two independent parameters, which can be generated each alone in the Monte-Carlo simulations.

The differences between adsorption and desorption parameters for the Lehstenbach isotherms were tested using a T-Test on connected samples. Between the sorption maximums *b* (log-transformed values) for adsorption and desorption no significant difference was ascertained. The initial slopes s_0 (log-transformed values) however, exhibit significantly lower values for adsorption isotherms than for desorption isotherms. This reflects the hysteresis effect (cf. Fig. 5.3). Sulphate is adsorbed in large quantities for high concentrations in solution.

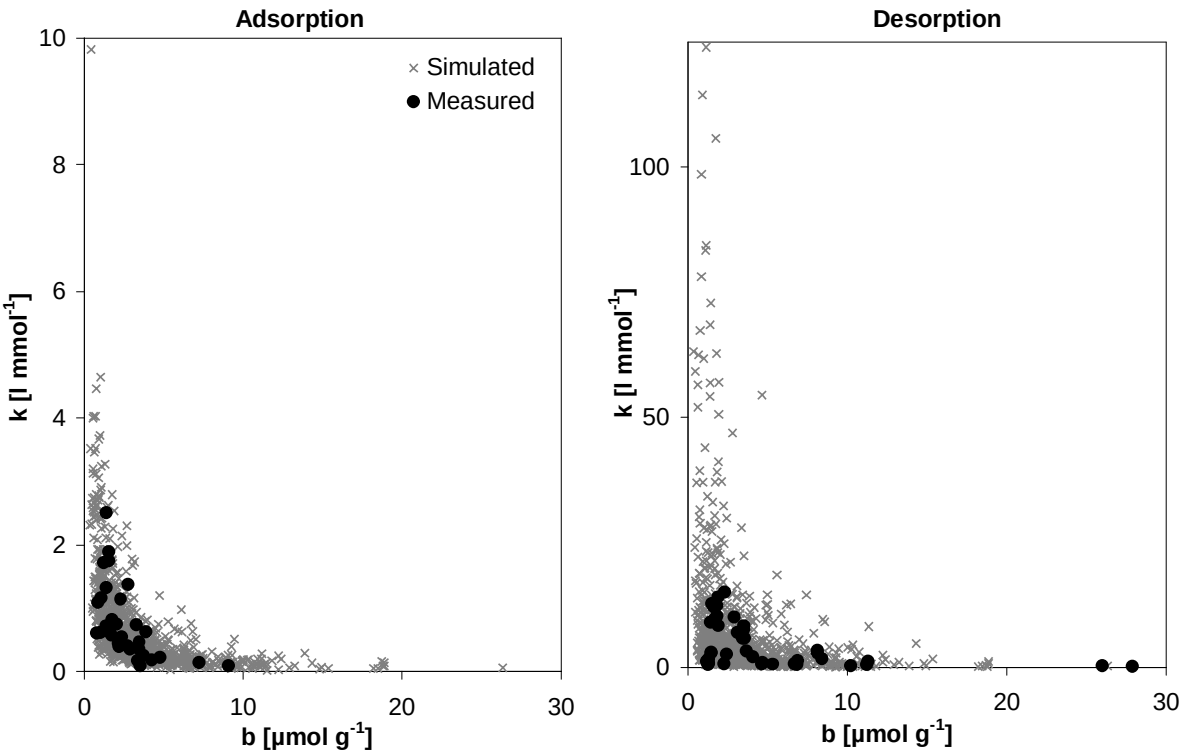

Fig. 6.7 Comparison of measured adsorption and desorption isotherm parameters for the Lehstenbach catchment (Schweisser, 1998) with 1000 simulated parameters each.

Thus, the initial slope of the adsorption isotherm is small. In contrast, large scale desorption takes place only at low concentrations in solution. The initial slope of the desorption isotherm is therefore great.

Based on these investigations, the distributions of isotherm parameters for the Monte-Carlo simulations are given by the arithmetic mean and the standard deviation of log-transformed parameters (Tab. 6.3B). The linear isotherms for the Lysina catchment are characterised by the coefficient K_d. Lehstenbach isotherms are described by the sorption maximum b and the initial slope s_0 (= $b \cdot k$). The sorption maximum is the same for adsorption and desorption. For the initial slope different distributions are specified with respect to adsorption and desorption. Consequently, the sorption behaviour of a point in space is characterised by the Monte-Carlo realisations of three parameters: one sorption maximum and two different initial slopes, which account for the hysteresis.

For the Lehstenbach catchment, adsorption and desorption parameters of 1000 random simulations are compared with the source data of the distribution, the experimental isotherm parameters of Schweisser (1998) (Fig. 6.7). For adsorption parameters, the agreement is good. For desorption parameters as well, the experimental distribution is well described by the simulation. However, in some cases the simulation tends to overestimate k values for small b values, but this error is accepted.

6.3.2 Scheme of Discretisation and Numerical Dispersion

Due to the numerical scheme applied, there are restrictions on discretisation in space as well as in time. Firstly, the minimisation of numerical dispersion requires the choice of a small Δx (equation (5.36)). Secondly, in order to meet the stability criterion of the scheme a fine discretisation in space necessarily leads to a fine discretisation in time (equation (5.34)). However, discretisation cannot be infinitely fine, as it is associated with an immense increase of the calculation effort.

On the basis of these considerations, the following standard scheme of discretisation was applied:

$\Delta t = 0.01$ yrs

Δx (unsaturated zone) = 0.5 m

Δx (groundwater) = 5 m

Different step widths are chosen for the unsaturated zone and the groundwater. For the groundwater Δx was selected, so that the numerical dispersivity caused by the discretisation in space is in the range of field-scale dispersivity values. For the unsaturated zone Δx was chosen to be smaller, as the overall length of that part of a flowline is only short (cf. Fig. 5.1). Additionally, a small Δx allows a better simulation of depths profiles such as the one given for the porosity in the Lehstenbach catchment (cf. Section 6.3.1). According to the stability criterion then (equation (5.34)) the greatest dispersivity value to be chosen is 1.5 m for the given resolution in time.

In the following, the effects of a modified scheme of discretisation on model results are investigated. For both catchments a flowpath of 500 m length was modelled with the standard parameterisation. In each case, 10 simulations with different random isotherm parameters were carried out. Different schemes of discretisation in space and time were tested, and one parameter was always modified with respect to the standard scheme of discretisation. In order to compare the different results a full record of the output curve was required. Due to retardation processes however, the concentration maximum is not always achieved at present. Therefore, for this purpose the model period was extended by 100 years. Sulphate deposition fluxes for the future were set to zero.

The results of this investigation are summarised in Tab. 6.4. The main characteristics of sulphate concentration in solution in model output time series are given in the form of numerical values (cf. Fig. 6.8). These are the maximum concentration achieved during the simulation, the year in which this concentration is achieved as well as the year in which concentrations first exceed a limit of 10^{-3} mmol l^{-1}. The numbers were determined for the 10 simulations of each modification and the maximum and the minimum of determined values are shown in the table.

For both catchments, differences in model results between the different schemes of discretisation are small and values differ only slightly from those of the standard scheme of

Tab. 6.4 Effects of the scheme of discretisation on model results. The main characteristics of modelled time series of dissolved sulphate are shown for a flowpath of 500 m length and 10 simulations each. **A**. Lehstenbach catchment. **B**. Lysina catchment.

A

Lehstenbach catchment	**Range of max. conc. [mmol l^{-1}]**	**Time range of max. conc. [yrs]**	**Time range of first increase [yrs]***
Standard	0.321 - 0.366	1995 - 2000	1891 - 1897
Δx = 1.5 m	0.320 - 0.364	1995 - 1998	1891 - 1897
Δx = 100 m	0.293 - 0.352	1994 - 1999	1882 - 1888
Δt = 0.001 yrs	0.328 - 0.364	1996 - 1999	1890 - 1898
Δt = 0.0001 yrs	0.338 - 0.369	1995 - 1999	1892 - 1895

B

Lysina catchment	**Range of max. conc. [mmol l^{-1}]**	**Time range of max. conc. [yrs]**	**Time range of first increase [yrs]***
Standard	0.284 - 0.293	1993 - 1996	1853 - 1856
Δx = 1.5 m	0.276 - 0.294	1992 - 1997	1854 - 1856
Δx = 100 m	0.267 - 0.289	1991 - 1998	1851 - 1856
Δt = 0.001 yrs	0.282 - 0.293	1993 - 1996	1854 - 1856
Δt = 0.0001 yrs	0.269 - 0.295	1991 - 1999	1853 - 1858

* first exceeding 10^{-3} mmol l^{-1}

discretisation. This is also expressed by a further investigation: The maximum deviation between the standard discretisation and a modified one was calculated from the medians of simulations. For all cases this difference is smaller than the range between maximum and minimum value of simulations of the standard discretisation at this point in time (cf. Fig. 6.8). This shows that the variation of model output due to random sorption isotherms is generally greater than the one associated with the modification of the scheme of discretisation.

Only in one case a slight difference is observed. This is for the Lehstenbach catchment and a great Δx of 100 m. With 0.29 to 0.35 mmol l^{-1} the maximum concentration is lower compared to the standard, which exhibits maximum concentrations of 0.32 to 0.37 mmol l^{-1} (Tab. 6.4). In addition, for that Δx the first increase of sulphate concentrations is between 1882 and 1888, which is early compared to 1891 to 1897 for the standard scheme. Thus, the curve is flatter and wider, which is clearly due to numerical dispersion. With respect to the modification of Δt, such features cannot be observed.

Generally, the alteration of the scheme of discretisation has only small effects on model results within the given limits. Hence, the chosen scheme is considered to be appropriate.

6.3.3 Sensitivity Analysis

Model sensitivity was tested with regard to the parameters maximum regolith depth, total porosity, field capacity, proportion of the fine soil fraction, and dispersivity. By analogy with the previous section a flowpath of 500 m length was modelled for each parameterisation. 10 simulations with different random isotherm parameters were always carried out. The model period was again extended by 100 years. In each case, only one parameter was modified with respect to the standard parameterisation.

The results are given in the way of the main characteristics of output concentrations of sulphate in solution (Tab. 6.5): the maximum concentration achieved during the simulation, the year in which this concentration is achieved, the year in which concentrations first exceed a limit of 10^{-3} mmol l^{-1} as well as the maximum deviation between the results of the standard parameterisation and the modified one. This value results from the comparison of the medians of time series for the 10 simulations each and it is only represented in the table if it is greater than the range of values (maximum - minimum) taken on in the standard parameterisation at this point in time. Fig. 6.8 illustrates these characteristics by means of the parameterisation, which exhibits the greatest deviation from the standard.

For the Lehstenbach catchment (Tab. 6.5A), the most crucial parameters are the maximum regolith depth and the proportion of the fine soil fraction. Their variation leads to a substantial change of the velocity of sulphate transport. For a maximum regolith depth of 35 m sulphate concentration peaks between 1993 and 1995, whereas for a depth of 50 m the peak is only between 1998 and 2003. This pattern is also reflected in a later initial increase of sulphate concentrations in the latter case. For the proportion of the fine soil fraction, the effects

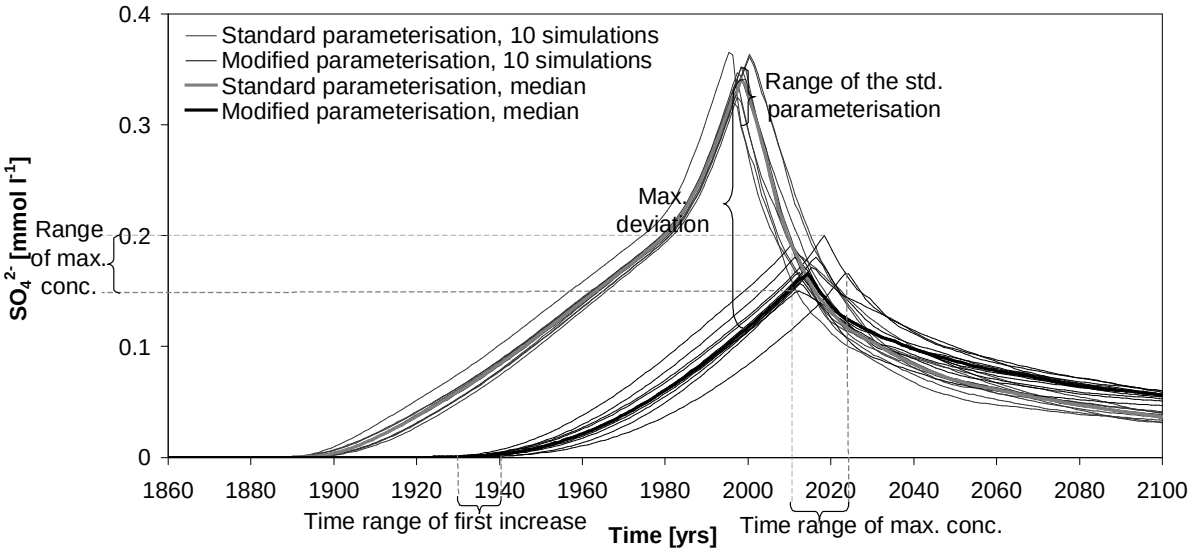

Fig. 6.8 Comparison of model results for the standard parameterisation and a modified one (fine soil fraction 0.79) for a 500 m flowpath in the Lehstenbach catchment. The characteristics by which the different parameterisations are described are included in the chart.

Tab. 6.5 Sensitivity analysis. The main characteristics of modelled time series of dissolved sulphate are shown for a flowpath of 500 m length and 10 simulations each. **A**. Lehstenbach catchment. **B**. Lysina catchment.

A

Lehstenbach catchment	**Range of max. conc. [mmol l^{-1}]**	**Time range of max. conc. [yrs]**	**Time range of first increase [yrs]***	**Max. deviation from the stand. [mmol l^{-1}]****
Standard	0.321 - 0.366	1995 - 2000	1891 - 1897	
Maximum regolith depth [m]				
35	**0.365 - 0.395**	**1993 - 1995**	**1884 - 1890**	**0.073**
50	**0.292 - 0.333**	**1998 - 2003**	**1897 - 1904**	**0.058**
Total porosity [-] (lower part)				
0.12	0.298 - 0.351	1994 - 1999	1892 - 1895	
0.22	0.331 - 0.371	1997 - 2000	1891 - 1898	
Field capac. [prop. of tot. poros.]				
0.3	0.315 - 0.356	1996 - 1999	1892 - 1896	
0.6	0.327 - 0.363	1997 - 1999	1893 - 1897	
Fine soil fraction [prop. of tot.]				
0.29	**0.350 - 0.399**	**1995 - 1999**	**1887 - 1895**	
0.79	**0.150 - 0.200**	**2010 - 2023**	**1929 - 1940**	**0.229**
Dispersivity [m]				
200	0.297 - 0.341	1993 - 1999	1877 - 1884	

B

Lysina catchment	**Range of max. conc. [mmol l^{-1}]**	**Time range of max. conc. [yrs]**	**Time range of first increase [yrs]***	**Max. deviation from the stand. [mmol l^{-1}]****
Standard	0.284 - 0.293	1993 - 1996	1853 - 1856	
Maximum regolith depth [m]				
3	**0.289 - 0.298**	**1989 - 1992**	**1850 - 1852**	**0.075**
5	**0.269 - 0.292**	**1996 - 1999**	**1857 - 1860**	**0.067**
Total porosity [-]				
0.34	0.275 - 0.295	1993 - 1995	1853 - 1857	
0.57	0.287 - 0.294	1993 - 1995	1854 - 1855	
Field capac. [prop. of tot. poros.]				
0.3	0.285 - 0.297	1992 - 1996	1853 - 1856	
0.6	0.279 - 0.294	1993 - 1996	1854 - 1856	
Fine soil fraction [prop. of tot.]				
0.68	**0.279 - 0.297**	**1991 - 1994**	**1852 - 1854**	
0.93	**0.270 - 0.290**	**1995 - 1997**	**1855 - 1858**	
Dispersivity [m]				
200	0.269 - 0.281	1991 - 1993	1851 - 1853	

*first exceeding 10^{-3} mmol l^{-1}

**comparing the medians of simulations; values are only given if they are greater than the range of the standard parameterisation at the same point in time

are even more pronounced. For a value of 0.29 sulphate concentrations peak between 1995 and 1999. For a value of 0.79 however, they do not peak until between 2010 and 2023. Maximum concentrations vary greatly as well. For the former they range from 0.35 to 0.40 mmol l^{-1}. The latter only exhibits maximum values between 0.15 and 0.20 mmol l^{-1}. In addition, these parameterisations result in a clear deviation from the standard. Shallower regolith depths and smaller fractions of the fine soil thereby accelerate sulphate transport, deeper regolith depths and greater fractions of the fine soil retard transport.

This is in agreement with the theory, according to which a decreased regolith depth leads to an increased Darcy velocity in the groundwater (equation (5.4)), which again results in an enhanced sulphate transport (equation (5.19)). Furthermore, the decreased regolith depth shortens the length of the unsaturated zone for a given flowpath (cf. Fig. 5.1), which further reduces sulphate residence times. Decreased fractions of the fine soil lead to a decreased effective bulk density (equation (5.13)) and further to a decreased retardation coefficient (equation (5.20) and (5.21)), which again enhances sulphate transport.

A variation of the total porosity and the field capacity leads to small changes of maximum sulphate concentrations. However, no effect on retardation can be observed. The dispersivity value of 200 m also only leads to minor changes by flattening (reduced maximum concentrations) and widening (earlier initial increase) the curve.

The results of the sensitivity analysis for the Lysina catchment (Tab. 6.5B) show the same pattern, even if the effects are less pronounced. The parameters maximum regolith depth and fine soil fraction alter the extent of the delay, whereas here the maximum regolith depth exhibits the greater effects. Total porosity and field capacity have a minor influence on model results. Finally, increased dispersivity values result in slightly decreased maximum sulphate concentrations and an earlier initial increase.

In summary, the model shows the greatest sensitivity with respect to the maximum regolith depth and the proportion of the fine soil fraction, whereas the parameters total porosity and field capacity do not lead to considerable alterations. The effects of enhanced dispersivity values are visible but small considering the fact that with 200 m an unrealistically high value was chosen.

6.3.4 Sulphate Adsorption, Desorption, and Hysteresis

For the Lehstenbach catchment the discrepancy between sulphate adsorption and desorption isotherms is taken into account in the model by introducing a hysteresis loop (cf. Fig. 5.3). Fig. 6.9 illustrates the effects of hysteresis on model results. For this, a 500 m flowpath was modelled with adsorption isotherms, desorption isotherms, and the combination of both given by the hysteresis loop. The standard parameterisation was applied and 10 simulations with different sets of isotherm parameters were carried out in each case. The simulation period was extended to the year 2100. Sulphate deposition fluxes for the future were set to zero.

For the adsorption isotherms, sulphate concentrations first increase around the year 1890. Maximum concentrations are achieved between 2000 and 2020. Desorption isotherms

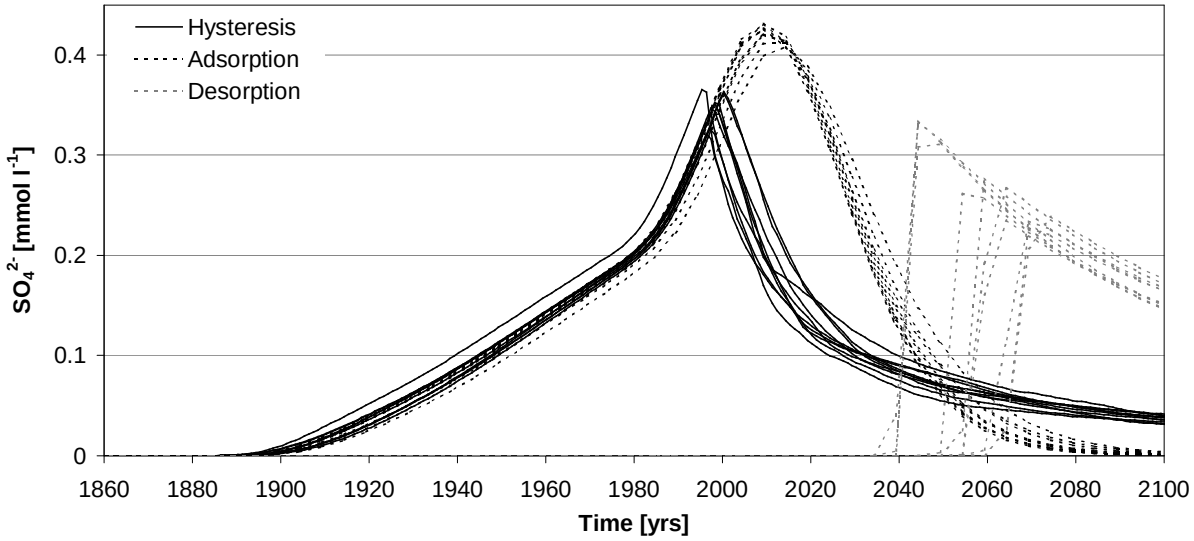

Fig. 6.9 Hysteresis effects. A 500 m flowpath for the Lehstenbach catchment and standard parameterisation is modelled with adsorption isotherms, desorption isotherms, and the hysteresis.

lead to completely different results. The first increase takes place between 2040 and 2060. It is very steep and sulphate concentrations peak only approximately 5 to 10 years later. For the hysteresis, the increase of sulphate concentrations is the same as for the adsorption isotherms. However, values do not achieve the same peak concentrations. The decrease sets in earlier. A further difference is given by the long tailing which is modelled with the hysteresis, but not with the adsorption isotherms.

6.4 Model Application

6.4.1 Lehstenbach Catchment

Modelling was performed using three different parameterisations. According to the results of the sensitivity analysis (cf. Section 6.3.3), the regolith depth and the proportion of the fine soil fraction were varied. As they both influence the delay of sulphate transport in a strictly monotonic way for a given flowpath length, they could be combined in such a way that maximum or minimum delay was achieved. Thus, parameterisation “standard” refers to the standard parameterisation represented in Tab. 6.3. For the parameterisation “fast” the regolith depth was set to 35 m and the proportion of the fine soil fraction to 0.29, and for the parameterisation “slow” the regolith depth was set to 50 m and the proportion of the fine soil fraction to 0.79. By means of these extreme parameterisations an estimate of the uncertainty of the results is given. In each case 10 simulations with different sets of random isotherm parameters were performed. For comparison, measured time series (Moritz *et al.*, 1994; Moritz, unpublished data; BITÖK, unpublished data) are included in the figures.

Simulated mean sulphate concentrations in stream water are represented in Fig. 6.10. The 10 simulations for each parameterisation exhibit only small differences, which indicates

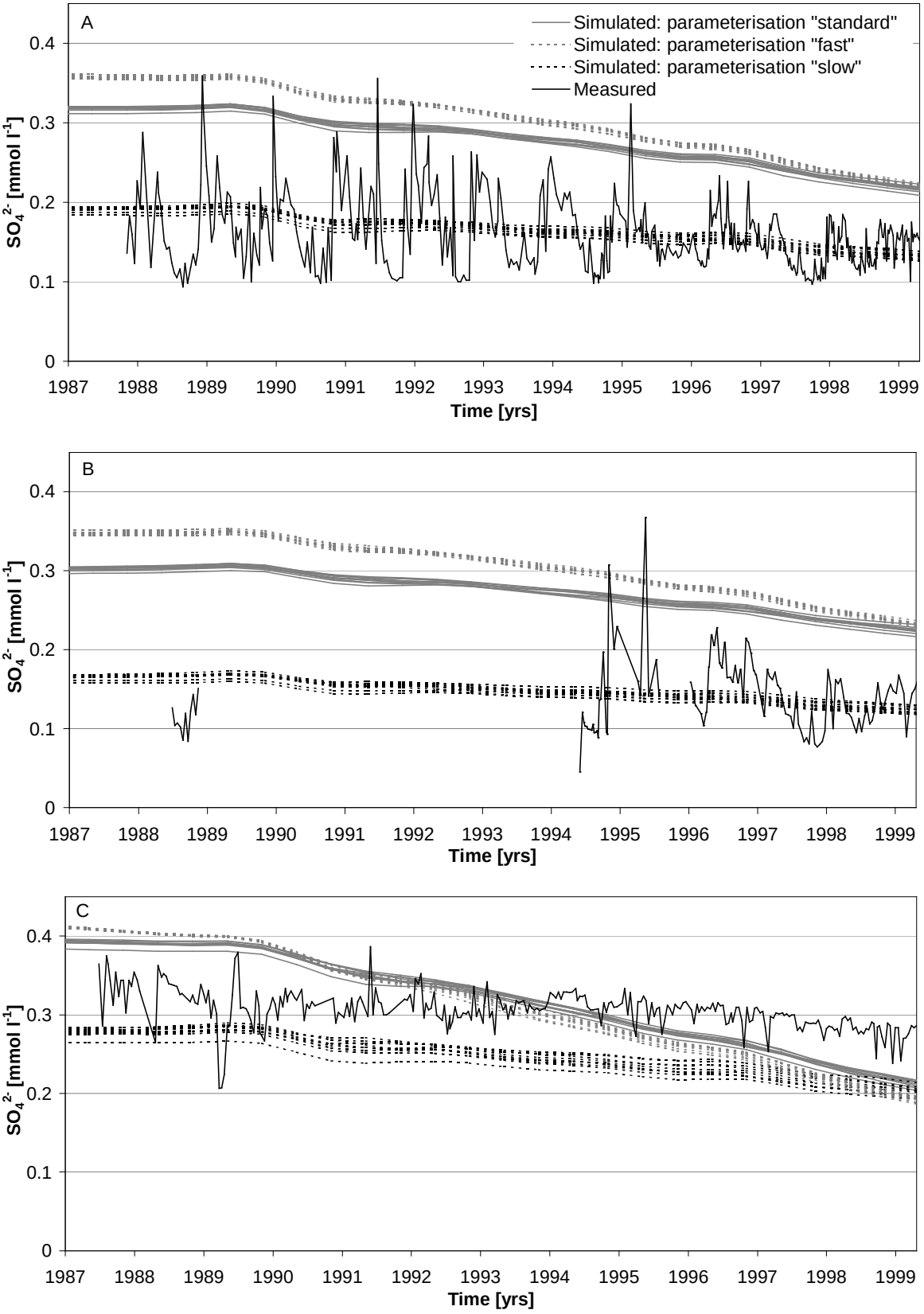

Fig. 6.10 Simulated time series of mean sulphate concentration and measured time series of sulphate concentrations in stream water in the Lehstenbach catchment. **A**. Main weir. **B**. Köhlerloh. **C**. Schlöppnerbrunnen.

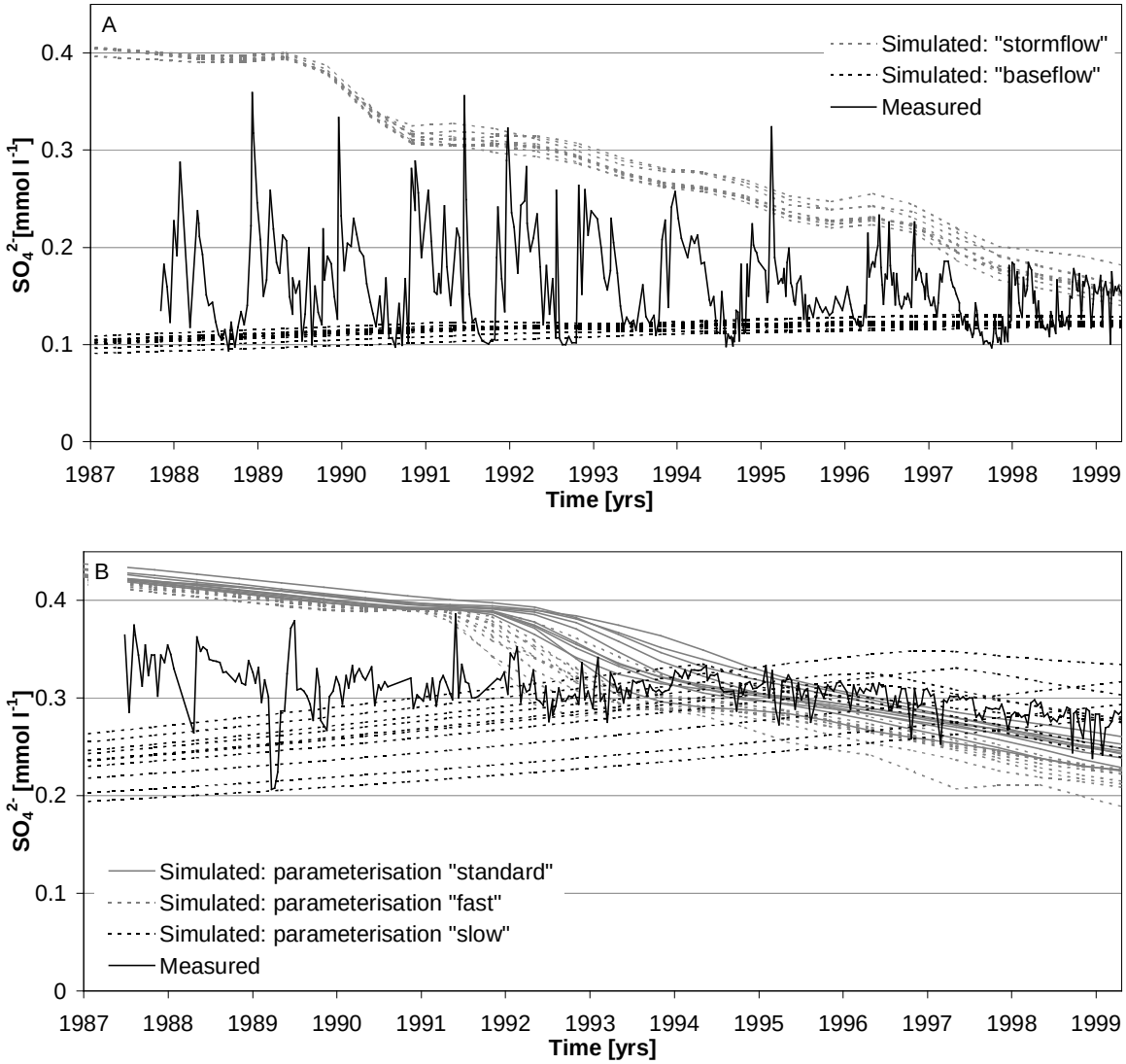

Fig. 6.11 Simulated time series of sulphate concentration in stream water considering split flowpaths and measured time series of sulphate concentrations in stream waters in the Lehstenbach catchment. **A**. Main weir, parameterisation “slow”. Flowpaths are divided into “stormflow” (three shortest flowpaths) and “baseflow” (the remaining flowpaths). **B**. Schlöppnerbrunnen, flowpath of 225 m length.

that on average the implemented random spatial heterogeneity of isotherm parameters levels out.

Sulphate concentrations simulated for the main weir (Fig. 6.10A) using the standard parameterisation are as high as 0.3 mmol l^{-1} in the late 1980s and decrease to 0.2 mmol l^{-1} during the 1990s. Therewith, they are clearly higher than measured concentrations, whose highest peaks just reach the simulated concentrations. The parameterisation “fast” is higher than the standard parameterisation. In contrast, the parameterisation “slow” leads to distinctly more reasonable concentrations, which start with values of 0.2 mmol l^{-1} in the late 1980s and slightly decrease to 0.15 mmol l^{-1} at present. Thus, they are in the mean range of measured concentrations.

For the Köhlerloh sampling site (Fig. 6.10B) the overall pattern looks very similar. Only the level of sulphate concentration in the late 1980s is marginally less. This fits very nicely to the observed concentrations, which also resemble values measured at the main weir. Consequently, the parameterisation “slow” is again the most appropriate.

The Schlöppnerbrunnen spring (Fig. 6.10C) exhibits a clearly higher level of sulphate concentrations for all three parameterisations compared to the main weir and Köhlerloh with values ranging from just below 0.3 mmol l^{-1} to 0.4 mmol l^{-1} in the late 1980s. This is in accordance with the measured time series. However, simulated values decrease since 1990, whereas measured concentrations do not start to decrease before 1995.

Simulated mean runoff consists of single flowpaths. A separate consideration of these may help to reveal if observed patterns in principle can be reproduced by the model (Fig. 6.11). With the parameterisation “slow” it is possible to split flowpaths to the main weir into baseflow and stormflow, thus forming the envelopes of measured concentrations (Fig. 6.11A). Stormflow thereby is generated by the three shortest flowpaths (25, 75, and 125 m) and approximates the maximums of the time series. Baseflow consists of the remaining flowpaths and is in the range of minimum concentrations. For this separation stormflow accounts for 29.5 % and baseflow for 70.5 % of total discharge. For the other parameterisations it is similarly possible to mix a baseflow which is in the range of measured baseflow values. It would comprise 8.2 % of total discharge with respect to the standard parameterisation and only 0.3 % with respect to the parameterisation “fast”. For these parameterisations however, it is not possible to mix a stormflow from the remaining shorter flowpaths with a similar decrease of concentrations such as observed during stormflow events. Further, for all parameterisations the simulated baseflow shows a slightly positive slope, which is not the case for the

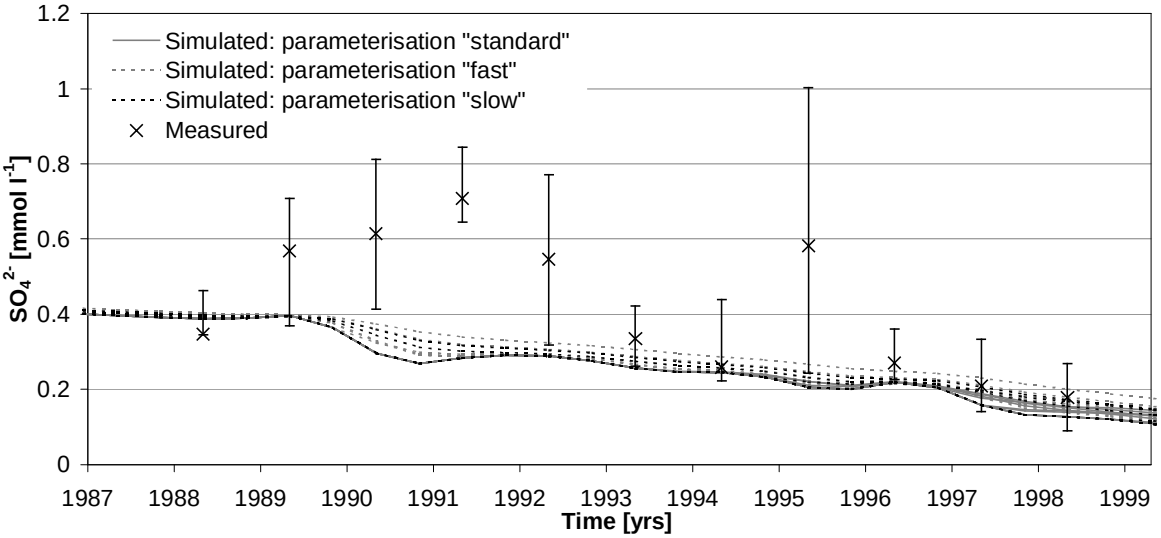

Fig. 6.12 Simulated time series of sulphate concentration in the soil solution in 1 m depth and annual medians and quartiles of measured sulphate concentration in the soil solution of that depth for the sampling sites GW 01, GW 03, GW 05, and GW 06 in the Lehstenbach catchment.

measured baseflow.

Mean sulphate concentrations simulated for the Schlöppnerbrunnen spring show a decrease since 1990, whereas measured concentrations do not decrease before 1995 (Fig. 6.10C). For this site the delimitation of the subcatchment is difficult, so that it is uncertain to which extent flowpaths really contribute to discharge. Therefore, single flowpaths were considered to examine the degree of a delayed decrease such as observed for the measured concentrations. As an example, Fig. 6.11B shows the 225 m flowpath. For the parameterisation "slow" it even exhibits slightly increasing values until about 1997, when the extremum is achieved and values start to decrease. Thereby, concentrations are similar to the measured ones.

Simulated sulphate concentrations for the soil solution in 1 m depth are shown in Fig. 6.12. They reflect the specified upper boundary of the model. Thus, the differences between the parameterisations are small. Additionally, the figure depicts the annual medians and quar-

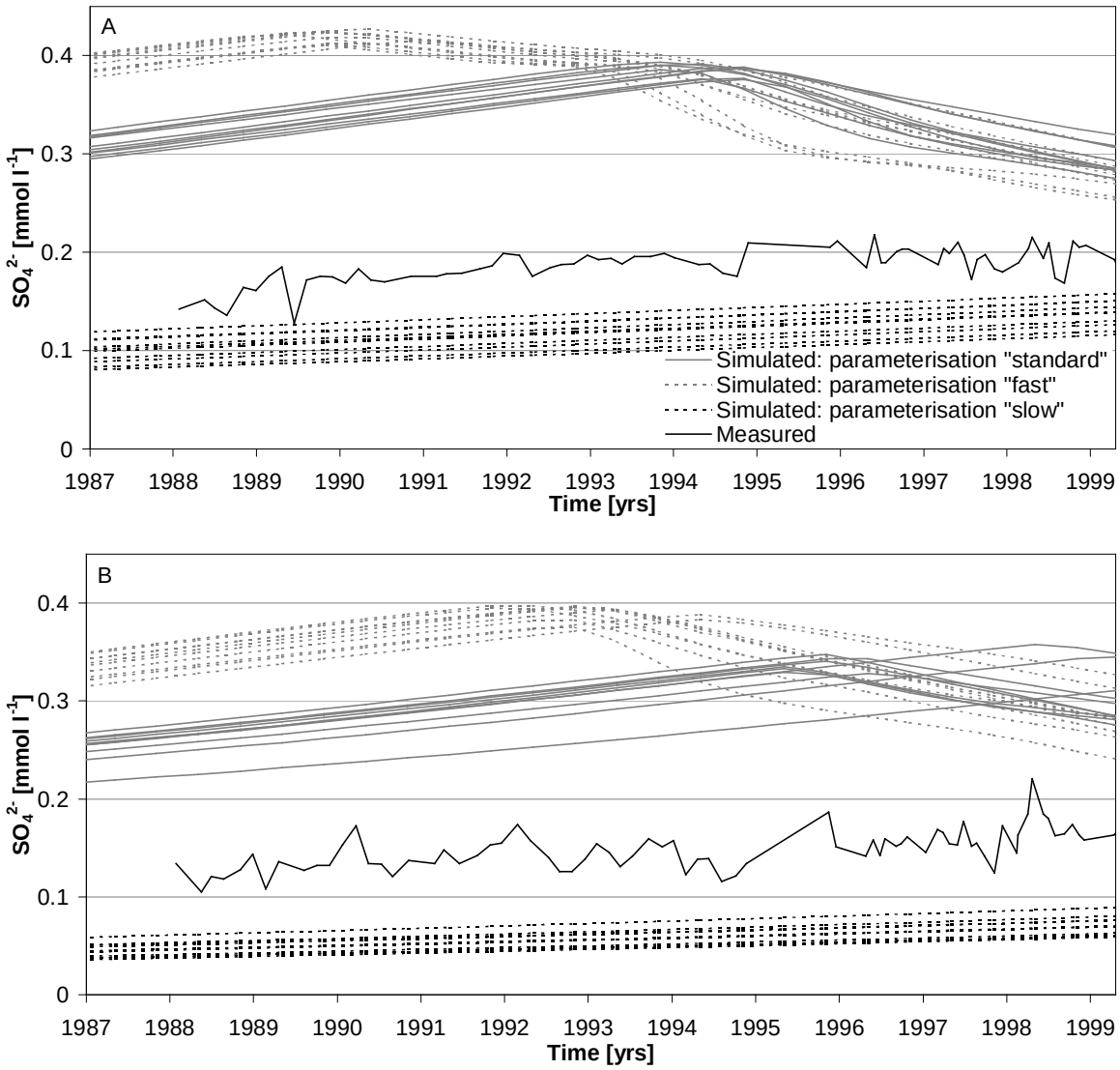

Fig. 6.13 Simulated and measured time series of sulphate concentration of the groundwater in the Lehstenbach catchment. **A**. Well GW 04, flowpath length 400 m. **B**. Well GW 05, flowpath length 200 m.

tiles of sulphate concentration measured in the soil solution in that depth at different places in the catchment. The spread of these values is great. Further, differences between the years are considerable as well. On the one hand, these may be due by the fact that the number of samples from different sites is not constant over time, but varies for different years. On the other hand, high concentrations may be caused by drying effects of the soil solution. This may especially be the case for the year 1991, which was the driest of the sampling period (Moritz *et al.*, 1994; Moritz, unpublished data). Thus, it can only be recorded that simulated concentrations are within the annual quartiles of measured concentrations for the majority of cases.

Sulphate time series at the groundwater wells GW 04 and GW 05 are represented by one flowpath each, whose range of depth approximately corresponds to that of the depth integrated samples (Fig. 6.13). For GW 04 a flowpath of 400 m length, for GW 05 one of 200 m length was selected. The depth of these changes according to the parameterisation. For GW 04 it ranges from 5.4 to 8.4 m, for GW 05 from 13.4 to 19.6 m. At both wells the differences between the parameterisations are considerable. Values simulated using the parameterisation "slow" are less than 0.15 mmol l^{-1}, whereas for the parameterisations "standard" and "fast"

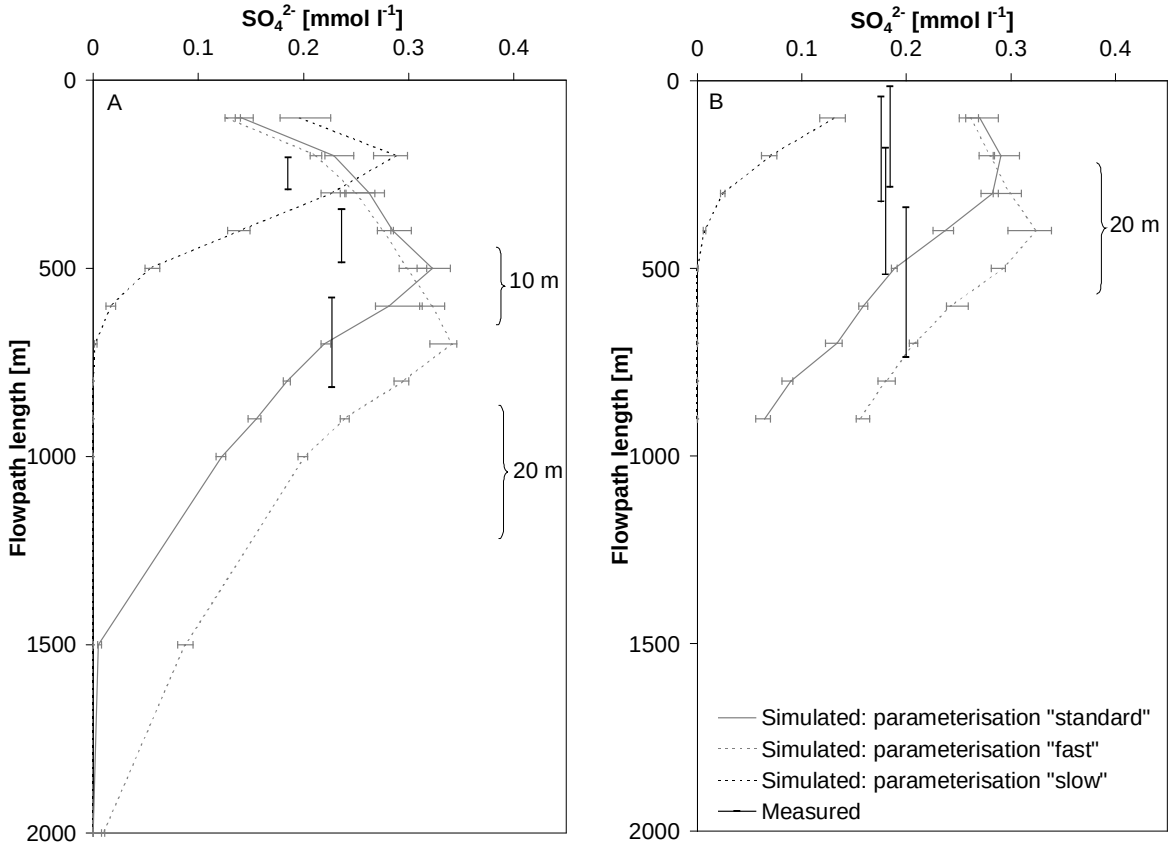

Fig. 6.14 Simulated groundwater sulphate concentrations (median and quartiles of 10 simulations each) for the Lehstenbach catchment and the year 1999. Concentrations are plotted versus the flowpath length in the way of a depth profile. Corresponding approximate depths are specified by braces. Depth specific groundwater samples of Rötting (2000) are given by vertical lines representing the range of flowpaths which corresponds to the sampled depth. **A**. Well GW 04. **B**. Well GW 05.

concentrations exceed 0.2 mmol l^{-1} during the whole period shown. Measured time series are in between the parameterisations “standard” and “slow” and interestingly show increases with similar slopes compared to the simulations with the parameterisations “standard” and “slow”.

Fig. 6.14 shows the depth profiles of sulphate concentrations the model generated for the wells GW 04 and GW 05 and the year 1999, which is the end of the simulation period. As the flowpath length was chosen to be the fixed quantity and the depth varies thus according to the parameterisation, the y-axis is given by the flowpath length, which is strictly monotonic connected with the depth. For both wells and all parameterisations (except from the parameterisation “slow” at GW 05) a clear peak with maximum sulphate concentrations of 0.35 mmol l^{-1} is simulated, which moves downwards through the profile. Therewith, it represents the divide between decreasing concentration with time above and still increasing concentration below. For the parameterisation “fast” this peak is located deepest, for the other parameterisations it is accordingly further above. At GW 04 it is situated between the flowpaths of 200 and 700 m length. At GW 05 it is between 0 and 400 m lengths. The well GW 05 is located in the middle of a slope and flowlines exhibit a long unsaturated zone (cf. Fig. 5.1). The delay is therefore more pronounced compared to GW 04, which is located in stream vicinity.

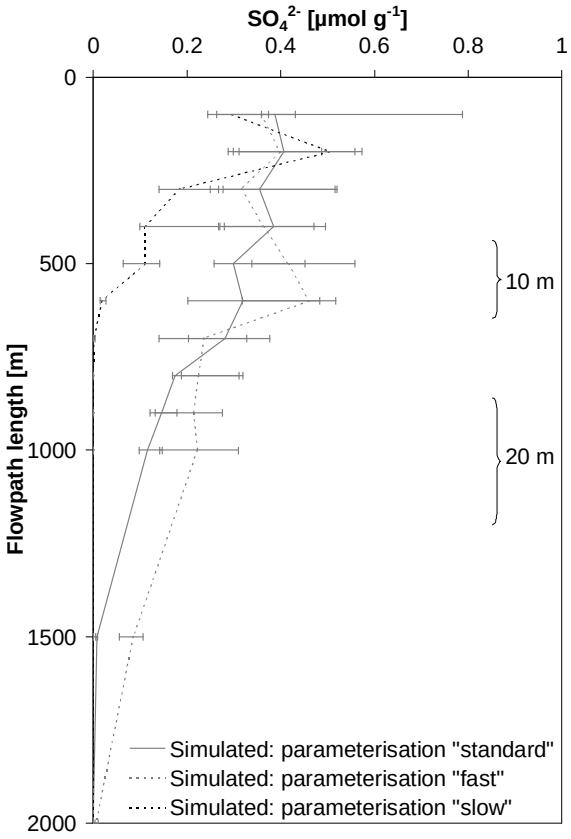

Fig. 6.15 Simulated sulphate contents of the fine soil fraction of the solid phase (median and quartiles of 10 simulations each) for the well GW 04 in the Lehstenbach catchment and the year 1999. Contents are plotted versus the flowpath length in the way of a depth profile. Corresponding approximate depths are specified by braces.

For the parameterisation “slow” the sulphate peak has even not yet completely reached the aquifer. Measured depth specific sulphate concentrations of the groundwater (Rötting, 2000) are within the broad range of simulated values, but in contrast to these they do not exhibit such a clear undulation.

Simulated sulphate contents of the solid phase (fine soil fraction) for the well GW 04 (Fig. 6.15) are represented in the same way as groundwater concentrations. Values exhibit a markedly greater spread than the corresponding groundwater values, so that in the upper part of the profile a trend cannot be observed. For flowpaths which are longer than 1000 m however values are clearly lower. The median of measured sulphate contents (NaH_2PO_4 extr.) for the upper 10 m of the regolith is 0.58 µmol g^{-1} (derived from Schweisser, 1998). This value is only achieved by the upper quartiles of simulated sulphate contents. On average simulated values are lower.

Catchment balances were calculated based on the model output (Fig. 6.16). They indicate that a considerable amount of sulphate is still stored in the catchment. With respect to the

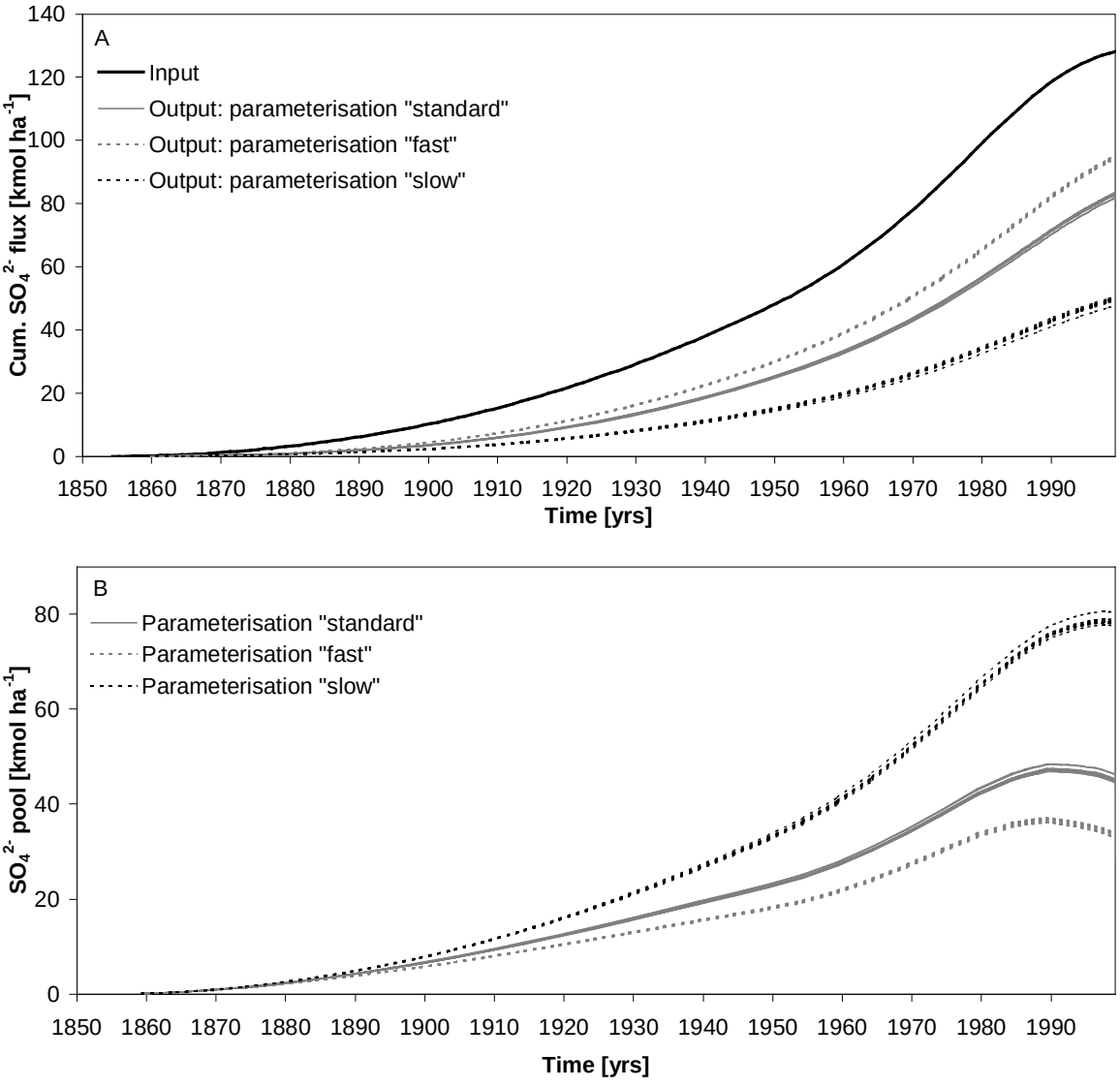

Fig. 6.16 Hindcast of the simulated sulphate balance for the Lehstenbach catchment. **A**. Cumulative sulphate input and output fluxes. **B**. Total sulphate pool.

year 1999, the cumulative sulphate output from the catchment (Fig. 6.16A) is greatest for the parameterisation “fast” with about 74 % of the total input. For the standard parameterisation approximately 65 % and for the parameterisation “slow” only 39 % have already been released. Consequently, the total pool of sulphate stored in the catchment is greatest for the parameterisation “slow” with about 78 kmol ha^{-1} (median) in the year 1999 (Fig. 6.16B). For the standard parameterisation it is 45 kmol ha^{-1} and for the parameterisation “fast” it is only 34 kmol ha^{-1}. For all parameterisations the maximum is achieved and a net release from the catchment is just on the way, which is due to the strongly decreased sulphate input fluxes during the last decade. This is in accordance with measurements of input and output fluxes for the catchment. They reveal a net release since 1994 except for the year 1996, where sulphate input approximately equalled output (Moritz *et al.*, 1994; Moritz, unpublished data). The total pool of sulphate, which consists of solid bound sulphate (approximately 90 % for the standard parameterisation) and dissolved sulphate (approximately 10 %), is underestimated by the model. Simulated values are clearly lower compared to the experimentally determined average pool of solid bound sulphate of 94 kmol ha^{-1} for the upper 10 m of the regolith (Schweisser, 1998).

6.4.2 Lysina Catchment

Analogously to the Lehstenbach catchment, modelling was performed using three parameterisations. The parameterisation “standard” refers to the standard parameterisation given in Tab. 6.3. For the parameterisation “fast” the regolith depth was set to 3 m and the proportion of the fine soil fraction to 0.68. For the parameterisation “slow” the regolith depth was set to 5 m and the proportion of the fine soil fraction to 0.93. For comparison measured time series (Hruška & Krám, unpublished data) are included in the figures.

Simulated time series of mean sulphate concentrations at weir 1 and weir 2 exhibit only small changes with respect to the different parameterisations (Fig. 6.17). For weir 1 (Fig. 6.17A) simulated sulphate concentrations strongly decrease with time and are between approximately 0.3 mmol l^{-1} in 1987 and 0.1 mmol l^{-1} at present. Therewith, they are in the range of measured concentrations. Only at the beginning of the sampling period in the early 1990s they do not match the measurements and show markedly lower concentrations.

For weir 2 a decrease of simulated sulphate concentrations can also be observed (Fig. 6.17B). It is however not as steep as the one at weir 1. Here, concentrations range from slightly more than 0.3 mmol l^{-1} in 1987 to approximately 0.2 mmol l^{-1} at present and are thus similar to measured concentrations at this site. Only the dimension of the decrease is not exactly the same. It is more pronounced for the simulations.

The separate consideration of the shortest and longest flowpath of the main and side catchment informs about the extent to which the observed short-term variability of sulphate at the weirs can in principal be reproduced by the model (Fig. 6.18). Sulphate concentrations of the shortest flowpath resemble the input to the system and represent an approximation of stormflow. Sulphate concentrations modelled for the longest flowpath show the greatest delay

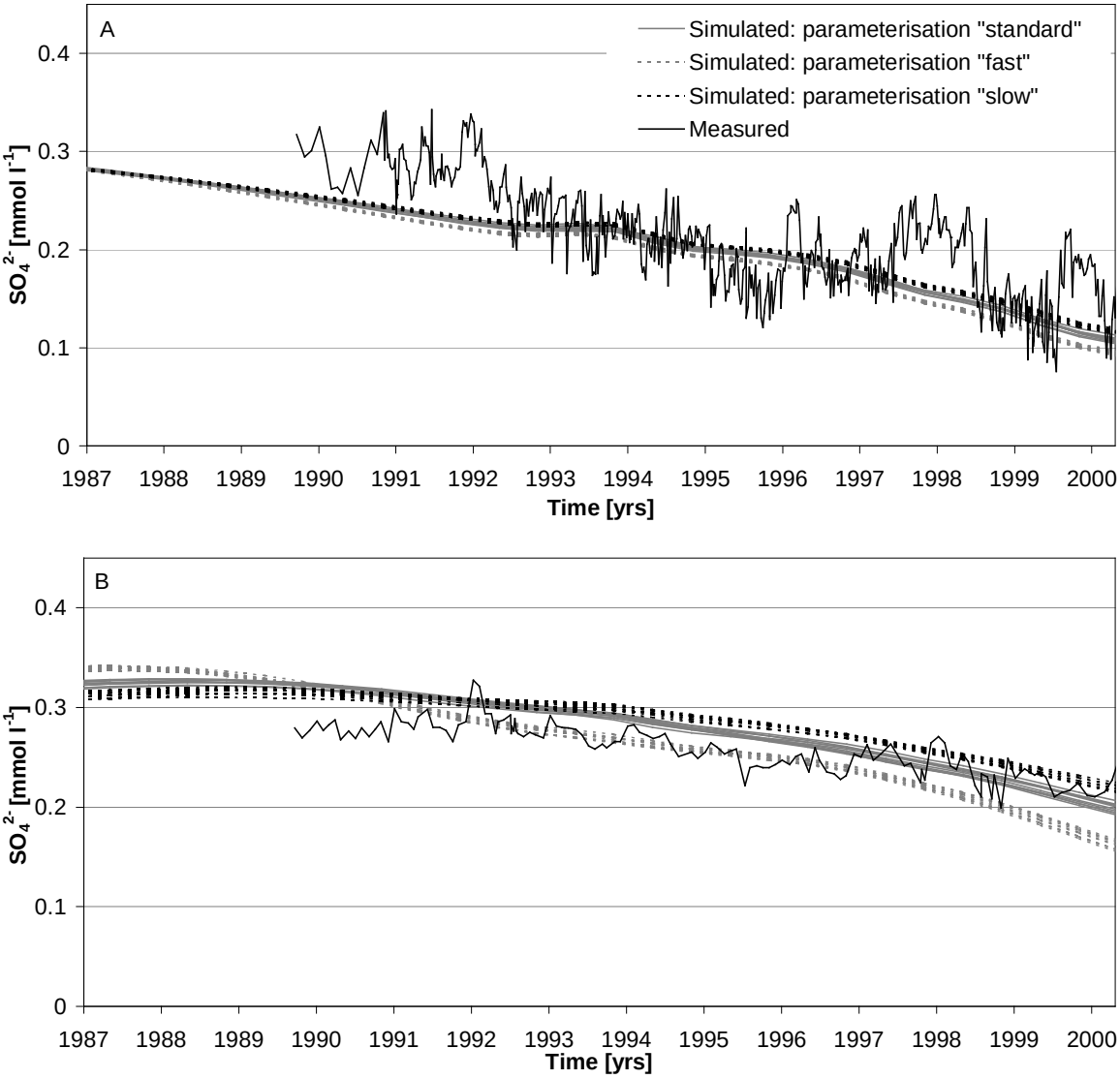

Fig. 6.17 Simulated time series of mean sulphate concentration and measured time series of sulphate concentrations in stream water in the Lysina catchment. **A**. Weir 1. **B**. Weir 2.

and approximate baseflow. For both catchments therefore envelopes arise, within which the measured concentrations can be found. For the shortest flowpath values strongly decrease. With respect to the longest flowpath values still increase until the early 1990s for the side catchment and even until the late 1990s for the main catchment. For weir 1 (Fig. 6.18A) some measurements however cannot be explained by the model. These are the high values of approximately 0.35 mmol l^{-1} in the early 1990s as well as the low values of about 0.13 mmol l^{-1} in 1995.

For the spring Lenka the idealised slope approach (cf. Fig. 5.1) was modified. A road intersects the slope directly below the spring. The height of the scarp in uphill direction is approximately 2 m. Therefore, there is no riparian zone with a shallow water table in the vicinity of the spring. The idealised slope however exhibits a shallow water table at the lower end of the slope and it is thus not appropriate for the given situation. For that spring therefore,

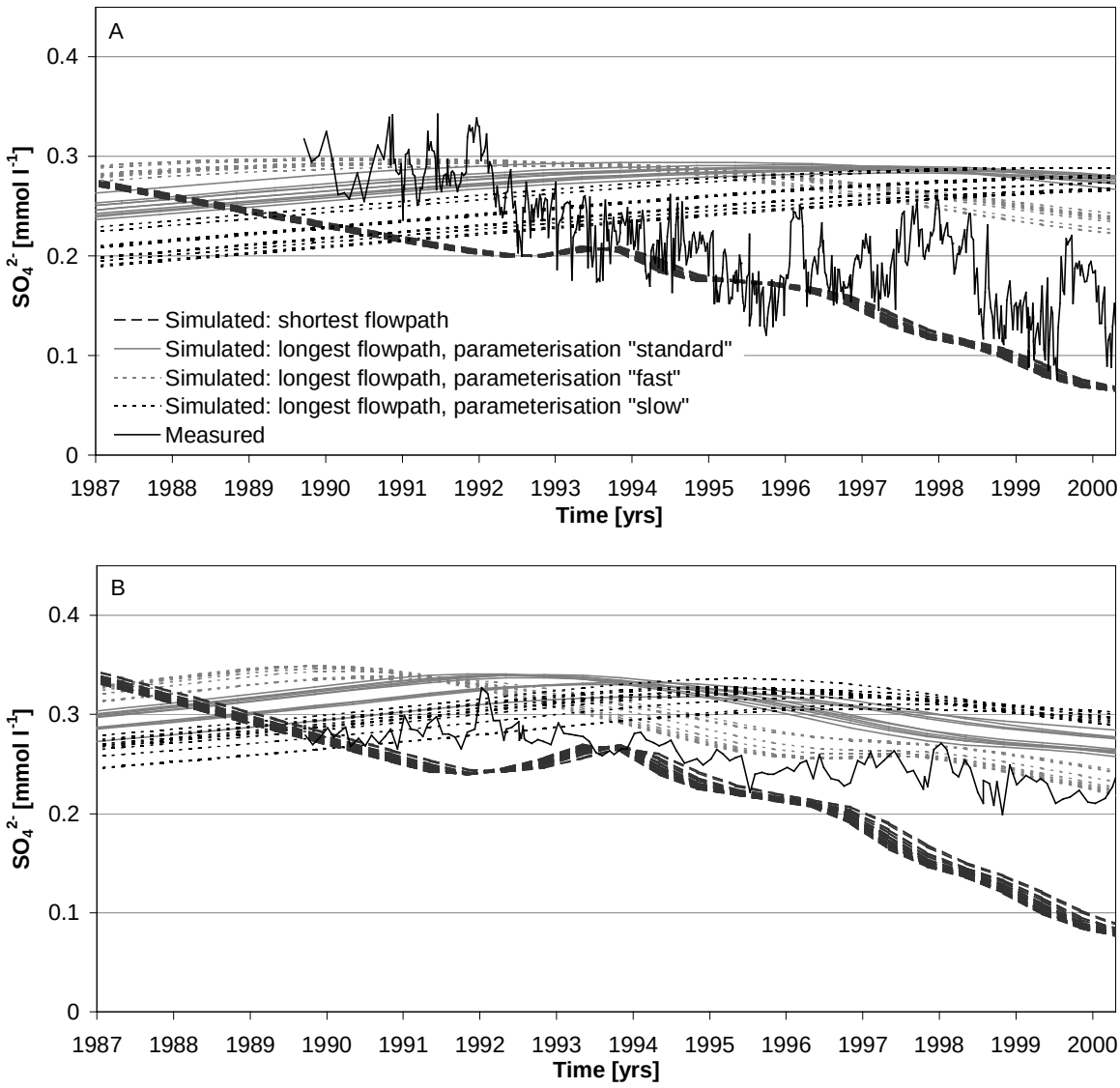

Fig. 6.18 Simulated time series of sulphate concentration for the shortest and the longest flowpath of the Lysina main and side catchment as well as measured time series at the weirs. For the shortest flowpath the different parameterisations are represented in the same way. **A**. Weir 1 (shortest flowpath: 25 m, longest flowpath: 575 m). **B**. Weir 2 (shortest flowpath: 25 m, longest flowpath: 325 m).

the lower end of the slope was left out and the spring was located in the middle of the slope. For this, the distance to the lower end of the slope was set equal to the distance of the spring from the watershed boundary.

Simulated time series of sulphate concentration at Lenka are shown in Fig. 6.19A. Values clearly decrease from 0.3 mmol l^{-1} to about 0.2 mmol l^{-1} since the early 1990s. This is not in accordance with measured concentrations, which do not decrease before 1999. Only for the longest flowpath a delay is modelled, which is similar to the one observed (Fig. 6.19B).

Depth profiles of sulphate concentrations in the groundwater and contents on the solid phase for the Lysina main catchment (Fig. 6.20) are represented in the same way as for the

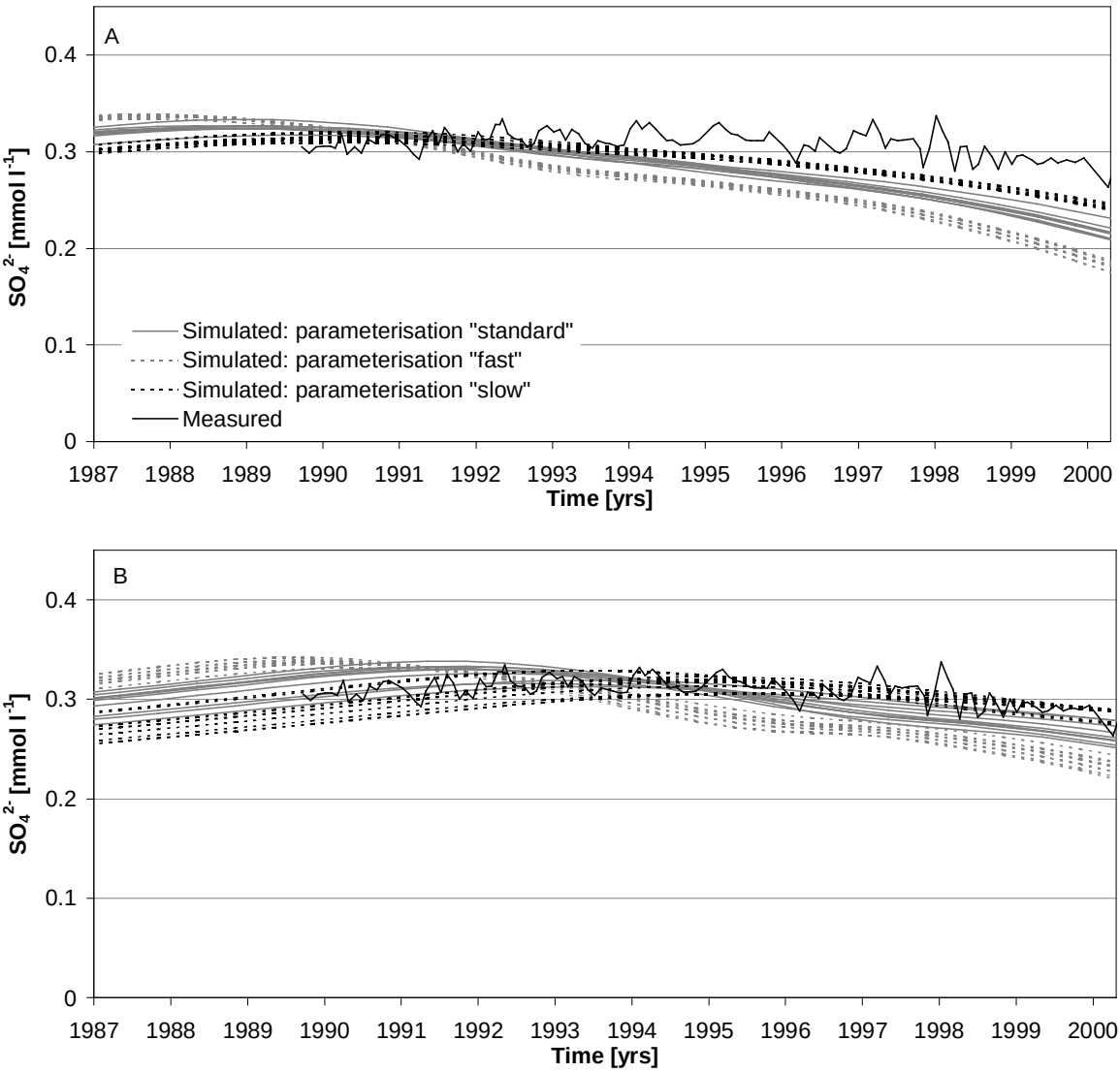

Fig. 6.19 Simulated and measured time series of sulphate concentration at the spring Lenka in the Lysina catchment. **A**. Mean concentrations. **B**. Longest flowpath (218 m).

wells in the Lehstenbach catchment. In this case however, they do not refer to a well, i.e. a distinct point at the basic slope, but to the lower end of the slope, i.e. a stream point (cf. Fig. 5.1). This enables the comparison with measured groundwater sulphate concentrations, since the piezometers installed in the main catchment are all located near streams.

Simulated concentrations of dissolved sulphate show a clear depth dependency (Fig. 6.20A). For the top layers values are low with less than 0.1 mmol l^{-1}. At the bottom of the regolith they are markedly higher and between 0.2 and 0.3 mmol l^{-1}, which indicates a recovery starting from the top. Measurements from the piezometers show the same general pattern with low concentrations in the shallow aquifer and higher concentrations in the deeper layers, but concentrations tend to be lower than the modelled ones.

Simulated sulphate contents of the solid phase exhibit a considerable spread (Fig. 6.20B). On the whole however, a depth dependency can be observed. Values range from less

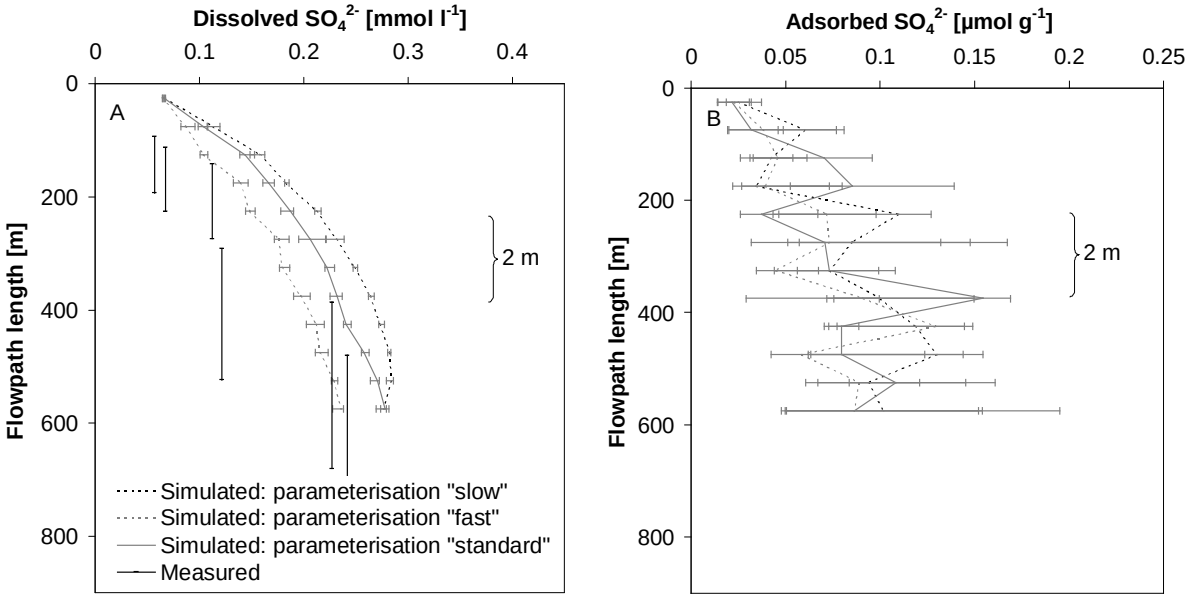

Fig. 6.20 Simulated groundwater sulphate concentrations and sulphate contents of the fine soil fraction of the solid phase (median and quartiles of 10 simulations each) for a stream point (lower end of the slope) in the Lysina main catchment and the year 2000. Values are plotted versus the flowpath length in the way of a depth profile. Corresponding approximate depths are specified by braces. The medians of groundwater samples from the piezometers are given by vertical lines representing the range of flowpaths which corresponds to the sampled depth. **A**. Dissolved phase. **B**. Solid phase.

than 0.05 µmol g^{-1} in the top layers to 0.1 µmol g^{-1} (median) at the bottom of the regolith. The median of measured sulphate contents (H_2O extr.) is 0.14 µmol g^{-1}. Therewith, it is higher than simulated contents and in the range of the upper quartiles of these. Furthermore, measured sulphate contents are significantly negatively correlated with depth (cf. Fig. 6.2A). Model results however exhibit a positive relationship with depth.

Due to the small sulphate contents of the solid phase the modelled sulphate pool in the main catchment is between 1 and 2 kmol ha^{-1} for the different parameterisations and therewith very small. Thus, sulphate in runoff rapidly reacts to changes in deposition fluxes, so that according to the simulations 97 to 99 % of the cumulative sulphate input has already left the catchment.

7 Discussion

7.1 Experimental Findings from the Lysina Catchment

7.1.1 Groundwater Solute Concentration

Sulphate concentrations in the groundwater exhibit a clear depth gradient with low values in the shallow aquifer and higher values in the deeper aquifer (Fig. 6.1). The gradient can even be observed at the two piezometers of each sampling site and indicates a recovery of the catchment starting from the top. The shallowest groundwater was sampled at GW IIIa. It is also the one with the lowest sulphate concentrations, which are characterised by a median of 0.06 mmol l^{-1}. Therewith, it is still distinctly higher than the present concentrations of 0.02 mmol l^{-1} in bulk precipitation and 0.04 mmol l^{-1} in throughfall (medians for the hydrologic year 2000, Hruška & Krám, unpublished data). On the one hand this can be attributed to the concentrating of sulphate in the topsoil resulting from evapotranspiration (Reuss & Johnson, 1986). The runoff coefficient of the catchment is 0.46 (Krám, pers. comm.). Thus, about half of the incoming precipitation is subject to evapotranspiration. On the other hand the higher sulphate concentrations in the shallow groundwater may indicate the buffering of the solid phase, which releases sulphate as a result of the decreasing depositions.

Aluminium concentrations are high in the shallow groundwater and markedly lower or even not detectable in the deeper groundwater. The high concentrations in the shallow aquifer are in accordance with observations from the soil solution in different depths. Concentrations showed a 20fold increase from throughfall to 80 cm depth (Krám, 1997). This indicates the considerable pool of mobile aluminium in the topsoil, which is highly acidified with a mean pH of about 4 for B horizons and a base saturation of less than 5 % for B as well as C horizons (Krám, 1997). Therefore, according to Ulrich (1981) aluminium buffering prevails. This mobile aluminium is ready to be leached into deeper layers and may therefore also be the source of the high aluminium concentrations measured in the groundwater of up to 1.5 m depth in this study.

The concentrations of the base cations, calcium and magnesium, are low in the shallow groundwater and clearly higher in the deeper part of the aquifer. There are three possible explanations. Firstly, the chemistry of water depends on the distance along the flowpath (Freeze & Cherry, 1979). The deeper groundwater has covered the longer flowpath. Therefore, it has been in contact longer with the solid phase and reflects the chemical composition of the rock. Secondly, the low base saturation of the topsoil exhibits no potential for an enrichment of waters with respect to base cations. Thirdly, the significantly positive correlation between sulphate, calcium, and magnesium gives evidence that the high base cation concentrations may be caused by the high sulphate concentrations in the deeper aquifer. Sulphate increases the ionic strength of the solution, which is indicated by a positive correlation with

the electrical conductivity. Reasons of electroneutrality require the balance of the increased negative charge resulting in the enhanced leaching of base cations (Reuss & Johnson, 1986).

In runoff, the elucidated chemical patterns of shallow and deep groundwater can be found again. Stormflow composition is similar to that of the shallow groundwater, but distinctly different to that of precipitation. So, sulphate in stormflow exceeds that in throughfall by a factor of 2, and aluminium in stormflow even exceeds that in throughfall by a factor of 109 with respect to the hydrologic year 2000 (derived from Hruška & Krám, unpublished data). Baseflow composition is similar to that of the deep groundwater. This is in accordance with findings of Buzek *et al.* (1995), who calculated the contribution of different components to runoff from oxygen isotopes and the anion deficit for the same catchment. Water originating in the upper soil horizons comprised 80 % during flood events and 0 % during baseflow conditions. Furthermore, the concentration of precipitation to runoff was generally low with a maximum of 20 % for the highest discharge peaks. The observation is also consistent with these from other catchments, in which also mainly pre-event water contributes to discharge during stormflow conditions (Anderson *et al.*, 1997, Lischeid *et al.*, 2001).

7.1.2 Pool of Solid Bound Sulphate and Sorption Isotherms

H_2O extractable (extr.) sulphate of the drilling cores is low with a median of 0.14 µmol g^{-1}. Corresponding values determined for the topsoil in the same catchment are higher with mean contents of 0.44 µmol g^{-1} for B_h horizons, 0.87 µmol g^{-1} for B_s horizons, and 0.59 µmol g^{-1} for C horizons (Krám, 1997). In the Lehstenbach catchment the median of sulphate contents (H_2O extr.) for the upper 10 m of the regolith is 0.41 µmol g^{-1} and hence is also higher than the value determined in this study (derived from Schweisser, 1998).

Values may be underestimated, as sulphate in the solution of the last extraction steps was below the identification limit and could therefore not be considered in the calculations. However, for the given soil and solution quantities this can only account for at maximum 0.05 µmol g^{-1}. Further, a grave mistake during the laboratory analysis is unlikely, as the extraction was also performed with the NaH_2PO_4 solution. Here as well the amount of extracted sulphate was very low. In general, sulphate concentrations in the extracting solution were below the identification limit, which was due to the dilution of the solution prior to the analysis (cf. Section 4.3.2).

Sulphate is significantly correlated with total carbon, pH (H_2O), and pH ($CaCl_2$). All these parameters however are also significantly correlated with depth. Consequently, the causality between the parameters is uncertain and in some cases the correlation may only be due to the common depth gradient.

It is widely accepted that pH plays an important role for sulphate sorption. In laboratory experiments, forest soils were exposed to solutions of varying pH. Maximum sorption capacities were found at pH values of 3.8 to 4.2. With increasing pH, sorption rapidly decreased (Meiwes *et al.*, 1980; Nodvin *et al.*, 1986; Courchesne & Hendershot, 1989). Values in this study are between 4.5 and 5.5 (pH (H_2O)) neglecting one sample (Fig. 6.2E). The sig-

nificantly negative correlation between pH and sulphate is in accordance with the relationship found in the literature. Thus, the pH values above 5 in the deeper part of the regolith might be seen as one explanation for the very low sulphate contents, which were measured there. Further, the relationship might also offer an explanation for the higher sulphate contents in the topsoil compared to the values of this study (see above). In the topsoil the pH (H_2O) is about 4 (Krám, 1997) and might thus be one cause for a greater sorption capacity compared to the deeper layers with the higher pH values.

Between the humus content in the soil and the sulphate retention generally a negative relationship is found (Singh & Johnson, 1986; Mitchell *et al.*, 1992). It is ascribed to the blockage of sorption sites by the organic matter. For the Lysina samples however, sulphate and total carbon are significantly positively correlated. A possible explanation for such a behaviour would be the release of sulphur from the organic pool by mineralisation prior to and during the laboratory analyses. For A horizons and temperatures of 15 to 20 °C Jungnickel (1996) calculated rates of mineralisation of 0.0025 to 0.009 µmol g^{-1} d^{-1}. These were based on findings of Maynard *et al.* (1984), Ghani *et al.* (1993), Sakadevan *et al.* (1993), and Valeur & Nilsson (1993) (cit. in Jungnickel, 1996). Samples however were stored at 2 °C and the extraction with the shaker took place at 5 °C. Samples were exposed to room temperature only for centrifugation and filtration (Tab. 4.4), which amounts to at maximum two days. Furthermore, carbon contents are with one exception clearly smaller than the ones common for A horizons. Therefore, mineralisation cannot be the reason for differences in the sulphate contents of approximately 0.2 µmol g^{-1} between the samples. Hence, it is concluded that the relationship between sulphate and total carbon might only be caused by the common correlation with depth.

Sulphate sorption mainly takes place on the hydroxides and oxides of iron and aluminium as well as on clay minerals (Scheffer & Schachtschabel, 1992). Thus, the proportion of clay minerals in the soil is positively related to the sorption capacity. This is consistent with the findings from the Lysina catchment. There are three samples which were classified as loam or clay and not as sand (cf. Appendix B). These are three out of the four samples exhibiting the highest sulphate contents. Moreover, the generally low proportion of the clay fraction in the samples might be seen as a further reason for the low sulphate contents.

On the whole, the very low sulphate contents in the deeper regolith are plausible and are likely be rooted in part in the high pH and the low proportion of the clay fraction. A connection with sulphate reduction processes is unlikely, as low contents were likewise measured in the boggy and the upslope areas of the catchment.

The determination of desorption isotherms proved to be problematic due to the low sulphate contents of the solid phase. Sulphate could only be detected for the first four (and in one case five) extraction steps. Thus, only four points were available for the fit of the desorption isotherms. It was not possible to fit Langmuir isotherms with the Levenberg-Marquardt algorithm. In most cases, an approximation was not reached after 300 iteration steps or the

coefficients exhibited negative or unreasonably high values. For that reason, the linear isotherms were opted for. Fitting was done for each sample separately by considering not only the desorption points but also the two adsorption points which were determined. This decision arose from the fact that the separate fit to adsorption and desorption points led to very similar slopes and a sorption maximum for the adsorption points did not seem to be achieved. It is concluded however, that there is a considerable uncertainty with respect to the shape of the isotherms, which has to be taken into consideration during the interpretation of the model results.

It would also have been possible to derive only one fit for all samples together. However, it was refrained from that, because the adsorption and desorption points, which are the source data of the fit, are clearly not normally distributed (cf. Fig. 4.1). Hence, the requirements for the validity of the fit statistics are not met (Bortz, 1999). Furthermore, single fits enabled the comparison of isotherms from different depth as well as from different sampling sites. Finally, reasons of consistency supported this decision, as Schweisser (1998) also determined separate isotherm curves for each soil sample from the Lehstenbach catchment.

Generally, isotherms run flat compared to the average isotherms Schweisser (1998) determined for the upper 10 m of the Lehstenbach regolith (Fig. 6.3). The slope is significantly negatively correlated with the pH (H_2O) and significantly positively correlated with the sulphate content. Thus, a low pH leads to a steeper slope of the isotherm, i.e. an enhanced sorption capacity, which again results in a greater amount of adsorbed sulphate. This confirms the importance of the pH for sulphate sorption as discussed above.

7.1.3 Sulphate Reduction Processes

Measured and smelled hydrogen sulphide at the sites GW II and GW III as well as the metal sulphides at GW Ib indicate that sulphate reduction plays a role in the catchment. This is confirmed by the oxygen and nitrate concentrations which were measured in the piezometers (Fig. 6.1E and F). According to the sequence of redox reactions in a closed aqueous system containing organic material, oxygen reduction and denitrification occur first. Sulphate reduction takes place only at much lower redox potentials (Stumm & Morgan, 1996).

At GW IV close to the well Lenka oxygen saturation and nitrate concentrations are high. Thus, sulphate reduction is very unlikely. At the site GW I close to the weir 1 oxygen saturation is at maximum 50 % and nitrate concentrations are clearly lower compared to GW IV. Here, denitrification is in progress. This is indicated by the presence of nitrite, which is an intermediate product of the process (Stumm & Morgan, 1996). For the sites GW II and GW III in the boggy part of the main catchment, oxygen saturation is less than 37 % and nitrate is below the identification limit. Therefore, denitrification is already completed at these sites and consequently they are the most likely ones for sulphate reduction to occur. This is in accordance with the rotten smell, which was only observed at these sites.

Measured hydrogen sulphide concentrations, however, are very low. The maximum concentration is 0.45 µmol l^{-1} at GW IIb, which is less than 1 % of the sulphate concentration

measured for samples from that piezometer. Further, sulphate concentrations do not indicate a considerable reduction. At all sites they are clearly higher than present concentrations in precipitation (Section 7.1.1). At the catchment scale as well, nothing points to a net sink of sulphate, which irreversible reduction would be. In the early 1990s the catchment was balanced with respect to sulphate. Input assessed by bulk precipitation and throughfall measurements and output assessed by runoff measurements were approximately equal (Hruška & Krám, 1994; Krám & Hruška, 1994; Krám *et al.*, 1997). At present, output fluxes are even twice as high as input fluxes (Krám, pers. comm.), which is due to the strongly decreased sulphate depositions in the last few years. Thus, the catchment acts as a net source of sulphate, which makes large scale reduction processes very unlikely. This is supported by stable sulphur isotope measurements, which were conducted in throughfall, bulk precipitation, and runoff. They did not show any shift in the isotopic composition (Hruška, pers. comm.), which should be observed for sulphate reduction, as it usually fractionates sulphur isotopes to a large degree (Thode, 1991).

Consequently, it is concluded that some sulphate reduction takes place in the boggy part of the catchment. However, it cannot be quantified by means of the conducted measurements and it only seems to play a minor role at the catchment scale.

7.1.4 Organic Pool of Sulphur

H_2O extractable sulphate in the Lysina soil samples comprises at maximum 17.3 % of total sulphur. At GW Ib metal sulphides might account for another large part of sulphur. For the other samples however, it is likely that the bulk of the remaining part is organic sulphur, which is common to form the greatest pool of sulphur in forest soils (Reuss & Johnson, 1986).

According to Gisi *et al.* (1990) the mean C:S ratio in topsoils is 140. Biederbeck (1978) reports on values of 57 to 271 for the surface horizons of different soils in north and south America. The median in the Lysina soil samples is 52.3. Therewith, it is in the lower range of values reported in the literature. However, that does not inevitably mean that there is another significant sulphur source in the regolith. Firstly, literature values refer to the topsoil, whereas samples in this study were taken from deeper layers. Values are therefore not absolutely equivalent. Secondly, total sulphate contents might be underestimated by the H_2O extraction. In general, H_2O does not extract total sulphate. For most forest soils it has been shown that more sulphate can be extracted using the NaH_2PO_4 extraction (Meiwes, 1979; Harrison *et al.*, 1989). Therefore, inorganic sulphur might make up a greater proportion of total sulphur than at maximum 17.3 %. This would explain a closer C:S ratio than observed in organic matter.

7.2 Model Design and Set-Up

7.2.1 Key Processes

The key processes which were implemented in the sulphate model are sulphate sorption and one-dimensional sulphate transport along flowpaths.

The general importance of sulphate sorption as a major retardation process of catchment recovery from acidification was already pointed out in Section 2.2. Furthermore, its specific importance for the catchments modelled is indicated by the observed sulphate time series. Deep groundwater sulphate concentrations at two wells in the Lehstenbach catchment are still significantly increasing (cf. Section 3.2), despite of strongly decreased depositions in the last 15 to 20 years. This cannot be explained by the water residence time, which is only between 2 and 3 years for these wells (Zahn, 1995). Correspondingly, in the Lysina catchment the well Lenka demonstrates the relevance of a retardation process, as sulphate concentrations do not decrease before the very late 1990s (cf. Section 3.2).

One-dimensional modelling of sulphate transport is in between the zero-dimensional lumped modelling approaches, which do not consider the catchment's hydrology and three-dimensional groundwater models such as MODFLOW (McDonald & Harbaugh, 1988). Lumped models do not offer a spatial resolution. Thus, they are unable to simulate both the spatial variability of sulphate patterns and the different concentrations of baseflow and stormflow in runoff observed in the catchments. However, three-dimensional models are also unsuitable for the given problem. In practice, the small scale distribution of the relevant parameters such as the soil's water retention curve, the hydraulic conductivity, or the porosity is not known at the required degree of precision. This leads to model results being of an immense uncertainty and non-uniqueness (Hauck, 1999). Hence, the coupling of such a groundwater model with a sorption model also does not appear to be the appropriate approach.

In hydrological modelling it is crucial to find the dominant processes acting at the given scale (Beven, 2001). Zero dimensional lumped models are too simple for the catchment scale, three-dimensional models of water flow are too sophisticated. The modelling approach of this study takes into account the well-known importance of water flowpaths on groundwater and runoff chemical patterns (Anderson *et al.*, 1997; Vogt & Muniz, 1997). On the one hand it offers the necessary spatial resolution for the simulation of different sampling sites in the catchments. On the other hand, the water flow regime of the basic slope (cf. Section 5.2.1) makes minimum demands on the parameterisation. Therewith, the model looses the possibility to simulate small scale heterogeneities. Using three-dimensional models however, this would also only be theoretically feasible.

7.2.2 Simplifications

Models are simplified pictures of reality. Thus, the model presented here also contains a number of simplifications with respect to the implemented processes. These will be addressed in the following.

Water Flow Concept of the Idealised Basic Slope

The main assumption of the water flow concept is that all water entering the system by precipitation contributes to groundwater recharge. Net-evapotranspiration is already subtracted. Other discharge generation processes such as overland flow and interflow, the lateral water flow occurring above the groundwater table, are neglected.

It is widely accepted that infiltration excess overland flow does not play a role in forested catchments in humid regions. Saturation excess overland flow during rainstorm events, however, has been shown to be important (Bonell, 1998). The proportion of direct precipitation to discharge in the Lysina and the Lehstenbach catchment has been assessed by hydrograph separation studies. For the Lysina catchment its average contribution was calculated to be 4 %, whereas it increased to 20 % during the highest discharge peaks (Buzek *et al.*, 1995). For the Lehstenbach catchment, hydrograph separation for peak discharge revealed a contribution of precipitation of 3 % based on sulphate and of 37 % based on silica. Silica, however, is likely to overestimate the proportion (Lischeid *et al.*, 2001). Hence, it is concluded that overland flow accounts for only a minor part of total discharge in both catchments.

Several authors have shown that interflow above the water table can occur during heavy rainstorms (McGlynn *et al.*, 1999; Scanlon *et al.*, 2000). For the Lehstenbach catchment however, hydrological as well as hydrochemical data indicate that it does not play an important role (Lischeid *et al.*, 2001). For the Lysina catchment, interflow cannot be precluded, but it is unlikely to occur at a large scale. In the boggy area of the catchment the groundwater level is close to the surface (cf. Tab. 4.1). Thus, there is no space for a lateral flow occurring above the water table. The areas with the deeper groundwater level are characterised by weathered granite. For the sites GW I and GW IV, which are located in such areas, the texture was classified as sand (Appendix B). Interflow, however, requires layers with a low hydraulic conductivity, above which the lateral water flow can take place. There are no indications for that.

On the whole, the above considerations show that overland flow and interflow can contribute to only a minor part of total discharge. Therefore, the assumption that all precipitation is groundwater recharge appears to be justifiable.

The model further assumes Darcian water flow, thus laminar flow in porous media. In both catchments the aquifer consists of weathered granite. It can therefore be understood as a pore aquifer, which justifies the assumption. At the large scale it should be one unconfined aquifer, such as required for the model. Locally however, heterogeneities in the regolith lead to exceptions. In the Lehstenbach catchment one out of 13 groundwater wells is characterised by confined groundwater (Lischeid, pers. comm.) and at the sampling site GW II in the Lysina catchment two different aquifers were encountered (cf. Section 6.1.3).

The lower confining bed of the aquifer in the model is given by the bedrock surface. Groundwater flow in the fractured granite is neglected. The Lehstenbach catchment exhibits a deep regolith and therefore a thick aquifer. Thus, on a quantitative basis groundwater cycling in deep fracture zones should be negligible. For the Lysina catchment nothing is really known

about the importance of groundwater cycling through fracture zones. The fast response of sulphate concentrations to decreased depositions at weir 1 (cf. Fig. 3.5A) however, rather indicates that groundwater flow is limited to the shallow regolith.

Besides, it is assumed that groundwater entirely discharges to the stream. For the Lehstenbach catchment this has been shown by groundwater gradients and subsequent discharge measurements along streams. These showed that the streams are gaining throughout their courses (Lischeid *et al.*, 2001). Groundwater contour maps generated for the sites GW I, GW II, and GW III in the Lysina catchment also indicate groundwater discharge to the streams (Fig. 6.4). Only the piezometer GW IIb exhibiting a second aquifer (cf. Section 6.1.3) does not seem to be connected to the local stream system.

The upwelling of groundwater in the vicinity of the stream is neglected in the model. In the Lysina catchment it should not play a great role due to the shallow regolith depth. In contrast, in the Lehstenbach catchment the deepest groundwater has to be uplifted by several tens of meters. In general however, this process is limited to the adjacent meters around a stream. Further, it is likely to take place very rapidly. All the water of a slope has to flow through the stream bed into the stream. This results in a substantial decrease of the flow's cross-section. Therefore, flow velocities strongly increase compared to the lateral groundwater flow and water residence times are likely to be very short in the vicinity of the stream.

Analysis of Flowpath Lengths

Often, the gradient of the groundwater table follows the topography. In most cases though, it may be to some extent flatter and local heterogeneities of the surface may level out. Therefore, it is appropriate to generate groundwater flowpaths along the topographic gradients (cf. Section 5.2.2). The error associated with this is likely to be small. The assumption that flowpaths terminate perpendicular to the stream, however, is problematic. The groundwater contour maps of the sampling sites in the Lysina catchment clearly indicate that groundwater flow occurs rather parallel to the stream (Fig. 6.4). Besides, obviously not all groundwater is directly connected to the adjacent stream such as observed at GW IIb, where a second aquifer was encountered (cf. Section 6.1.3). Hence, it is concluded that the derived flowpath lengths underestimate the ones prevailing in the catchments.

Concept of Sulphate Dynamics

The sulphate model considers convection, hydrodynamic dispersion, and equilibrium sorption. All sulphate in the system is of anthropogenic atmospheric origin.

Natural sulphate deposition, which occurred before the industrialisation, is neglected. It should be small compared to the peak deposition of the 1970s and 1980s. This is indicated by present deposition fluxes measured in the catchments. They comprise only 20 % of peak fluxes, but should still be higher compared to the pre-industrial ones. In New Zealand e.g., sulphate depositions of 0.03 kmol ha^{-1} yr^{-1} were measured (Scheffer & Schachtschabel, 1992).

The maximum deposition of the Lehstenbach scenario however is 2.25 kmol ha^{-1} yr^{-1}. The actual deposition is 0.46 kmol ha^{-1} yr^{-1} (cf. Appendix D).

Sulphur sources of the bedrock are not taken into account. Granite in general contains only traces of sulphur and the release by weathering is very small as well (Mückenhausen, 1993). Further, in the Lysina catchment stable sulphur isotope ratios were measured in throughfall, bulk precipitation, and runoff. These were very similar. Values of bedrock however, were distinctly different (Novák, 1998; Novák, pers. comm.). Hence, the influence of bedrock sulphur on the catchment's sulphate dynamics seems to be negligible.

The organic pool of sulphur is assumed to be stable and not to influence sulphate dynamics. In most forested catchments it exhibits the greatest part of the sulphur pool (Reuss & Johnson, 1986). However, under natural conditions the main part of that seems to be stable and hardly reactive (McLaren *et al.*, 1985; Mitchell *et al.*, 1989). Nevertheless, stable sulphur isotope studies for both catchments revealed that cycling of sulphate through the organic pool takes place (Novák *et al.*, 1996; Alewell & Gehre, 1999). The influence of this pool on sulphate dynamics should have played a minor role during peak depositions, as inorganic sulphate deposition largely exceeded organic cycling (Alewell, 2001). The role of the pool for the recovery from acidification, however, is uncertain. Net-mineralisation of sulphur being immobilised during peak depositions might occur and might lead to a greater retardation than associated with the sulphate desorption (Torssander & Mörth, 1998).

Reduction processes as net sulphate sinks in the catchments are neglected in the model. For the Lysina catchment it is already discussed in Section 7.1.3 that their importance at the catchment scale is limited. For the Lehstenbach catchment stable sulphur isotope studies indicate sulphate reduction to occur in the wetland soils of the catchment (Alewell & Gehre, 1999). Lischeid *et al.* (2000) however, who investigated sulphate patterns in runoff, conclude that the significance of this sink is only small at the catchment scale.

Sulphate transport in transverse directions to the water flow direction is not taken into account in the model. It can only occur by dispersion. Comparing field-scale dispersivities however, Gelhar *et al.* (1992) found that transverse dispersivities in general were at least one order of magnitude smaller compared to the longitudinal dispersivities. Even high longitudinal dispersivities have only minor effect on model results (cf. Section 6.3.3). Thus, effects should even be less for transverse dispersion considering the fact that concentration gradients between adjacent flowpaths should be similar to these occurring within one flowpath.

Sorption is modelled as equilibrium sorption. The kinetics of the sorption process are neglected, as for sulphate adsorption and desorption occur very rapidly. This is already pointed out in Section 2.2. Irreversible sorption, i.e. sulphate being adsorbed but never released again, is also excluded from the model. For the Lehstenbach regolith however, Schweisser (1998) found only 65% of sulphate to be reversibly bound. Thereby, NaH_2PO_4 is defined to extract total solid bound sulphate. H_2O is defined to extract the reversibly bound fraction. The latter fraction however, is likely to be underestimated due to the analytical procedure. This is indicated by sulphate contents which resulted from the experimental determi-

nation of desorption isotherms using the same samples (Schweisser, 1998). These isotherm determinations were conducted in the same way as the determination of H_2O extractable sulphate. Only the soil : solution ratios and the number of extraction steps were different. Both methods should therefore extract the same pool of sulphate. However, sulphate contents which resulted from the isotherm determinations were markedly higher than those of the H_2O extraction and in the range of values of the NaH_2PO_4 extraction. This suggests that the delimitation between the total and the reversibly bound pool of sulphate is not so clear. Hence, it was refused from the implementation of the process in the model.

7.2.3 Sulphate Adsorption, Desorption, and Hysteresis

Laboratory investigations on sulphate adsorption and desorption behaviour in soils revealed a clear discrepancy between the two (Alewell, 1995; Gobran *et al.*, 1998; Schweisser, 1998). Adsorption isotherms were found to run flat. Hence, large amounts of sulphate can only be adsorbed for high sulphate concentrations in solution. Desorption however, the reversal, was found to take place only at small concentrations in solution, but then in large quantities. This leads to the typical convex shape of the desorption isotherm, whereas the adsorption isotherm is rather linear for the given range of concentrations in solution (cf. Fig. 5.3). The effect of different adsorption and desorption pathways is often referred to as hysteresis.

For the Lehstenbach catchment, it is distinguished between adsorption and desorption. Adsorption isotherms are considered for increasing sulphate concentrations at a given point in space and time. For decreasing sulphate concentrations, desorption isotherms are taken into consideration (cf. Section 5.2.3). The problem, however, is the transition from the adsorption isotherm to the desorption isotherm for the change from increasing to decreasing concentrations in solution. Schweisser (1998), from whom the isotherm parameterisation was taken, only determined adsorption isotherms for high sulphate concentrations in solution and desorption isotherms for low concentrations in solution. Based on the observations of Alewell (1995) and Gobran *et al.* (1998), the model simplistically assumes stable sulphate contents on the solid phase for the transition phase. This has the implication that adsorbed sulphate is released from the solid phase at only much lower concentrations in solution. For the Lysina catchment, the process is not implemented, as isotherms are very uncertain. They do not allow for the distinction between different adsorption and desorption pathways (cf. Section 7.1.2).

Modelling the Lehstenbach catchment with either adsorption or desorption isotherms leads to completely different model results (Fig. 6.9). Adsorption isotherms run fairly linear for the given concentrations in solution (cf. Fig. 5.3). Thus, retardation is hardly dependent on the concentration in solution (very low k value; cf. equation (5.21)), and for a single flowline the shape of the modelled output curve resembles the deposition fluxes, which define the upper boundary.

Desorption isotherms have been used to model sulphate dynamics in the Lehstenbach catchment with the zero-dimensional lumped MAGIC model (Alewell, 1995; Jungnickel, 1996; Schweisser, 1998; Manderscheid *et al.*, 2000a; Matzner *et al.*, 2001). Fig. 6.9, however,

reveals that these isotherms lead to very unrealistic results when including transport processes in the model. For a 500 m flowpath, which corresponds to a depth of 8.9 m, and the standard parameterisation, the breakthrough does not take place before 2040. Further, the increase is very steep, and maximum concentrations are achieved only 5 to 10 years after the first breakthrough. This behaviour is due to the convex shape of the desorption isotherm (cf. Fig. 5.3). For small sulphate concentrations in solution retardation is great, as the slope of the isotherm is steep. For higher concentrations, the slope of the isotherm markedly flattens. Thus, retardation is clearly less. The peak concentrations therefore move faster compared to the initial concentrations from the beginning of the industrialisation and they finally catch up the lower concentrations. Such steep increases, however, have not been observed in the catchments. Furthermore, retardation is too pronounced with the desorption isotherms. Even for the parameterisation "fast" the maximum depth of sulphate at present is only 10 m (flowpath length 575 m). For the other parameterisations it is less. This is neither in accordance with the depth specific groundwater samples (Rötting, 2000) nor with the sulphate contents on the solid phase (Schweisser, 1998). In 10 m depth Schweisser (1998) found sulphate contents of more than 1 µmol g^{-1} on the solid phase. Rötting (2000) found sulphate concentrations of more than 0.2 mmol l^{-1} in depths below 10 m. It is concluded that the desorption isotherms are unsuitable to describe the catchment's sulphate dynamics of the last one and a half centuries.

The hysteresis combines adsorption and desorption properties. For increasing concentrations in solution simulated values resemble these which are modelled with the adsorption isotherms (Fig. 6.9). However, values do not reach the same maximum, but show a rapid decrease, which starts earlier. Due to decreasing sulphate concentrations in precipitation, the transition phase between adsorption and desorption isotherms sets in (Fig. 5.3). The solid phase therefore becomes inactive. Retardation is zero, and sulphate is convected through the system, which leads to the earlier decrease. Only at low sulphate concentrations of approximately 0.1 mmol l^{-1} desorption sets in. The slope of the desorption isotherm is steep. Thus, retardation is great, which results in the pronounced tailing of the curve compared to the one, which is modelled with only adsorption isotherms.

7.2.4 Parameterisation

The parameterisation of the sulphate model is associated with a number of uncertainties and simplifying assumptions. Spatial heterogeneity is only taken into account for the sorption isotherms by the Monte-Carlo simulations. All other parameters are modelled homogeneously. Certainly, this is a great simplification. However, the most sensitive parameters, the proportion of the fine soil fraction and the regolith depth, influence the delay of sulphate transport in a monotonic way for a given flowpath length. The maximum proportion of the fine soil fraction and maximum regolith depth result in a maximum delay. The minimum proportion of the fine soil fraction and minimum regolith depth result in a minimum delay (cf. Section 6.3.3). As the extent of delay is the main cause of different model results, the given

extreme parameterisations lead to extreme model results. Therewith, the limits of the model results are obtained for the given heterogeneity and uncertainty of the parameterisation.

In the following, the single parameters will be addressed in detail.

Deposition Scenario

The deposition scenario defines the time series of sulphate input into the catchment. It is therefore crucial for the model results. On site measurements, however, have only been conducted since the late 1980s and early 1990s. For the one and a half centuries before only estimates are available, which are highly uncertain. For the Lysina catchment these estimates are based on local coal mining activity (Hruška & Krám, unpublished data). In this catchment sorption isotherms are flat, the regolith is shallow, and flowpaths are short. Thus, sulphate retention is small and stream and groundwater sulphate concentrations depend on the deposition of a few preceding years. Therefore, the scenario is of minor relevance. For the Lehstenbach catchment greater sorption capacities, a deeper regolith, and longer flowpaths lead to a greater retention. Consequently, deposition fluxes of a longer preceding period are important. Local estimates, however, are not available. Different authors therefore have used different scenarios for their sulphate simulations, which differ significantly (Alewell, 1995; Schweisser, 1998; Manderscheid *et al.*, 2000a). The total cumulative sulphate deposition flux of the scenario employed by Manderscheid *et al.* (2000a) is 197 kmol ha^{-1} for the period from the beginning of the industrialisation until present. The scenario of Alewell (1995) amounts only to 128 kmol ha^{-1}. In this study the scenario of Alewell (1995) was applied. On the one hand this resulted from the fact that in first model runs the scenario of Manderscheid *et al.* (2000a) led to unreasonably high sulphate concentrations in model results. On the other hand, the scenario of Alewell (1995) is more similar to the Lysina local scenario (cf. Appendix D), when rescaled by the present ratio of throughfall fluxes of 0.85. This should be expected due to the vicinity of the catchments and the fact that the main part of sulphate deposition in the Lehstenbach catchment during the last decades was delivered from East. This is indicated by increased SO_2 concentrations which were measured in the air during easterly wind directions (Peters & Gerchau, 1995).

Isotherms

The isotherm is the controlling factor of sulphate retardation and has therefore a great influence on model results. Its spatial heterogeneity is taken into account by Monte-Carlo simulations. The step width in space in the model is 0.5 m for the unsaturated zone and 5 m for the aquifer. For each point of discretisation in space a new set of random isotherm parameters is generated. Therewith, the assumed correlation length of the isotherms is smaller than 0.5 m. This assumption is justifiable. In the Lehstenbach catchment, isotherms determined in the topsoil did not show any spatial dependencies at sampling grid sizes of 20 x 20 m (Manderscheid *et al.*, 2000a). Further, vertical profiles of isotherms at a scale of less than a meter revealed a great variability in some cases (Schweisser, 1998). Lysina isotherms also

indicate a great spread for samples from single drilling cores (cf. Appendix C), so that a significant difference between different sampling sites could not be detected (cf. Section 6.1.2).

The model does not consider the higher sorption capacities in the topsoil. In the Lehstenbach catchment the mean soil pH (H_2O) in the B horizons is 4.2, in the deeper regolith it is 5.3 (Manderscheid *et al*., 2000a; Manderscheid *et al.*, 2000b). In the Lysina catchment the mean pH (H_2O) of B horizons is about 4 (Krám, 1997), in the deeper regolith values of above 5 were measured (Fig. 6.2E). Several authors showed that sulphate sorption is highly dependent on soil pH with maximum sorption capacities occurring at a pH of about 4 (Nodvin *et al.*, 1986; Courchesne & Hendershot, 1989). Further, Alewell (1995) found clearly steeper adsorption isotherms in the B horizons of the Lehstenbach catchment than Schweisser (1998) found in the deeper regolith. However, it has to be taken into consideration that the sorption capacity in the topsoil might have changed over time. Increased acid depositions especially in the second half of the last century are likely to have caused a decrease of pH in the soils. For instance, forest soils in Germany were generally found to have lower pH values compared to soils from New Zealand, which developed under similar climatic and geological conditions (Matzner & Davis, 1996). Decreased pH values might then only have led to an increase of sulphate sorption capacities in the topsoil. Due to these uncertainties associated with the topsoil isotherms, neglecting them seems to be justifiable when considering the whole regolith.

On the whole, the uncertainty associated with the isotherms is considerable. In addition to the above considerations on topsoil isotherms, in the Lehstenbach catchment isotherms were only determined at eight sites for the upper 10 m of the regolith (cf. Section 5.4.2). Nothing is known about sorption properties in the deeper regolith. Lysina isotherms are highly uncertain as well, which is due to the problems with the laboratory method (cf. Section 7.1.2). Within the scope of this, the uncertainty associated with the distribution of isotherm parameters (Section 6.3.1) seems to be negligible. However, for the Lehstenbach desorption isotherms it has to be considered that k values are likely to be overestimated for low maximum sorption capacities b (cf. Fig. 6.7). In these cases, the initial slopes of the isotherms tend to be too steep. Thus, following adsorption and the hysteresis loop, the desorption sets in at too low concentrations in solution (cf. Fig. 5.3).

Proportion of the Fine Soil Fraction

The fine soil fraction was introduced, as only this effectively contributes to sulphate sorption. Especially for the Lehstenbach catchment drilling profiles reveal a very heterogeneous regolith (Rüdiger, 1993a; Schweisser, 1998). Loamy sand and fine grained weathered granite alternate with massive granitic woolsacks of up to several meters in diameter. The estimation of the proportion of the fine soil fraction by upscaling of values determined for single drilling profiles (cf. Section 5.4.2), however, is highly uncertain.

Theoretically, a change of the proportion of the fine soil fraction equals a change of the isotherm parameters. A decrease, for instance, results in a smaller proportion of active surfaces which are available for sorption. For the model, this has the same effect as a decrease

of the sorption capacity (K_d in equation (5.20) and b in equation (5.21)) for a constant proportion of the fine soil fraction. Therewith, the considerable sensitivity of the model with respect to the proportion of the fine soil fraction also demonstrates the influence of the isotherms on model results.

Regolith Depth and Water Flow Regime

For both catchments the regolith depth is uncertain. In the Lehstenbach catchment geophysical measurements are only available for 11 points (Rüdiger, 1993a). The derived regolith depth varies between 5 and 42 m. For the Lysina catchment measurements along three horizontal profiles revealed a regolith depth between 0.5 and 4 m (Gurtler & Nikl, 1999). The small scale heterogeneity was considerable. Therefore, the maximum regolith depth is the most uncertain parameter of the basic slope, which defines the water flow regime in the model (cf. Section 5.2.1).

From the parameterisation of the basic slope a hydraulic conductivity of the aquifer arises. Further, theoretical residence times of the stream water sampling sites can be calculated based on the water flow velocity and the distribution of flowpath lengths. A comparison with measured values may indicate the extent to which the basic slope approach and its parameterisation are consistent with independent data. The values given in the following refer to the standard parameterisation. For the Lehstenbach catchment the hydraulic conductivity of the deeper aquifer in the model is 8.6×10^{-6} m s^{-1}. Pumping tests revealed a mean hydraulic conductivity of 2.8×10^{-6} m s^{-1} (Hauck, 1999). Water residence times calculated from the model are 4.1 yrs for the main weir, 4.6 yrs for the Köhlerloh sampling site, and 2.3 yrs for the Schlöppnerbrunnen spring. Therewith, they are in the same range as values determined by oxygen isotope studies. These are 3.6 yrs for the main weir and 4 yrs for the Schlöppnerbrunnen spring (Zahn, 1995). For the Lysina catchment the hydraulic conductivity of the aquifer in the model is 2.3×10^{-5} m s^{-1}. This is in accordance with literature values for weathered granite, which range from 0.3 to 5.2×10^{-5} m s^{-1} (Morris & Johnson, 1967, cit. in Spitz & Moreno, 1996). Calculated residence times are 1 yr for weir 1, 1.9 yrs for weir 2, and 2.1 yrs for the Lenka spring. Oxygen isotope studies were only conducted for the main catchment (Buzek *et al.*, 1995). They revealed a mean water residence time of 1.1 to 1.5 yrs for weir 1, which is very similar to the model residence time of 1 yr. On the whole, measurements and model values are in the same range for both catchments. Therefore, it is concluded that the basic slope approach is appropriate for the description of the water flow regime at the catchment scale.

Porosity, Field Capacity, and Dispersivity

The parameters porosity, field capacity, and dispersivity are likely to be subject to substantial spatial heterogeneity. However, not much is know about this. The field capacity is only estimated by values determined for C horizons in the Lehstenbach catchment. Dispersivity values are entirely based on literature values, as are the porosity values for the Lysina catchment (cf. Section 5.4.1 and 5.4.2). The model, however, is not very sensitive with re-

spect to these parameters (cf. Section 6.3.3). Therefore, the rough estimates are assumed to be appropriate.

Effective porosity values for the Lehstenbach catchment were determined by investigating groundwater level fluctuations. The intention was to reveal possible depth gradients. Fig. 6.6, however, demonstrates that values show a considerable spread. The method assumes that all precipitation of a given period directly infiltrates into the soil and entirely contributes to groundwater recharge (cf. Section 5.4.1). Only periods of shorter than a month were considered, in order to ascertain little lateral groundwater discharge. For a mean hydraulic conductivity in the aquifer of 2.8×10^{-6} m s^{-1}, an effective porosity of 0.05 (both values: Hauck, 1999), and an angle of inclination of 4.6° (model parameterisation; cf. Section 5.4.1) the lateral groundwater flow amounts to 12 m for a month and is therefore small. Furthermore, only winter periods were considered, as for these periods evapotranspiration is negligible. However, winter periods are often characterised by snowfall, a snow covering, and thaw. So, all but one of the considered periods exhibited temperature values below 0 °C for the period itself or the week before. Snow is therefore likely. Due to the snow storage groundwater recharge is then not necessarily given anymore by the amount of precipitation in the considered period. This may explain the great variability of determined porosity values. A depth gradient could not be determined. Thus, the median of values was taken for the model parameterisation. It amounts to 0.09 (and to 0.17 when converted to total porosity; cf. Section 5.4.1 and 6.3.1). This value is similar to the value of 0.08 determined by Rüdiger (1993b) and that of 0.05 determined by Hauck (1999). Using the value in the model parameterisation therefore seems to be justifiable.

7.2.5 Rounding Errors

Rounding errors arise from the fact that on the computer numbers are stored as floating-point numbers, which have a limited number of mantissa digits. Rounding is performed after each arithmetic operation. Unsuitable operations such as the subtraction of almost equal numbers can lead to a maximum deletion of digits. The results of such operations are therefore associated with a great error (Bronstein *et al.*, 1999). For the applied explicit numerical scheme (cf. Section 5.3.1) this could lead to fatal consequences, as the error would be passed on from one timestep to the next. For a simulation period of 250 years 25000 timesteps have to be passed through.

The error is assessed by comparing the cumulative sulphate input flux into the system with the cumulative sulphate output flux. For a sufficiently long time interval all sulphate which has entered the system should have left it. Thus, sulphate input should equal sulphate output. In fact, it is only the 15th digit, for which these numbers differ. This exactly reflects the given inaccuracy of the employed “double” numbers (Breymann, 1999). Hence, it is concluded that rounding errors are negligible and do not have any effects on model results.

7.3 Model Application

7.3.1 Lehstenbach Catchment

Model results for the Lehstenbach catchment exhibit great differences with respect to the employed parameterisations. This is illustrated by the profiles of groundwater sulphate concentrations of the wells GW 04 and GW 05 (Fig. 6.14). For the parameterisation “fast”, which represents minimum delay of sulphate transport (cf. Section 6.4.1), sulphate has already reached the bottom of the regolith. In contrast, for the parameterisation “slow”, which represents maximum delay, the breakthrough of sulphate has only taken place for the shortest third of flowpaths. Hence, with the given uncertainties of the parameterisation model results exhibit a great range and are clearly not unique. In the following, single sites will be addressed separately.

Main Weir

For the main weir, simulated sulphate concentrations in the middle-term trend (Fig. 6.10A) are lowest for the parameterisation “slow”. For the other parameterisations concentrations are substantially higher. This behaviour can be explained by considering the depth profile of concentrations. It is not explicitly given for a stream point, thus the lower end of the basic slope (cf. Fig. 5.1). The well GW 04, however, is located in stream vicinity. Therefore, its profile is very similar to the one of a stream point and it will be referred to this during the following considerations (Fig. 6.14A). For the parameterisations “standard” and “fast” the breakthrough of sulphate has taken place for the main proportion of flowpaths and sulphate has reached great depths. Thus, the main proportion of flowpaths contributing to discharge, which reach up to 1550 m length (cf. Fig. 5.5A), contains sulphate. For the parameterisation “slow” the sulphate breakthrough has only taken place for the short flowpaths. Consequently, there is a considerable proportion of flowpaths contributing to discharge which does not contain any sulphate. It is this proportion, which leads to the lower sulphate concentrations in the middle-term trend.

Observed sulphate concentrations at the weir are best described by the simulations of the parameterisation “slow”. Simulated values of the other parameterisations are too high. Such a behaviour could be ascribed to an overestimation of sulphate input fluxes. However, this is very unlikely, as the scenario with the lowest input fluxes available was chosen for the parameterisation. For this, peak fluxes in the late 1970s are only 20 % higher than maximum measured fluxes in the late 1980s (cf. Appendix D). Therefore, the low concentrations measured can only be explained by a clear depth gradient.

The model is able to reproduce the envelopes of the considerable short-term variability of measured sulphate concentrations. For the parameterisation “slow” this is done in Fig. 6.11A. Stormflow is mixed by the three shortest flowpaths representing the interval of 0 to 150 m length. These flowpaths exhibit a maximum depth of 1.9 m. This is in agreement with

the conception according to which stormflow in the Lehstenbach catchment is primarily generated from the topsoil layers in the riparian zone (Lischeid *et al.*, 2001). It is not possible to model stormflow sulphate concentrations by only considering the very shortest flowpath (25 m). It reacts very rapidly to the strongly decreased depositions of the last decade. Thus concentrations in 1999 are only approximately 0.1 mmol l^{-1}, whereas measured values are around 0.17 mmol l^{-1}. This indicates that even water generating stormflow has some retention time. At present it may not anymore be the uppermost layer which is responsible for the higher stormflow concentrations, but slightly deeper layers, which exhibit still higher concentrations.

The remaining flowpaths represent the deeper groundwater, thus baseflow. As with the mean runoff it is again the clear depth gradient which leads to the low concentrations, which are in the range of measured baseflow concentrations. For the parameterisations “standard” and “fast”, which do not exhibit such a pronounced depth gradient, it is also possible to mix a baseflow with concentrations similar to the measured ones. In these cases, however, such low concentrations can only be generated by considering the very longest flowpaths (cf. Fig. 6.14A). Therewith, it is not anymore possible to mix a stormflow from the remaining shorter flowpaths. It would not show a similar quick response to decreased depositions such as the measured stormflow does.

Köhlerloh

The distribution of flowpath lengths of the Köhlerloh sampling site is very similar to that of the main weir with respect to both the shape and the range of flowpath lengths (Fig. 6.5). As it is only the distribution of flowpath lengths, which distinguishes between the sites, simulated middle-term trends of both sites are also very similar (Fig. 6.10A and B). This is in accordance with the observed patterns, which exhibit very much the same sulphate dynamics for both sites in the middle- and the short-term trend.

Schlöppnerbrunnen

The distribution of flowpath lengths of the Schlöppnerbrunnen subcatchment is distinctly different compared to that of the whole catchment and the Köhlerloh subcatchment (Fig. 6.5). The maximum flowpath length is less than 500 m. Consequently, runoff is generated from only short flowpaths, for which sulphate concentrations are high (cf. Fig. 6.14A). For that reason the level of simulated concentrations at the Schlöppnerbrunnen site is higher compared to that of Köhlerloh and the main weir (Fig. 6.10C). The difference is most pronounced for the parameterisation “slow”. This parameterisation exhibits the clearest depth gradient (cf. Fig. 6.14A). Therefore, the effect of omitting the long flowpaths is strongest.

Measured sulphate concentrations at the Schlöppnerbrunnen spring are also markedly higher compared to these of Köhlerloh and the main weir. The model is able to reproduce this general difference by only altering the contribution of different flowpath lengths. However, in the simulations the decrease of sulphate concentrations starts clearly earlier compared to the observations. There are two possible explanations. Firstly, the delimitation of the subcatch-

ment for the Schlöppnerbrunnen spring is difficult, as it is situated at a slope with diverging flowpaths. Therefore, the distribution of flowpath lengths is uncertain. Secondly, the length of the unsaturated zone of the subcatchment is likely to be underestimated by the model. The maximum flowpath length of the subcatchment is about 500 m. This corresponds to a maximum depth of the theoretical groundwater level of 8.9 m below surface (b.s.) (standard parameterisation). However, two drillings were performed at the same slope, one approximately 250 m north-west of the spring, the other one approximately 500 m north-east of the spring. For both of them, in 10 m depth the water table was not reached. An underestimation of the length of the unsaturated zone by only a few meters has great effects on model results. This is due to the small water flow velocity in the unsaturated zone in the model compared to that in the aquifer (cf. Section 5.2.1). Thus, water residence times for that part of a flowline (cf. Fig. 5.1) are fairly high. For a 10 m long unsaturated zone, for instance, the mean water residence time is 1.9 yrs. For 20 m it amounts to 3.6 yrs. Such an underestimation would also explain the shorter water residence time calculated from the model parameterisation of 2.3 yrs (standard parameterisation) compared to the measured one of 4 yrs (Zahn, 1995). Further, a longer unsaturated zone leads to a longer residence time of sulphate. It may thus be one important reason for the delayed decrease of observed concentrations at the spring.

The Schlöppnerbrunnen spring does not exhibit a pronounced short-term variability of runoff chemical patterns such as the main weir and Köhlerloh. Lischeid (2001b) deduces this to the absence of a riparian zone with a shallow groundwater table. He concludes that stormflow runoff at this spring generates from the deeper groundwater by piston flow displacement and has therefore the same origin as baseflow. For sulphate, the model reveals a further explanation. The range of flowpaths is small compared to that of the main weir and Köhlerloh (Fig. 6.5). Thus, there are no long flowpaths for which the breakthrough of sulphate has not yet taken place (cf. Fig. 6.14A). These however are the flowpaths, which enable the low baseflow concentrations at the main weir. Hence, for the Schlöppnerbrunnen site there is no potential for the generation of a low concentration baseflow and thus the range of concentrations could never be so large.

Groundwater Wells

The middle-term trend of sulphate concentration at the groundwater wells GW 04 and GW 05 is simulated by one flowpath each. When comparing these values with the measured time series of depth integrated samples, it has to be taken into account that for the latter groundwater from different depths and thus different flowpaths is mixed. There are groundwater flow logs of the wells (Rötting, 2000). Hence, the approximate range of depths of the integrated samples is known. However, these depths are subject to local water flow patterns and do not correspond to the schematic approach of the basic slope. It is thus uncertain which flowpaths really contribute to the depth integrated samples.

The differences between the parameterisations are great (Fig. 6.13). For the parameterisation “slow” an increasing trend is simulated until present. It is due to the delay of the

sulphate breakthrough for the considered flowpath. This is in accordance with the observed concentrations, which exhibit a clear increase at GW 05 until present and at GW 04 until the mid 1990s. These increases can therefore be explained quantitatively by sorption processes with the given isotherm parameterisation.

Profile of Groundwater Sulphate Concentrations

The simulated profile of dissolved sulphate exhibits a clear peak for both groundwater wells modelled, which slowly moves into greater depths (Fig. 6.14). Such a pattern is consistent with the significantly negative correlation of sulphate concentrations with depth for the depth integrated groundwater samples, which is found at six out of 13 wells in the Lehstenbach catchment (cf. Section 3.2). At the well GW 03 a change of this relationship with time can even be observed. Since the late 1980s concentrations at a high groundwater level slightly decreased, whereas concentrations at a deep groundwater level slightly increased (Lischeid, pers. comm.). This indicates a relocation of sulphate into deeper layers such as obtained with the simulations.

Depth profiles of dissolved sulphate could further be observed at other sites. Robertson *et al.* (1989) investigated groundwater profiles at a distance of approximately 100 km from the Sudbury nickel-copper smelters, which were the largest point source of atmospheric sulphur emissions in North America. In an unconfined silty sand aquifer of 40 m depth peak sulphate concentrations were observed in about 5 to 10 m depth. Values above and below this depth were markedly lower. This pattern is explained by the high sulphate depositions in the area during the 1960s. Further, Meiwes *et al.* (1994) reports on sulphate gradients in a Triassic sandstone in northern Germany with high sulphate concentrations in the upper up to 7 m and clearly lower concentrations below.

In the Lehstenbach catchment depth specific groundwater sampling in the upper half of the aquifer did not reveal a clear pattern (Rötting, 2000). This discrepancy between measurements and simulations may be due to the following reasons. Firstly, at maximum four samples were taken at a profile. This resolution might not be sufficient to see any profiles such as an undulation. Secondly, measurements and simulations consider a different scale. At the small scale of the measurements local heterogeneities prevail. These lead to different water flow patterns and sorption capacities compared to these of the schematic basic slope approach of the model. Clear shapes are most likely to be disturbed by this. Therefore, a comparison of values is difficult and the depth specific samples cannot be seen as a proof for a non-existing gradient at the larger scale.

Profile of Solid Bound Sulphate

For the given range of concentrations in solution the adsorption isotherms run fairly linear (cf. Fig. 5.3). A sorption maximum is therefore clearly not reached.

Simulated solid bound sulphate contents for the well GW 04 exhibit a considerable spread (Fig. 6.15), which results from the random sorption properties of the Monte-Carlo

simulations. For the upper part of the profile, a clear shape cannot be observed. Besides the random isotherms, this effect is due to the implemented hysteresis between adsorption and desorption isotherms (cf. Fig. 5.3). When sulphate concentrations in solution start to decrease, the transition period between the adsorption and the desorption isotherm sets in. The solid phase therefore becomes inactive until the desorption isotherm is reached. This is at only low concentrations in solution of about 0.1 to 0.2 mmol l^{-1}. At present these concentrations are only achieved for the very top layers (cf. Fig. 6.14). For the main part of the upper profile therefore, the transition period predominates. Hence, simulated solid bound sulphate contents represent the values, which were attained during peak concentrations, and are rather constant with respect to the last decade. For other wells, i.e. different positions at the basic slope (cf. Fig. 5.1), the profile resembles that of GW 04. Highest sulphate contents are achieved in the upper parts of the profiles, which the peak of dissolved sulphate has already passed. Below, sulphate contents decrease with depth.

Generally, simulated sulphate contents (cf. Fig. 6.15) are lower than the median of measured sulphate contents (NaH_2PO_4 extr.) of 0.58 µmol g^{-1} for the upper 10 m of the regolith (Schweisser, 1998). This indicates an underestimation of the sorption capacities of the solid phase. Adsorption isotherms are slightly too flat. Besides, the sorption capacities being too low, also explains the underestimation of the total pool of sulphate in the model compared to the measured one of Schweisser (1998).

Parameterisation “slow” versus “standard” and “fast”

The middle-term trend of sulphate concentrations at the main weir is best matched by the parameterisation “slow”. Only a strong depth gradient with long flowpaths for which the breakthrough of sulphate has not yet taken place enables the low concentrations. The envelopes of short-term variability for the main weir can also only be reproduced with the strong depth gradient of the parameterisation “slow”. Further, the difference between the Schlöppnerbrunnen spring with high level sulphate concentrations and only short flowpaths and the main weir with lower sulphate concentrations in the middle-term trend and a large proportion of long flowpaths is best reproduced with the strong depth gradient of the parameterisation “slow”.

Therefore, the system is best described by the parameterisation “slow” and there is evidence that sulphate has not yet reached greater depths. At the well GW 04, for instance, the maximum flowpath lengths exhibiting sulphate for the parameterisation “slow” is 600 m (Fig. 6.14A). This corresponds to a depth of the sulphate front of 13.5 m for that well.

A clear depth gradient is also the only way to approximately bring in line the deposition scenario with a cumulative sulphate flux of 128 kmol ha^{-1} (Alewell, 1995) and the sulphate pool of the upper 10 m of the regolith of 94 kmol ha^{-1} (Schweisser, 1998). Extrapolating this sulphate pool to the mean regolith depth of 32 m (Rüdiger, 1993a) would result in a pool of 300 kmol ha^{-1}. Such a value could never be explained by the sulphate deposition of the last one and a half centuries.

There is another implication of the above considerations: For the parameterisation "slow" not even half of the sulphate which has entered the system by anthropogenic deposition has left it at present (Fig. 6.16A).

7.3.2 Lysina Catchment

The main differences of the Lysina catchment compared to the Lehstenbach catchment are the shorter flowpaths, the shallower regolith depth, and the flatter isotherms (cf. Tab. 6.3). Therewith, the delay of sulphate transport is generally low and differences between the different parameterisations, which control the extent of delay, are much less pronounced than for the Lehstenbach catchment.

Weir 1

More than 50 % of the flowpaths of the main catchment are shorter than 50 m. For a 50 m flowpath the length of the unsaturated zone is 0.35 m, the water residence time derived from the model is 0.55 yrs, and the mean sulphate residence time amounts to 1.25 yrs (all values refer to the standard parameterisation). Hence, sulphate retention is very low and the simulated time series of mean sulphate concentration are very strongly determined by the specified sulphate input to the system (Fig. 6.17A).

This is in accordance with the observations. The middle-term trend of concentrations shows a quick response to decreased depositions. In the early 1990s sulphate output fluxes from the catchment approximately equalled input fluxes (Hruška & Krám, 1994; Krám & Hruška, 1994; Krám *et al.*, 1997), which indicated a rapid transport of sulphate through the catchment. At present however, the output from the catchment is about twice as high as the input (hydrologic year 2000; Krám, pers. comm.). This is attributed to the very low input fluxes and shows that in the catchment some retention takes place with respect to sulphate, even if it is very small. Due to the short flowpaths, sulphate output from the catchment lags only shortly behind the input. Therefore, meeting the middle-term trend of sulphate concentrations for that weir is very easy, if only the input fluxes are correct.

For the early 1990s measurements and simulations differ from each other (Fig. 6.17A). It is exactly this period, for which the input fluxes to the catchment are uncertain, as throughfall and bulk precipitation sampling was first initiated in 1991. The discrepancy indicates that estimated normalised input concentrations (cf. equation (5.22)) for that period are approximately 0.05 mmol l^{-1} too low.

The short-term variability of measured sulphate concentrations at weir 1 can be reproduced by the model. This is demonstrated by the range between the shortest and the longest flowpath (Fig. 6.18A). The shortest flowpath reacts very rapidly to the decreased depositions. The longest flowpath leads to a greater delay and exhibits still high concentrations. Thus, the range between the two clearly gapes during the 1990s. Such a pattern is also observed for the measured concentrations during baseflow and stormflow conditions at the weir. Until 1992 stormflow events generate both maximum and minimum sulphate concentrations, whereas

baseflow concentrations are in between the extremes. Since 1993 only the minima are generated during stormflow events and baseflow accounts for the high concentrations. This indicates that the pronounced depth gradient of concentrations with low concentrations in the top layers generating stormflow and high concentrations in the deeper layers generating baseflow (cf. Section 7.1.1) developed only during the early 1990s.

High sulphate concentrations measured in the early 1990s and low sulphate concentrations measured in 1995 cannot be explained by the range of concentrations between the shortest and the longest flowpath (Fig. 6.18A). For the high concentrations in the early 1990s this may be attributed to an underestimation of the sulphate input concentrations in the model as discussed above. The low concentrations measured in 1995 may be due to dilution effects as the amount of bulk precipitation in this year was 1154 mm. Therewith, it was distinctly higher than the mean annual precipitation of 933 mm in the catchment (Hruška & Krám, unpublished data).

Weir 2

In the simulations weir 2 differs from weir 1 by the higher deposition fluxes (entirely forested; cf. Section 5.4.2) and the different shape of the distribution of flowpath lengths with a markedly higher proportion of longer flowpaths (Fig. 6.5D and E). The higher deposition fluxes lead to the higher sulphate concentrations in the middle-term trend compared to weir 1 (cf. Fig. 6.17B). The contribution of longer flowpaths results in a delayed response to reduced deposition. This is consistent with the measured differences between the sites and may thus be an explanation for these.

Weir 2 does not show a clear short-term variability such as observed at weir 1, although it would be possible by the range of sulphate concentrations between the shortest and the longest flowpath in the model (cf. Fig. 6.18B). Especially low concentrations such as achieved for stormflow events at weir 1 do not occur at this site. The catchment of weir 2 is long and narrow (Fig. 3.3). There is only a small riparian zone with a shallow groundwater table in the vicinity of the weir. Further, the contribution of flowpaths being shorter than 50 m to discharge is only 13 % compared to 52 % for weir 1 (cf. Fig. 6.5D and E). Thus, compared to the main catchment, there is no such potential for the mobilisation of large amounts of shallow groundwater with low sulphate concentrations.

Lenka

For the spring Lenka, simulated and measured time series of sulphate concentrations do not match (Fig. 6.19A). The delay to decreased deposition is much more pronounced for measured values than for simulated ones. Only simulated values for the longest flowpath are approximately able to meet the observations (Fig. 6.19B). One reason for the discrepancy may be the great uncertainty which is associated with the isotherms (cf. Section 7.1.2). Sorption capacities might be underestimated by the model and retardation would therefore be too low. However, the problem is more likely to be rooted in the water flow regime of the model.

Lenka and weir 2 exhibit approximately the same distribution of flowpath lengths (cf. Section 6.2). Thus, simulated time series of sulphate concentration are very similar for the two. For weir 2 the simulations match the observations well. For Lenka it is not the case. The differences between the Lenka catchment and the catchment of weir 2 are very unlikely to be caused by different isotherms, as the catchments are only few meters apart from each other, the bedrock is the same, and for the main proportion of both the water table is deep. A different underlying hydrology is more likely. Firstly, the distribution of flowpath lengths for the Lenka catchment is very uncertain. An equal distribution was assumed, as the delimitation of a subcatchment is not possible due to diverging flowpaths (cf. Section 6.2). Secondly, the regolith depth is uncertain. Geophysical measurements revealed an approximate depth of 2 m for the lower part of the slope at which the Lenka catchment is situated (Gurtler & Nikl, 1999). Drilling at the site GW IV however, which is also located at that slope, could easily be performed until 3 m depth. The bedrock was not yet reached. Thus, the length of the unsaturated zone may be underestimated in the model. A longer unsaturated zone would explain the greater retardation of measured concentrations. Finally, groundwater cycling in the fractures of the granitic bedrock may play a role. It would lead to a longer residence time of water and therefore to a greater retardation as well.

Profile of Groundwater Sulphate Concentrations

The model reveals an increasing trend of sulphate concentrations with depth (Fig. 6.20A). This is a result of the rapid response of short flowpaths to reduced deposition, whereas long flowpaths exhibit a longer delay. Measured sulphate concentrations from the piezometers show the same general trend. Values however do not exactly match. As for the groundwater profiles in the Lehstenbach catchment (cf. Section 7.3.1) this may be attributed to local scale heterogeneities disturbing the clear pattern produced by the model.

Profile of Solid Bound Sulphate

The Lysina catchment is modelled with linear isotherms. For these, solid bound sulphate contents are proportional to the sulphate concentrations in solution (cf. equation (5.14)). Therefore, the profile of adsorbed sulphate resembles that of dissolved sulphate and exhibits an increasing trend with depth (Fig. 6.20B). Only the spread of values is greater which is a result of the random isotherms generated by Monte-Carlo simulations. The trend of measured sulphate contents is reverse (Fig. 6.2A). Thereby, measured and simulated values of the deeper layers agree well. Sulphate contents of the top layers, however, are very clearly underestimated by the model. There might therefore be a depth gradient of sorption capacity, which would explain the higher sulphate contents in the upper part of the profile. There might also be a hysteresis between adsorption and desorption isotherms, which would conserve higher sulphate contents in the top layers until sulphate concentration in solution are low (cf. Fig. 5.3). The uncertainty of the isotherms however is too great to reveal such features.

7.4 Potentials and Limitations of the Modelling Approach

The sulphate model considers transport and equilibrium sorption processes along one-dimensional flowpaths. The hydrology is described by the strongly simplified basic slope approach (cf. Fig. 5.1). The parameterisation is the same within a catchment and only the distribution of flowpath lengths distinguishes between different sites. Therewith, only a minimum number of processes which are discussed in connection with sulphate dynamics at the catchment scale is taken into consideration. This allows to examine the extent to which the observed patterns can be ascribed to individual processes. The model can therefore serve as a tool for the quantitative understanding of observed patterns.

The approach follows the suggestion of Beven (2001) according to which there is need to include spatially distributed observation in model application. The internal structure of the model allows to make use of all the available information provided by the observed sulphate time series. For evaluation, the spatial variability and further the short-term temporal variability is explicitly taken into account.

The parameterisation is based on measurements. None of the parameters was fitted by inverse modelling. Hence, model results and observations are entirely independent and no degrees of freedom are used for calibration.

The model is able to successfully reproduce the different observed middle-term dynamics at different sampling sites. Moreover, it is possible to simulate the envelopes of the considerable range of short-term dynamics at single stream water sampling sites by considering long and short flowpaths separately. The successful reproduction of the observed patterns with the simple model structure suggests that sulphate transport and sorption along flowpaths are in fact the decisive processes which shape sulphate dynamics at the catchment scale. For both the Lysina and the Lehstenbach catchment the consideration of other processes such as bacterial dissimilatory sulphate reduction, net-mineralisation from the organic pool or the precipitation and dissolution of sulphate mineral phases is not necessary.

The limits of the model are observed at a smaller scale than the catchment scale. It is not entirely possible to meet the middle-term trends of sulphate dynamics at the spring Schlöppnerbrunnen in the Lehstenbach catchment and the spring Lenka in the Lysina catchment. These limits, however, turn out to be potentials again, as they indicate the scale for which the model is not suitable anymore and at which other processes may become relevant. For both sites the discrepancy between simulations and observations is mainly attributed to hydrology (cf. Section 7.3.1 and 7.3.2). Firstly, for both the delimitation of a subcatchment is difficult. Therefore, the distribution of flowpath lengths assumed in the model may differ from the one prevailing in the field. Secondly, the regolith depth is uncertain and the validity of the basic slope approach (cf. Fig. 5.1) is not given anymore. In these cases the water flow regime of the model is too simplified for an appropriate description of the underlying hydrology. At the catchment scale these local deviations are likely to level out.

8 Conclusions

The observed spatial variability of sulphate patterns in stream water and groundwater in the Lysina and in the Lehstenbach catchment is reproducible. The sulphate model matches the different observed middle-term dynamics at different sampling sites. In addition, it succeeds in simulating the envelopes of the considerable range of short-term dynamics at single stream water sampling sites. This gives evidence that sulphate transport and sorption along flowpaths are the decisive processes which shape sulphate dynamics at the catchment scale. It further suggests that the different distribution of flowpath lengths, which is the only characteristic distinguishing between different sites in a catchment, is one of the main causes of the observed spatial variability. The patterns can therefore be explained quantitatively and are not subject to random variability.

The considerable proportion of short flowpaths in the Lysina main catchment (52 % are shorter than 50 m), which react very rapidly to decreasing atmospheric sulphur deposition, is responsible for the clear decrease of sulphate concentrations in the middle-term trend at the catchment outlet. In contrast, the greater proportion of longer flowpaths (up to 350 m) in the side catchment and the catchment of the Lenka spring causes the delay of recovery, which is observed at their outlets. In the Lehstenbach catchment, very long flowpaths of up to 1550 m length for the catchment outlet and Köhlerloh can explain that at these sites a recovery in the middle-term trend can hardly be observed. The Schlöppnerbrunnen spring, however, is characterised by shorter flowpaths with at maximum 500 m length, which leads to the decrease of sulphate concentration observed at this side.

For both catchments, modelling reveals a distinct depth gradient of dissolved sulphate. For the Lysina catchment, which exhibits a shallow regolith of at maximum 4 to 5 m depth, simulated concentrations are low in the upper part of the aquifer and markedly higher in the deeper layers. This pattern is confirmed by groundwater sampling and indicates a recovery of the catchment starting from the top. For the Lehstenbach catchment with a regolith depth of up to 40 m, modelling with different parameter sets reveals that sulphate has not yet reached greater depths. Accordingly, recovery has started in the very top layers, high sulphate concentrations are attained in the remaining part of the upper regolith, and no sulphate can be found in the deeper regolith.

Short flowpaths correspond to shallow depths. Long flowpaths correspond to greater depths. The given pronounced depth gradient of dissolved sulphate and a great range of different flowpath lengths contributing to runoff can therefore explain the considerable short-term variability of sulphate time series, which is observed at single stream water sampling sites.

Furtermore, for the Lehstenbach catchment only a combined implementation of adsorption and desorption isotherms, which are connected by a hysteresis loop, leads to reason-

able model results. Desorption isotherms alone cannot reproduce the observed patterns, as the retardation would be too pronounced.

The limits of the model are observed at a smaller scale than the catchment scale. It does not entirely meet the middle-term trend of sulphate concentration at the spring Schlöppnerbrunnen in the Lehstenbach catchment and the spring Lenka in the Lysina catchment. This is attributed to the simplified hydrology of the model, which differs from the local water flow regime.

Further research is recommended at three levels. Firstly, for a better understanding of sulphate dynamics in the two catchments it would be useful to have more precise information on the following points. The Schlöppnerbrunnen and the Lenka catchment, for which model results and observations do not entirely match, should be investigated with respect to the delimitation of their subcatchments, the regolith depth, and the depth of the water table. In addition, especially for the Lehstenbach catchment, where sulphate retention is high, the shape of the sorption isotherms is crucial. The schematic hysteresis loop, which is implemented in the model, indicates a pronounced retardation of sulphate transport starting with the set-in of desorption. However, there is much uncertainty about the process. The hysteresis of sulphate sorption should therefore be examined in more detail. Moreover, for the Lehstenbach catchment the model indicates a clear depth gradient of sulphate according to which high concentrations are only achieved in the upper part of the profile and sulphate has not yet reached deeper layers. Data however are only available for the upper part of the regolith. For model evaluation it would therefore be interesting to have further data on groundwater sulphate concentrations and solid bound sulphate contents from deeper layers of the regolith.

Secondly, the model worked well for two catchments. It should be applied to further ones. On the one hand, the given hypothesis that it is mainly the different distribution of flowpath lengths which shapes sulphate dynamics at different sites would be challenged in a broader sense. On the other hand, comparing where the model works and where is does not work would elucidate its potentials and limits. Discrepancies between model results and observations would further help to spot other relevant processes.

Finally, models which are designed in a simple way by only considering very few processes, but explicitly taking into account the temporal and spatial information of the available observations, offer a tool for the quantitative understanding of observed patterns and represent a promising path to follow in hydrochemical modelling.

9 Summary

The Lehstenbach catchment in south-eastern Germany and the Lysina catchment in the western part of the Czech Republic are substantially impacted by anthropogenic atmospheric acid deposition. Despite of the strongly decreasing sulphur depositions of the last two decades, sulphate concentrations in groundwater and stream water do not indicate a distinct recovery. In particular, the observed spatial variability both in the short-term trend (days) and the middle-term trend (years) complicates the understanding of the predominant processes. In both catchments, clearly decreasing concentrations at single stream water sampling sites stand beside stable or even still increasing concentrations at single groundwater wells exhibiting water from greater depths.

The objective of this study was to examine the extent to which the observed spatial patterns can be ascribed to individual processes. A model was developed, which considers sulphate transport and equilibrium sorption along one-dimensional flowpaths. A Monte-Carlo simulation provided for spatial heterogeneity of sorption isotherms. The uncertainty of the remaining parameters was taken into account using varying parameter sets. In the model, the only difference between individual sampling sites within a catchment is the different shape of their subcatchments. According to this shape, each site is characterised by the contribution of flowpaths of different lengths.

For model parameterisation and evaluation additional groundwater and soil sampling was performed in the Lysina catchment in up to 4.5 m depth. Groundwater sulphate concentrations revealed a distinct depth gradient, indicating a recovery of the catchment starting from the top. Concentrations in the shallow groundwater were below 0.1 mmol l^{-1}, whereas concentrations in the deeper aquifer exceeded 0.2 mmol l^{-1}. Solid bound sulphate contents (H_2O extractable) were low with a median of 0.14 µmol g^{-1}.

The model was able to reproduce the different observed middle-term dynamics at different sampling sites without a calibration by inverse modelling. According to the model, short flowpaths, which react very rapidly to decreasing atmospheric sulphur depositions, are responsible for the decrease of concentrations at single stream water sampling sites. In contrast, long flowpaths, which lead to a greater delay, can explain the still increasing concentrations at single groundwater wells. Moreover, the considerable range of short-term variability which is observed at single stream water sampling sites could be reproduced by considering long and short flowpaths separately. For the Lehstenbach catchment, modelling with different parameter sets further revealed a distinct depth gradient of sulphate with high concentrations only in the upper regolith.

Model results give clear evidence that different flowpath lengths are one of the main causes of the observed spatial variability of sulphate patterns. Therefore, the patterns can be explained quantitatively.

10 Zusammenfassung

Das Wassereinzugsgebiet Lehstenbach im Fichtelgebirge und das Wassereinzugsgebiet Lysina in Westböhmen nahe Marienbad sind erheblich durch anthropogene atmosphärische Säureeinträge belastet. Trotz der seit nunmehr zwei Jahrzehnten stark sinkenden Schwefeldepositionen deuten die Sulfatkonzentrationen im Grund- und Oberflächenwasser noch nicht auf eine deutliche Erholung hin. Dabei erschwert besonders die beobachtete räumliche Variabilität der kurzfristigen (Tage) sowie der mittelfristigen (Jahre) Dynamik das Verständnis der relevanten Prozesse. In beiden Einzugsgebieten reicht die Spannweite von mittelfristig deutlich abnehmenden Konzentrationen in einzelnen Vorflutern bis hin zu stabilen oder sogar weiterhin kontinuierlich ansteigenden Konzentrationen im tieferen Grundwasser an einzelnen Messstellen.

Im Rahmen dieser Arbeit wurde untersucht, inwieweit die räumlichen Muster auf einzelne Prozesse zurückgeführt werden können. Dazu wurde ein Modell entwickelt, das Sulfattransport und Gleichgewichtssorption entlang eindimensionaler Fließwege beschreibt. Die räumliche Heterogenität der Sorptionsisothermen wurde durch eine Monte-Carlo-Simulation berücksichtigt. Der Unsicherheit der verbleibenden Parameter wurde mit unterschiedlichen Parametrisierungsvarianten Rechnung getragen. Der einzige Unterschied zwischen verschiedenen Messstellen eines Einzugsgebietes ergibt sich im Modell aus der Form ihres jeweiligen Teileinzugsgebietes. Entsprechend dieser Form wurden Fließwege verschiedener Länge kombiniert.

Für die Modellparametrisierung und -evaluierung wurden im Einzugsgebiet Lysina zusätzlich zum vorhanden Datensatz weitere Grundwasser- und Bodenproben aus bis zu 4,5 m Tiefe entnommen. Für die Sulfatkonzentrationen im Grundwasser ergab sich ein deutlicher Tiefengradient, der auf eine von oben einsetzende Erholung des Einzugsgebietes hindeutet. Im oberflächennahen Grundwasser lagen die Konzentrationen unter 0,1 mmol l^{-1}, im tieferen Aquifer hingegen bei über 0,2 mmol l^{-1}. Die Sulfatgehalte an der Bodenmatrix (H_2O extrahierbar) waren mit einem Median von 0,14 µmol g^{-1} gering.

Mit dem Modell war es ohne Kalibrierung durch inverse Modellierung möglich, die verschiedenen mittelfristigen Dynamiken einzelner Messstellen nachzubilden. Danach sind kurze Fließwege, die sehr schnell auf die sinkenden atmosphärischen Schwefeleinträge reagieren, für den deutlichen Rückgang der Sulfatkonzentrationen in einzelnen Vorflutern verantwortlich zu machen. Lange Fließwege hingegen, die zu einer größeren Verzögerung führen, erklären die weiterhin kontinuierlich ansteigenden Konzentrationen im tieferen Grundwasser an einzelnen Brunnen. Weiterhin erlaubte die separate Betrachtung kurzer und langer Fließwege für einzelne Vorflutermessstellen die Nachbildung der großen Spanne der dort beobachteten kurzfristigen Variabilität. Für das Einzugsgebiet Lehstenbach ergab die Modellierung mit verschieden Parametrisierungsvarianten zudem einen deutlichen Tiefengradienten

von Sulfat, wobei hohe Konzentrationen nur in den oberen Schichten der Verwitterungsdecke auftreten.

Die Modellergebnisse lassen darauf schließen, dass unterschiedliche Fließwegslängen tatsächlich eine der Hauptursachen für die beobachteten räumlichen Muster darstellen und diese somit quantitativ zu erklären sind.

11 References

Alewell, C., 1995, Sulfat-Dynamik in sauren Waldböden – Sorptionsverhalten und Prognose bei nachlassenden Depositionen, Bayreuther Forum Ökologie, Vol. 19, Bayreuther Institut für Terrestrische Ökosystemforschung, Universität Bayreuth, 185 pp.

Alewell, C., 2001, Predicting reversibility of acidification: The European sulphur story, *Water, Air and Soil Poll.* (in press).

Alewell, C. & Gehre, M., 1999, Patterns of stable S isotopes in a forested catchment as indicators for biological S turnover, *Biogeochemisty*, **47**, 319-333.

Alewell, C. & Novák, M., 2001, Spotting zones of dissimilatory sulfate reduction in a forested catchment: the ^{34}S-^{35}S approach, *Environmental Pollution*, **112**, 369-377.

Alewell, C., Manderscheid, B., Gerstberger, P. & Matzner, E., 2000a, Effects of reduced atmospheric deposition on soil solution chemistry and elemental contents of spruce needles in NE-Bavaria, Germany, *J. Plant Nutr. Soil Sci.*, **163**, 509-516.

Alewell, C., Manderscheid, B., Meesenburg, H. & Bittersohl, J., 2000b, Is acidification still an ecological threat?, *Nature*, **407**, 856-857.

Anderson, S.P., Dietrich, W.E., Torres, R., Montgomery, D.R. & Loague, K., 1997, Concentration-discharge relationships in runoff from a steep, unchanneled catchment, *Water Resour. Res.*, **33**, 211-225.

Anlauf, R. & Liu, L.Y., 1990, Simulation of simple one-dimensional transport processes, in: Richter, J. (ed.), Models for processes in the soil, Catena paperback, Cremlingen-Destedt, pp. 9-29.

Armbruster, M., 1998, Zeitliche Dynamik der Wasser- und Elementflüsse in Waldökosystemen, Freiburger Bodenkundliche Abhandlungen, 38, Inst. für Bodenkunde und Waldernährungslehre, Freiburg im Breisgau, 301 pp.

Ball, J. & Trudgill, S.T., 1995, Overview of Solute Modelling, in: Trudgill, S.T. (ed.), Solute Modelling in Catchment Systems, John Wiley & Sons, Chichester, pp. 3-56.

Beier, C., Gundersen, P., Hansen, K. & Rasmussen, L., 1995, Experimental manipulations of water and nutrient input to a Norway spruce plantation at Klosterhede, Denmark: 2) Effects on tree growth, and nutrition, *Plant and Soil*, **168-169**, 613-622.

Beven, K.J.,1993, Prophecy, reality and uncertainty in distributed hydrological modelling, *Advances in Water Resources*, **16**, 41-51.

Beven, K.J., 2001, How far can we go in distributed hydrological modelling?, *Hydrology and Earth System Sciences*, **5**, 1-12.

Biederbeck, V.O., 1978, Soil Organic Sulfur and Fertility, in: Schnitzer, M. & Khan, S.U. (eds.), Soil Organic Matter, Elsevier Scientific Publishing Company, Amsterdam, pp. 273-310.

Bonell, M., 1998, Selected challenges in runoff generation research in forests from the hillslope to headwater drainage basin scale, *Journal of the American Water Resources Association*, **34**, 765-785.

Bortz, J., 1999, Statistik für Sozialwissenschaftler, Springer Verlag, Berlin Heidelberg, 836 pp.

Bortz, J., Lienert, G.A. & Boehnke, K., 1990, Verteilungfreie Methoden in der Biostatistik, Springer Verlag, Berlin Heidelberg, 939 pp.

Böttcher, G., 1992, Wechselwirkungen zwischen Festphasen und Lösungen (z.B. unter Bildung basischer Aluminiumsufate) in 5 Bodenprofilen über verschiedenartigen Gesteinen in der Sösmulde (Oberharz), Berichte des Forschungszentrums Waldökosysteme, Reihe A, Bd. 93, Universität Göttingen, 84 pp.

Boxmann, A.W., van Dam, D., van Dijk, H.F.G., Hogervorst, R.F. & Koopmans, C.J., 1995, Ecosystem responses to reduced nitrogen and sulphur inputs into two coniferous forest stands in the Netherlands, *Forest Ecology and Management*, **71**, 7-29.

Bredemeier, M., Blanck, K., Lamersdorf, N. & Wiedley, G.A., 1995, Response of soil water chemistry to experimental 'clean rain' in the NITREX roof experiment at Solling, Germany, *Forest Ecology and Management*, **71**, 31-44.

Breymann, U., 1999, C++, Eine Einführung, 5.Auflage, Carl Hanser Verlag, München, 713 pp.

Bronstein, I.N., Semendjajew, K.A., Musiol, G. & Mühlig, H., 1999, Taschenbuch der Mathematik, 4. Auflage, Verlag Harri Deutsch, Frankfurt am Main, Thun, 1152pp.

Buzek, F., Hruška, J. & Krám, P., 1995, Three-Component Model of Runoff Generation, Lysina Catchment, Czech Republic, *Water, Air and Soil Poll.*, **79**, 391-408.

Chadwick, M.J., Kuylenstierna, J.C.I. & Gough, C.A., 1991, The Stockholm Environmental Institue map of relative sensitivity to acidic depositions in Europe, in: Hettelingh, J.O., Downing, R.J. & de Smet, P.A.M. (eds.), Mapping critical loads in Europe, Coordination Center for Effects Technical Report No. 1, National Institute of Public Health and Environmental Protection, Bilthoven, pp. 49-57.

Christophersen, N. & Wright, R.F., 1981, Sulphate budget and a model for sulphate concentrations in stream waters at Birkenes, a small forested catachment in southernmost Norway, *Water Resour. Res.*, **17**, 377-389.

Christophersen, N., Neal, C. & Hooper, R.P., 1993, Modelling the hydrochemistry of catchments: a challenge for a scientific method, *J. Hydrol.*, **152**, 1-12.

Cosby, B.J., Hornberger, G.M., Galloway, J.N. & Wright, R.F., 1985a, Modelling the effects of acid deposition: assessment of a lumped parameter model of soil water and stream water chemistry, *Water Resour. Res.*, **21**, 51-63.

Cosby, B.J., Hornberger, G.M. & Galloway, J.N., 1985b, Modelling the effects of acid deposition: estimation of long term water quality response in a small forested catchment, *Water Resour. Res.*, **21**, 1591-1601.

Cosby, J., Wright, R.F., Hornberger, G.M. & Galloway, J.N., 1984, Model of Acidification of Groundwater In Catchments, Report to the NCSU Acid Precipitation Program, Task Group Project: E2-14, Oslo.

Courchesne, F. & Hendershot, W.H., 1989, Sulfate retention in some podzolic soils of the southern Laurentians, Quebec, *Can. J. Soil Sci.*, **69**, 337-350.

Courchesne, F. & Hendershot, W.H., 1990, Kinetics of sulphate desorption from two spodosols of the Laurentians, Quebec, *Soil Sci.*, **150**, 858-866.

De Vries, W., Posch, M. & Kämäri, J., 1989, Simulation of the long term soil response to acid deposition in various buffer ranges, *Water, Air and Soil Poll.*, **48**, 349-390.

Eshleman, K.N., Predicting Regional Episodic Acidification of Surface Waters Using Empirical Models, *Water Resour. Res.*, **24**, 1118-1126.

Finnern, H., Grottenthaler, W., Kühn, D., Pälchen, W., Schraps, W.-G. & Sponagel, H., 1994, Bodenkundliche Kartieranleitung, 4. Auflage, Bundesanstalt für Geowissenschaften und Rohstoffe und Geologische Landesämter der Bundesrepublik Deutschland, Hannover, 392 pp.

Freeze, R.A. & Cherry, J.A., 1979, Groundwater, Prentice-Hall, Englewood Cliffs, 604 pp.

Galloway, J.N., Likens, G.E. & Edgerton, E.S., 1976, Acid precipitation in the northeastern United States: pH and acidity, *Science*, **194**, 722-724.

Gelhar, L.W., Welty, C. & Rehfeldt, K.R., 1992, A Critical Review of Data on Field-Scale Dispersion in Aquifers, *Water Resour. Res.*, **28**, 1955-1974.

Ghani, A., McLaren, R.G. & Swift, R.S., 1993, Mobilization of recently-formed soil orgnic sulphur, *Soil Biol. Biochem.*, **25**, 1739-1744.

Giblin, A.E. & Wieder, R.K., 1992, Sulphur cycling in marine and freshwater wetlands, in: Howarth, R.W., Stewart, J.W.B. & Ivanov, M.V. (eds.), Sulphur Cycling on the Continents: Wetlands, Terrestrial Ecosystems, and Associated Water Bodies, Scope 48, John Wiley & Sons, Chichester, pp. 85-123.

Gisi, U., Schenker, R., Schulin, R., Stadelmann, F.X. & Stichler, H., 1990, Bodenökologie, Georg Thieme Verlag, Stuttgart, 304 pp.

Gobran, G.R., Courchesne, F. & Dufresne, A., 1998, Relationships Between Sulfate Retention and Release, solution pH and DOC in the Gårdsjön Soils, in: Hultberg, H. & Skeffington, R. (eds.), Experimental Reversal of Acid Rain Effects: The Gårdsjön Roof Project, John Wiley & Sons, Chichester, pp. 207-229.

Gundersen, P., Rasmussen, L., Andersen, B.R. & Beier, C., Experimental manipulations of water and nutrient input to a Norway spruce plantation at Klosterhede, Denmark: 1) unintended physical and chemical changes by roof experiments, *Plant and Soil*, **168-169**, 601-611.

Gurtler, R. & Nikl, P., 1999, Experimentální povodí Lysina ve Slavkovském lese - Geofyzikální průzkum, Geonika Ltd., Prague.

Hansen, K., Beier, C., Gundersen, P. & Rasmussen, L., 1995, Experimental manipulations of water and nutrient input to a Norway spruce plantation at Klosterhede, Denmark: 3)

Effects on throughfall, soil water chemistry and decomposition, *Plant and Soil*, **168-169**, 623-632.

Harrison, R.B., Johnson, D.W. & Todd, D.E., 1989, Sulfate Adsorption and Desorption Reversibility in a Variety of Forest Soils, *J. Environ. Qual.*, **18**, 419-426.

Hauck, A., 1999, Hydrogeologische Charakterisierung des Lehstenbach-Einzugsgebiets am Großen Waldstein, Messung und Simulation, Diplomarbeit, Bayreuther Institut für Terrestrische Ökosystemforschung, Universität Bayreuth, 73 pp.

Haunschild, H. & Jerz, H. (eds.), 1981, Geologische Karte von Bayern und Erläuterungen 1:500000, Bayrisches Geologisches Landesamt, München, 168 pp.

Heindl, B., Ostendorf, B. & Köstner, B., 1995, Lage und forstliche Charakterisierung des Einzugsgebietes Lehstenbach, in: Manderscheid, B. & Göttlein, A., Wassereinzugsgebiet 'Lehstenbach' – das BITÖK-Untersuchungsgebiet am Waldstein (Fichtelgebirge, NO-Bayern), Bayreuther Forum Ökologie, Vol. 18, Bayreuther Institut für Terrestrische Ökosystemforschung, Universität Bayreuth, pp. 7-14.

Hodges, S.C. & Johnson, G.C., 1987, Kinetics of Sulphate Adsorption and Desorption by Cecil Soil Using Miscible Displacement, *Soil Sci. Soc. Am. J.*, **51**, 323-331.

Houle, D. & Carignan, R., 1995, Role of SO_4 adsorption and desorption in the long-term S budget of a coniferous catchment on the Canadian Shield, *Biogeochemistry*, **28**, 161-182.

Hrdlička, M., 1989, Map of the Lysina catchment 1:1000, Archive, Czech Geological Survey, Prague.

Hruška, J. & Krám, P., 1994, Hydrochemical monitoring of a forested catchment with extremely high aluminium concentrations in runoff: the Lysina catchment, Czech Republic, *International Association of Hydrological Sciences Publication*, **219**, 357-368.

Hultberg, H. & Skeffington, R. (eds.), 1998, Experimental Reversal of Acid Rain Effects: The Gårdsjön Roof Project, John Wiley & Sons, Chichester, 466 pp.

Jungnickel, C., 1996, Sulfat-Desorptionsisothermen saurer Waldböden, Räumliche Heterogenität und Abhängigkeit von Bodenparametern, Diplomarbeit, Bayreuther Institut für Terrestrische Ökosystemforschung, Universität Bayreuth, 78 pp.

Jury, W.A., Gardner, W.R. & Gardner, W.H., 1991, Soil Physics, John Wiley & Sons, New York, 328 pp.

Karltun, E., 1994, Principal Geographic Variation in the Acidification of Swedish Forest Soils, *Water, Air and Soil Poll.*, **76**, 353-362.

Krám, P., 1997, Biogeochemistry of forest catchments in the Czech Republic with contrasting lithology under conditions of acidic deposition, PhD thesis, Syracuse University, New York, 158 pp.

Krám, P. & Hruška, J., 1994, Influence of bedrock geology on elemental fluxes in two forested catchments affected by high acidic deposition, *Applied Hydrogeology*, **2/2**, 50-58.

Krám, P., Hruška, J., Driscoll, C.T. & Johnson, C.E., 1995, Biogeochemistry of Aluminium in a Forest Catchment in the Czech Republic Impacted by Atmospheric Inputs of Strong Acids, *Water, Air and Soil Poll.*, **85**, 1831-1836.

Krám, P., Hruška, J., Wenner, B.S., Driscoll, C.T. & Johnson, C.E., 1997, The biogeochemisty of basic cations in two forest catchments with contrasting lithology in the Czech Republic, *Biogeochemistry*, **37**, 173-202.

Lischeid, G., 2001a, Investigating short-term dynamics and long-term trends of SO_4 in the runoff of a forested catchment using artificial neural networks, *J. Hydrol.*, **243**, 31-42.

Lischeid, G., 2001b, Neither macropores nor interflow: generation of spiky discharge peaks in small forested catchments and its implications on stream water chemistry, *Hydrological Processes* (submitted).

Lischeid, G., Moritz, K., Bittersohl, J., Alewell, C. & Matzner, E., 2000, Sinks of anthropogenic nitrogen and sulphate in the Lehstenbach catchment (Fichtelgebirge): Lessons learned concerning reversibility., *Silva Gabreta*, **4**, 41-50.

Lischeid, G., Kolb, A. & Alewell, C., 2001, Short-term groundwater recharge and streamwater discharge: a comprehensive survey in the Lehstenbach catchment, *Water Resour. Res.* (submitted).

Lückewille, A., 1994, Billion Dollar Problem, Billion Dollar Solution? Transboundary Air Pollution Calls for Transboundary Solutions, in: Steinberg, C.E.W. & Wright, R.F. (eds.), Acidification of Freshwater Ecosystems: Implications for the Future, John Wiley & Sons, Chichester, pp. 17-31.

Lückewille, A., 1995, Rekonstruktion der Boden- und Gewässerversauerung in der Langen Bramke (Harz), Bayreuther Forum Ökologie, Vol. 21, Bayreuther Institut für Terrestrische Ökosystemforschung, Universität Bayreuth, 189 pp.

Lynch, J.A., Hanna, C.M. & Corbett, E.S., 1986, Predicting pH, Alkalinity, and Total Acidity in Stream Water During Episodic Events, *Water Resour. Res.*, **22**, 905-912.

Malessa, V., 1993, Depositionsbedingte Tiefengradienten der Bodenversauerung in der Sösemulde, Berichte des Forschungszentrums Waldökosysteme, Reihe A, Bd. 98, Universität Göttingen, 233 pp.

Manderscheid, B., Jungnickel, C. & Alewell, C., 2000a, Spatial variability of sulfate isotherms in forest soils at different scales and its implications for the modeling of soil sulfate fluxes, *Soil Science*, **165**, 848-857.

Manderscheid, B., Schweisser, T., Lischeid, G., Alewell, C. & Matzner, E., 2000b, Sulfate pools in the weathered substrata of a forested catchment, *Soil Sci. Soc. Amer. J.*, **64**, 1078-1082.

Marsal, D., 1976, Die numerische Lösung partieller Differentialgleichungen in Wissenschaft und Technik, B.I.-Wissenschaftsverlag, Zürich, 574 pp.

Matzner, E. & Meiwes, K.J., 1994, Long-Term Development of Element Fluxes with Bulk Precipitation and Throughfall in Two German Forests, *J. Environ. Qual.*, **23**, 162-166.

Matzner, E. & Davis, M., 1996, Chemical soil conditions in pristine Nothofagus forests of New Zealand as compared to German forests, *Plant and Soil*, **186**, 285-291.

Matzner, E., Alewell, C., Bittersohl, J., Lischeid, G., Kammerer, G., Manderscheid, B., Matschonat, G., Moritz, K., Tenhunen, J.D. & Totsche, K., 2001, Biogeochemistry of a Spruce Forest Catchment of the Fichtelgebirge in Response to Changing Atmospheric Deposition, in: Tenhunen, J.D., Lenz, R. & Hantschel, R. (eds.), Ecosystem Approaches to Landscape Management in Central Europe, Ecological Studies, Vol.147, Springer-Verlag, Berlin Heidelberg, pp. 463-503.

Maynard, D.G., Stewart, J.W.B. & Bettany, J.R., 1984, Sulfur cycling in grassland and parkland soils, *Biogeochemisty*, **1**, 97-111.

McDonald, M.G. & Harbaugh, A.W., 1988, A modular three-dimensional finite-difference ground-water flow model, U.S. Geological Survey Techniques of Water Resources Investigations, Book 6, Chapter A1.

McGlynn, B.L., McDonnell, J.B., Shanley, J.B. & Kendall, C., 1999, Riparian zone flowpath dynamics during snowmelt in a small headwater catchment, *J. Hydrol.*, **222**, 75-92.

McLaren, R.J., Keer, J.I. & Swift, R.S., Sulphur transformations in soils using sulphur-35 labelling, *Soil Biol. Biochem.*, **17**, 73-79.

Meiwes, K.J., 1979, Der Schwefelhaushalt eines Buchenwald- und eines Fichtenwaldökosystems im Solling, Göttinger Bodenkundliche Berichte, 60, Anstalt für Bodenkunde, Göttingen, 108 pp.

Meiwes, K.J., Khanna, P.K. & Ulrich, B., 1980, Retention of sulphate by an acid brown earth and its relationship with the atmospheric input of sulphur to forest vegetation, *Z. Pflanzenernaehr. Bodenkd.*, **143**, 402-411.

Meiwes, K.J., Merino, A. & Fortmann, H., 1994, Untersuchung der Versauerung in Bohrprofilen von Meßstellen des Grundwassergütemeßnetzes (GÜN) des Landes Niedersachsen, Berichte des Forschungszentrums Waldökosysteme, Reihe B, Bd. 34, Universität Göttingen, 86 pp.

Mitchell, M.J., Driscoll, C.T., Fuller, R.D., David, M.B. & Likens, G.E., 1989, Effect of Whole-Tree Harvesting of the Sulfur Dynamics of a Forest Soil, *Soil Science Society of America Journal*, **53**, 933-940.

Mitchell, M.J., David, M.J. & Harrison, R.B., 1992, Sulfur dynamics of forested ecosystems, in: Howarth, R.W., Stewart, J.W.B. & Ivanov, M.V. (eds.), Sulphur Cycling on the Continents: Wetlands, Terrestrial Ecosystems, and Associated Water Bodies, Scope 48, John Wiley & Sons, Chichester, pp. 215-254.

Moldan, B. & Schnoor, J.L., 1992, Czechoslovakia: Examining a Critically Ill Environment, *Environ. Sci. Technol.*, **26**, 14-21.

Moritz, K., Bittersohl, J., Müller, F.X. & Krebs, M., 1994, Auswirkungen des sauren Regens und des Waldsterbens auf das Grundwasser, Dokumentation der Methoden und Meßdaten des Entwicklungsvorhabens 1988 – 1992, Bayrisches Landesamt für Wasserwirtschaft, München, 387 pp.

Morris, D.A. & Johnson, A.I., 1967, Summary of hydrological and physical properties of rock and soil materials as analyzed by the hydrologic laboratory of the U.S. Geological Survey, USGS Water Supply Paper 1839-D.

Mörth, C.-M., Torssander, P., Kusakabe, M. & Hultberg, H., 1999, Sulfur isotope values in a forested catchment over four years: Evidence for oxidation and reduction processes, *Biogeochemisty*, **44**, 51-71.

Mückenhausen, E., 1993, Die Bodenkunde und ihre geologischen, geomorphologischen, mineralogischen und petrologischen Grundlagen, DLG-Verlag, Frankfurt am Main, 579 pp.

Nodvin, S.C., Driscoll, C.T. & Likens, G.E., 1986, The effect of pH on sulfate adsorption by a forest soil, *Soil Science*, **142**, 69-75.

Novák, M., 1998, $\delta^{34}S$ dynamics in the system bedrock-soil-runoff-atmosphere: Results from the GEOMON network of small catchments, Czech Republic, in: Arehart, G.B. & Hulston, J.R. (eds.), Water-Rock-Interaction, Balkema, Rotterdam, pp. 67-70.

Novák, M. & Wieder, R.K., 1992, Inorganic and organic sulfur profiles in nine Sphagnum peat bogs in the United States and Czechoslovakia, *Water, Air and Soil Poll.*, **65**, 353-369.

Novák, M., Bottrell, S.H., Fottová, D., Buzek, F., Groscheová H. & Žak, K., 1996, Sulfur Isotope Signals in Forest Soils of Central Europe along an Air Pollution Gradient, *Envion. Sci. Technol.*, **30**, 3473-3476.

Novák, M., Kirchner, J.W., Groscheová, H., Havel, M., Černý, J., Krejčí, R. & Buzek, F., 2000, Sulfur isotope dynamics in two Central European watersheds affected by high atmospheric deposition of SO_x, *Geochimica et Cosmochimica Acta*, **64**, 367-383.

Olsen, T., 1980, Ground-water-level fluctuations as a measure of the effective porosity and ground-water recharge, Sveriges Geologiska Undersökning, Rapporter och meddelanden nr 21, Uppsala, 46 pp.

Pačés, T., 1985, Sources of acidification in Central Europe estimated from elemental budgets in small basins, *Nature*, **315**, 31-36.

Peters, K. & Gerchau, J., 1995, Klima und luftchemische Situation des Fichtelgebirges unter besonderer Berücksichtigung des Einzugsgebietes Lehstenbach, in: Manderscheid, B. & Göttlein, A., Wassereinzugsgebiet 'Lehstenbach' – das BITÖK-Untersuchungsgebiet am Waldstein (Fichtelgebirge, NO-Bayern), Bayreuther Forum Ökologie, Vol. 18, Bayreuther Institut für Terrestrische Ökosystemforschung, Universität Bayreuth, pp. 15-39.

Peters, K., Huber, G., Netsch, S. & Frevert, T., 1984, Methode zur direktpotentiometrischen In-situ-Registrierung von Schwefelwasserstoff in einer Kläranlage, *gwf-wasser/abwasser*, **125**, 386-390.

Reuss, J.O., Cosby, B.J. & Wright, R.F., 1987, Chemical processes governing soil and water acidification, *Nature*, **329**, 27-32.

Reuss, J.O. & Johnson, D.W., 1986, Acid Deposition and the Acidification of Soils and Waters, Springer Verlag, New York, 119 pp.

Robertson, W.D., Cherry, J.A. & Schiff, S.L., 1989, Atmospheric Sulfur Deposition 1950-1985 inferred from Sulfate in Groundwater, *Water Resour. Res.*, **25**, 1111-1123.

Rötting, T., 2000, Entwicklung einer Methode der tiefenorientierten Grundwasserbeprobung in durchgehend verfilterten Brunnen, Diplomarbeit, Bayreuther Institut für Terrestrische Ökosystemforschung, Universität Bayreuth, 103 pp.

Rüdiger, F., 1993a, Geologische Kartierung und geophysikalische Untersuchungen im Einzugsgebiet der Quellbäche des Lehstenbaches (Fichtelgebirge), Diplomarbeit Teil 1, Institut für Allgemeine und Angewandte Geologie, Universität München, 35 pp.

Rüdiger, F., 1993b, Hydrogeologische Untersuchung des Einzugsgebietes der Lehstenbachquellbäche (Fichtelgebirge), Diplomarbeit Teil 2, Institut für Allgemeine und Angewandte Geologie, Universität München, 51 pp.

Sachs, L., 1997, Angewandte Statistik, Springer Verlag, Berlin Heidelberg, 881 pp.

Sakadevan, K., Hedley, M.J. & Mackay, A.D., 1993, Sulphur cycling in New Zealand hill county pastures. I. Laboratory sulphur, nitrogen and carbon mineralization studies, *J. Soil Sci.*, **44**, 73-83.

Scanlon, T.M., Raffensperger, J.P., Hornberger, G.M. & Clapp, R.B., 2000, Shallow subsurface storm flow in a forested headwater catchment: Observations and modeling using a modified TOPMODEL, *Water Resour. Res.*, **36**, 2575-2586.

Scheffer, F. & Schachtschabel, P., 1992, Lehrbuch der Bodenkunde, Ferdinand Enke Verlag, Stuttgart, 491 pp.

Schnoor, J.L., Galloway, J.N. & Moldan, B., 1997, East Central Europe: An Environment in Transition, *Environ. Sci. Technol.*, **31**, A412-A416.

Schulze, E.-D., Oren, R. & Lange, O.L., 1989, Processes Leading to Forest Decline: A Synthesis, in: Schulze, E.-D., Lange, O.L. & Oren, R. (eds.), Forest Decline and Air Pollution, Springer Verlag, Berlin Heidelberg, pp. 459-468.

Schweisser, T., 1998, Sulfatsorptions- und –desorptionsverhalten des oberflächennahen, geologischen Untergrundes im Wassereinzugsgebiet Lehstenbach (Fichtelgebirge), Diplomarbeit, Bayreuther Institut für Terrestrische Ökosystemforschung, Universität Bayreuth, 94 pp.

Singh, B.R. & Johnson, D.W., 1986, Sulfate content and adsorption in soils of two forest watersheds in southern Norway, *Water, Air and Soil Poll.*, **31**, 847-856.

Sobol, I.M., 1991, Die Monte-Carlo-Methode, Deutscher Verlag der Wissenschaften, Berlin, 108 pp.

Spitz, K., Moreno, J., 1996, A Practical Guide to Groundwater and Solute Transport Modelling, John Wiley & Sons, New York, 461 pp.

Steinberg, C.E.W. & Wright, R.F., 1994, Introduction, in: Steinberg, C.E.W. & Wright, R.F. (eds.), 1994, Acidification of Freshwater Ecosystems: Implications for the Future, John Wiley & Sons, Chichester, pp. 1-4.

Stettner, G., 1964, Erläuterungen zur Geologischen Karte von Bayern 1:25000, Blatt Nr. 5837 Weißenstadt, Bayrisches Geologisches Landesamt, München, 194 pp.

Stettner, G., 1981, Grundgebirge, in: Haunschild, H. & Jerz, H. (eds.), Geologische Karte von Bayern und Erläuterungen 1:500000, Bayrisches Geologisches Landesamt, München, pp. 7-33.

Stoddard, J.L., Jeffries, D.S., Lückewille A., Clair, T.A., Dillon, P.J., Driscoll, C.T., Forsius, M., Johannessen, M., Kahl, J.S., Kellogg, J.H., Kemp, A., Mannio, J., Monteith, D.T., Murdoch, P.S., Patrick, S., Rebsdorf, A., Skjelkvåle, B.L., Steinton, M.P., Traan, T., van Dam, H., Webster, K.E., Wieting, J. & Wilander, A., 1999, Regional trends in aquatic recovery from acidification in North America and Europe, *Nature*, **401**, 575-578.

Strikwerda, J.C., 1997, Finite Difference Schemes and Partial Differential Equations, International Thomson Publishing, New York, 385 pp.

Stumm, W. & Morgan, J.J., 1996, Aquatic Chemistry, John Wiley & Sons, New York, 1022 pp.

Sverdrup, H., Warvinge, P. & von Bromssen, U., 1987, A mathematical model for acidification and neutralisation of soil profiles exposed to acid deposition, in: Air Pollution and Ecosystems, Reidel, Dordrecht.

Thode, H.G., 1991, Sulphur Isotopes in Nature and the Environment: An Overview, in: Krouse, H.R. & Grinenko, V.A. (eds.), Stable Isotopes, Natural and Anthropogenic Sulphur in the Environment, John Wiley & Sons, Chichester, pp. 1-41.

Torssander, P. & Mörth, C.-M., 1998, Sulfur Dynamics in the Roof Experiment at Lake Gårdsjön Deduced from Sulfur and Oxygen Isotope Rations in Sulfate, in: Hultberg, H. & Skeffington, R. (eds.), Experimental Reversal of Acid Rain Effects: The Gårdsjön Roof Project, John Wiley & Sons, Chichester, pp. 185-206.

Ulrich, B., 1981, Ökologische Gruppierung von Böden nach ihrem chemischen Bodenzustand, *Z. Pflanzenernähr. Bodenkd.*, **144**, 289-305.

Ulrich, B., 1983, Stabilität von Waldökosystemen unter dem Einfluß des "sauren Regens", *Allgemeine Forstzeitschrift*, **26-27**, 670-677.

Ulrich, B., 1985, Natürliche und anthropogene Komponenten der Bodenversauerung, *Mitteilgn. Dtsch. Bodenkundl. Gesellsch.*, **43**, 159-187.

UN ECE, 2000, Protocol to the 1979 Convention of Long-Range Transboundary Air Pollution on Further Reduction of Sulphur Emissions, www.unece.org/env/lrtap/protocol/94sulp.htm.

Urban, N.R., Eisenreich, S.J. & Grigal D.F., 1989, Sulfur cycling in a forested sphagnum bog in northern Minnesota, *Biogeochemistry*, **7**, 81-109.

Valeur, I. & Nilsson. I., 1993, Effects of lime and two incubation techniques on sulfur mineralization in a forest soil, *Soil Biol. Biochem.*, **25**, 1343-1350.

Vogt, R.D. & Muniz, I.P., 1997, Soil and stream water chemistry in a pristine and boggy site in mid-Norway, *Hydrobiologica*, **348**, 19-38.

Wright, R.F., Lotse, E. & Semb, A., 1988, Reversibility of acidification shown by whole-catchment experiments, *Nature*, **334**, 670-675.

Zahn, M.T., 1995, Transport von Säurebildnern in Untergrund und Bedeutung für die Grundwasserversauerung, in: Bittersohl, J., Krebs, M., Müller, F.X. & Zahn, M.T., Internationales Symposium, Grundwasserversauerung durch atmosphärische Deposition, Ursachen – Auswirkungen – Sanierungsstrategien, Informationsberichte des Bayrischen Landesamtes für Wasserwirtschaft, Heft 3/95, Bayrisches Landesamt für Wasserwirtschaft, München, pp. 143-151.

Zhang, P.C. & Sparks, D.L., 1990, Kinetics and Mechanisms of Sulphate Adsorption/Desorption on Goethite Using Pressure-Jump Relaxation, *Soil Sci. Soc. Am. J.*, **54**, 1266-1273.

12 Appendices

Appendix A:

Chemical Parameters of the Weekly Groundwater Samples from the Lysina Catchment

and identification limits and coefficients of variation of the analytical methods

grey font: samples taken before the screen was cleaned

Sampling Site	Date	Type of Sample*	In situ measurements: Colour	Smell	Gr. Lev.	pH	Electr. Cond.	T	O_2	H_2S	Redox Pot.	Laboratory measurements: SO_4	S	NO_3	NO_2	NH_4	Cl	PO_4	Al	Fe	Ca	Mg	K	Na	Mn	Si	DOC	DIC	DN
Unit			-	-	m b.s.	-	µS cm⁻¹	°C	%	µmol l⁻¹	mV	mmol l⁻¹																	
Identification Limit			-	-	-	-	-	-	-	-	-	0.003	0.009	0.005	0.001	0.003	0.008	0.003	0.007	0.001	0.005	0.002	0.006	0.009	3.640E	0.007	0.062	0.062	0.011
Coeff. of Var. [%]			-	-	-	-	-	-	-	-	-	2.954	2.199	3.118	1.12	1.92	2.518	2.606	2.011	1.477	1.214	0.521	1.554	2.932	1.541	1.937	1.55	1.98	2.6
GW Ia	25/08/2000	new	orange-brown	neutral	1.90	6.28	92	12.1	n.d.	n.d.	n.d.	0.222	0.201	0.018	0.002	0.009	<	<	<	0.013	0.104	0.036	0.108	0.106	0.012	0.263	0.282	<	0.054
	06/09/2000	old	slightly beige	neutral	1.77	6.12	89	9.9	n.d.	n.d.	n.d.	0.232	0.216	0.016	0.003	0.010	<	<	<	0.039	0.142	0.050	0.092	0.103	0.015	0.268	0.291	0.249	0.067
	06/09/2000	new	no	neutral	-	6.12	86	8.9	15.8	n.d.	n.d.	0.227	0.212	0.023	0.002	0.010	0.063	<	<	0.028	0.140	0.049	0.090	0.094	0.014	0.262	0.307	<	0.077
	14/09/2000	old	n.d.	n.d.	1.80	5.72	80	11	n.d.	n.d.	n.d.	0.204	0.204	0.025	<	0.013	0.083	<	<	0.010	0.135	0.048	0.078	0.114	0.011	0.254	0.487	<	0.097
	14/09/2000	new	no	neutral	-	5.41	68	13.2	37.2	<	176	0.207	0.210	0.024	<	0.005	0.044	<	<	0.013	0.125	0.049	0.050	0.115	0.010	0.254	<	<	0.056
	21/09/2000	old	n.d.	n.d.	1.75	n.d.	n.d.	n.d.	n.d.	n.d.	n.d.	0.220	0.226	0.029	<	0.008	0.050	<	<	<	0.154	0.051	0.059	0.099	0.011	0.247	<	<	0.061
	21/09/2000	new	no	neutr., minerally	-	5.02	73	7.9	46.3	<	190	0.239	0.243	0.028	<	0.010	0.053	<	<	<	0.158	0.051	0.047	0.221	0.011	0.246	<	<	0.063
	28/09/2000	old	n.d.	n.d.	1.76	n.d.	n.d.	n.d.	n.d.	n.d.	n.d.	0.233	0.221	0.030	<	0.004	0.054	<	0.008	<	0.153	0.053	0.055	0.109	0.011	0.237	<	<	0.050
	28/09/2000	new	no	neutral, clayey	-	5.1	75	11.4	32.3	<	209	0.233	0.223	0.030	<	0.006	0.051	<	0.007	<	0.154	0.053	0.052	0.099	0.011	0.235	<	<	0.058
	05/10/2000	old	n.d.	n.d.	n.d.	n.d.	n.d.	n.d.	n.d.	n.d.	n.d.	0.221	0.214	0.029	<	0.014	0.057	<	<	<	0.145	0.048	0.071	0.150	0.010	0.231	0.237	<	0.059
	12/10/2000	new	no	n.d.	1.64	5.15	73	8.7	30.6	<	205	0.225	0.215	0.032	<	0.003	0.056	<	0.007	<	0.154	0.054	0.056	0.107	0.010	0.235	<	<	0.042
	26/10/2000	new	slightly orange	mineral	n.d.	5.22	77	8.3	53	<	298	0.219	0.224	0.031	<	0.013	0.072	<	<	<	0.153	0.052	0.067	0.120	0.012	0.226	0.229	<	0.057
	09/11/2000	new	no	slightly minerally	n.d.	5.06	78	7	30.8	<	321	0.231	0.235	0.032	<	0.022	0.067	<	<	<	0.162	0.056	0.054	0.124	0.010	0.216	0.225	<	0.076
	23/11/2000	new	no	minerally	n.d.	4.97	75	6	33.7	<	296	0.247	0.254	0.029	<	0.003	0.051	<	<	<	0.228	0.058	0.042	0.136	0.010	0.217	<	<	0.041
	30/11/2000	old	n.d.	n.d.	1.71	n.d.	n.d.	n.d.	n.d.	n.d.	n.d.	0.229	0.263	0.029	<	<	0.057	<	0.008	<	0.160	0.056	0.039	0.112	0.009	0.198	<	<	0.037
GW Ib	06/09/2000	old	brown	neutral	1.40	5.87	96	10	n.d.	n.d.	n.d.	0.185	0.130	<	<	0.027	0.161	<	<	0.059	0.060	0.020	0.150	0.155	0.056	0.097	11.822	0.388	0.156
	21/09/2000	old	n.d.	n.d.	1.81	n.d.	n.d.	n.d.	n.d.	n.d.	n.d.	0.226	0.236	0.014	0.009	0.011	0.056	<	<	<	0.159	0.049	0.130	0.186	0.051	0.305	0.215	0.350	0.056
	21/09/2000	new	slightly light brown	minerally	-	5.84	92	7.6	43.2	<	-60	0.194	0.219	0.014	0.003	0.013	0.058	<	<	<	0.156	0.048	0.108	0.167	0.042	0.286	0.315	0.251	0.056
	28/09/2000	old	n.d.	n.d.	1.77	n.d.	n.d.	n.d.	n.d.	n.d.	n.d.	0.244	0.231	0.023	0.003	0.006	0.063	<	<	<	0.166	0.052	0.099	0.150	0.039	0.276	<	0.236	0.048
	28/09/2000	new	no	neutral	-	5.72	89	12.7	37.5	<	-77	0.240	0.235	0.018	<	0.011	0.056	<	<	<	0.162	0.051	0.083	0.139	0.034	0.265	<	<	0.049
	05/10/2000	old	n.d.	n.d.	1.68	n.d.	n.d.	n.d.	n.d.	n.d.	n.d.	0.256	0.250	0.019	<	0.004	0.054	<	<	<	0.175	0.055	0.079	0.146	0.036	0.274	<	<	0.031
	12/10/2000	new	no	n.d.	1.64	5.8	89	8.9	12.8	<	149	0.245	0.242	0.007	<	0.009	0.067	<	<	<	0.170	0.054	0.094	0.153	0.035	0.280	<	0.239	0.029
	19/10/2000	old	n.d.	n.d.	1.71	n.d.	n.d.	n.d.	n.d.	n.d.	n.d.	0.244	0.240	0.013	0.003	0.005	0.055	<	<	<	0.178	0.056	0.073	0.131	0.033	0.267	<	<	0.030
	26/10/2000	new	slightly orange	neutral	1.68	5.6	85	8.3	53.9	<	260	0.235	0.256	0.017	<	0.006	0.058	<	<	<	0.174	0.056	0.065	0.130	0.034	0.257	<	<	0.031
	02/11/2000	old	n.d.	n.d.	1.73	n.d.	n.d.	n.d.	n.d.	n.d.	n.d.	0.236	0.266	0.018	<	0.005	0.071	<	<	<	0.181	0.057	0.059	0.157	0.031	0.257	<	<	0.030
	09/11/2000	new	no	neutral	1.68	5.38	87	6.6	8.1	<	243	0.234	0.259	0.018	<	0.010	0.059	<	<	<	0.170	0.054	0.063	0.137	0.036	0.252	<	<	0.047
	16/11/2000	old	n.d.	n.d.	1.76	n.d.	n.d.	n.d.	n.d.	n.d.	n.d.	0.244	0.259	0.019	<	0.006	0.060	<	<	<	0.185	0.058	0.056	0.134	0.029	0.250	<	<	0.033
	23/11/2000	new	slightly light brown	slightly minerally	1.86	5.41	87	6.2	16.1	<	244	0.242	0.270	0.014	<	<	0.054	<	<	<	0.176	0.056	0.061	0.125	0.033	0.254	<	<	0.024
	30/11/2000	old	n.d.	n.d.	n.d.	n.d.	n.d.	n.d.	n.d.	n.d.	n.d.	0.243	0.291	0.019	<	<	0.045	<	<	<	0.188	0.060	0.043	0.117	0.025	0.238	<	<	0.024
GW IIa	25/08/2000	old	brown	rotten	0.51	4.66	54	12.3	n.d.	n.d.	n.d.	0.112	0.117	<	<	0.011	0.062	<	0.062	0.008	0.046	0.016	0.047	0.179	0.003	0.406	3.081	<	0.071
	06/09/2000	old	light brown	slightly rotten	0.49	5.09	52	9.7	29.1	n.d.	n.d.	0.106	0.115	<	<	0.014	0.041	<	0.035	0.022	0.045	0.018	0.050	0.097	0.003	0.367	1.682	<	0.066
	06/09/2000	new	brown	slightly rotten	-	4.94	49	10.1	n.d.	n.d.	n.d.	0.103	0.112	<	<	<	0.034	<	0.052	0.022	0.040	0.018	0.049	0.104	0.002	0.409	1.882	<	0.057
	14/09/2000	old	yellowish	neutral	0.62	4.8	48	11.4	25.6	<	164	0.113	0.119	<	<	0.006	0.028	<	0.030	0.035	0.052	0.021	0.026	0.095	0.006	0.346	1.299	<	0.050
	21/09/2000	old	n.d.	n.d.	0.5	n.d.	n.d.	n.d.	n.d.	n.d.	n.d.	0.119	0.127	<	<	0.038	0.061	<	0.019	0.005	0.052	0.021	0.057	0.159	0.004	0.339	1.124	0.356	0.076
	21/09/2000	new	light brown	slightly rotten	-	4.7	50	7.4	2.9	<	161	0.108	0.120	<	<	0.018	0.047	<	0.028	0.012	0.072	0.023	0.044	0.121	0.005	0.331	1.191	0.321	0.057
	28/09/2000	old	n.d.	n.d.	0.55	n.d.	n.d.	n.d.	n.d.	n.d.	n.d.	0.117	0.128	<	<	0.016	0.039	<	0.031	0.011	0.063	0.023	0.026	0.117	0.004	0.337	1.099	0.259	0.050
	28/09/2000	new	beige	slightly rotten	-	4.68	51	10.8	6.2	<	271	0.117	0.132	<	<	0.035	0.052	<	0.030	0.013	0.060	0.022	0.043	0.130	0.004	0.328	1.174	<	0.080
	05/10/2000	old	n.d.	n.d.	0.45	n.d.	n.d.	n.d.	n.d.	n.d.	n.d.	0.121	0.129	<	<	0.015	0.039	<	0.030	0.007	0.064	0.025	0.031	0.137	0.004	0.345	1.141	<	0.040
	12/10/2000	new	brown	n.d.	0.45	5.04	53	8.5	8.5	<	105	0.116	0.123	<	<	0.013	0.054	<	0.037	0.018	0.065	0.024	0.052	0.125	0.004	0.339	1.216	<	0.044
	19/10/2000	old	n.d.	n.d.	0.55	n.d.	n.d.	n.d.	n.d.	n.d.	n.d.	0.113	0.116	<	<	0.006	0.036	<	0.035	0.012	0.062	0.024	0.026	0.110	0.004	0.332	1.149	<	0.032
	26/10/2000	new	light brown	very slightly rotten	0.52	4.89	51	8.6	36.5	<	286	0.109	0.125	<	<	0.018	0.047	<	0.031	0.022	0.064	0.023	0.040	0.119	0.004	0.339	1.174	<	0.052
	02/11/2000	old	n.d.	n.d.	0.53	n.d.	n.d.	n.d.	n.d.	n.d.	n.d.	0.111	0.122	<	<	0.008	0.064	<	0.034	0.015	0.142	0.023	0.023	0.147	0.003	0.330	1.116	<	0.036
	09/11/2000	new	slightly brownish	slightly rotten	0.54	4.56	51	6.9	9.8	<	261	0.110	0.123	<	<	0.015	0.048	<	0.032	0.019	0.062	0.022	0.037	0.120	0.004	0.322	1.124	<	0.052
	16/11/2000	old	n.d.	n.d.	0.54	n.d.	n.d.	n.d.	n.d.	n.d.	n.d.	0.116	0.126	<	<	0.008	0.050	<	0.032	0.016	0.064	0.023	0.023	0.123	0.004	0.336	1.166	<	0.036
	23/11/2000	new	light brown	slightly rotten	0.51	4.52	47	5.8	16.8	8E-04	287	0.111	0.141	<	<	0.003	0.038	<	0.035	0.026	0.061	0.022	0.024	0.104	0.004	0.318	1.174	<	0.027
	30/11/2000	old	n.d.	n.d.	n.d.	n.d.	n.d.	n.d.	n.d.	n.d.	n.d.	0.110	0.122	<	<	0.004	0.036	<	0.032	0.021	0.059	0.023	0.014	0.104	0.004	0.318	1.116	<	0.025
GW IIb	25/08/2000	old	dark brown	rotten	0.6	4.36	77	12.6	n.d.	n.d.	n.d.	0.119	0.129	<	<	0.022	0.107	<	0.050	0.021	0.065	0.039	0.055	0.171	0.006	0.427	0.747	<	0.106
	06/09/2000	old	brown	neutral	1.41	4.59	77	11.3	n.d.	n.d.	n.d.	0.035	0.066	<	<	0.036	1.348	<	0.111	0.211	0.150	0.071	0.266	0.196	0.014	0.591	0.780	<	0.185
	21/09/2000	old	brown	rotten	1.62	5.4	75	7.7	41.1	<	131	0.086	0.112	<	<	0.032	0.066	<	0.240	0.034	0.062	0.042	0.101	0.197	0.006	0.719	1.107	<	0.084

*old or new water from the piezometers   < below identification limit

	28/09/2000	old	n.d.	n.d.	1.51	n.d.	n.d.	n.d.	n.d.	n.d.	n.d.	0.125	0.127	<	<	0.007	0.038	<	0.012	0.006	0.098	0.032	0.035	0.143	0.009	0.353	0.883	0.286	0.040
	28/09/2000	new	light brown	rotten	-	5.32	60	13.3	27.3	<	115	0.128	0.138	<	<	0.012	0.040	<	0.009	0.005	0.081	0.027	0.036	0.134	0.008	0.351	0.823	0.235	0.046
	05/10/2000	old	n.d.	n.d.	1.48	n.d.	n.d.	n.d.	n.d.	n.d.	n.d.	0.126	0.131	<	<	0.003	0.033	<	0.012	0.008	0.089	0.030	0.032	0.135	0.008	0.370	0.841	<	0.023
	12/10/2000	new	brown	n.d.	1.33	5.49	62	8.8	7.7	0.08	-41	0.125	0.130	<	<	0.009	0.051	<	0.011	0.007	0.088	0.029	0.053	0.148	0.008	0.363	0.793	0.299	0.030
	19/10/2000	old	n.d.	n.d.	1.49	n.d.	n.d.	n.d.	n.d.	n.d.	n.d.	0.117	0.123	<	<	0.012	0.039	<	0.010	0.007	0.094	0.031	0.036	0.130	0.009	0.351	0.832	0.257	0.036
	26/10/2000	new	brown	rotten	1.45	5.53	60	8.3	33.5	0.45	129	0.121	0.138	<	<	0.015	0.053	<	0.008	0.008	0.081	0.027	0.040	0.140	0.008	0.349	0.778	<	0.044
	02/11/2000	old	n.d.	n.d.	1.42	n.d.	n.d.	n.d.	n.d.	n.d.	n.d.	0.119	0.129	<	<	0.010	0.050	<	0.007	0.006	0.086	0.029	0.033	0.145	0.008	0.353	0.811	<	0.032
	09/11/2000	new	grey-brown	rotten	1.41	5.04	60	6.7	9.0	<	50	0.122	0.132	<	<	0.009	0.046	<	0.007	0.010	0.082	0.027	0.035	0.135	0.008	0.349	0.828	<	0.034
	16/11/2000	old	n.d.	n.d.	1.54	n.d.	n.d.	n.d.	n.d.	n.d.	n.d.	0.128	0.131	<	<	0.009	0.054	<	0.010	0.006	0.091	0.030	0.031	0.168	0.009	0.353	0.891	<	0.031
	23/11/2000	new	grey	rotten	1.51	5.11	59	6.0	9.2	0.12	188	0.121	0.134	<	<	0.010	0.041	<	0.008	0.010	0.089	0.029	0.034	0.124	0.008	0.333	0.800	<	0.033
	30/11/2000	old	n.d.	n.d.	n.d.	n.d.	n.d.	n.d.	n.d.	n.d.	n.d.	0.118	0.130	<	<	0.009	0.034	<	<	0.011	0.092	0.030	0.031	0.123	0.009	0.344	0.849	<	0.026
GW IIIa	21/09/2000	old	n.d.	n.d.	0.11	n.d.	n.d.	n.d.	n.d.	n.d.	n.d.	0.043	0.057	<	<	0.004	0.080	<	0.031	0.029	0.093	0.029	0.083	0.137	0.003	0.434	2.689	0.483	0.078
	21/09/2000	new	brown	like liquid manure	-	4.5	55	7.8	9.8	<	245	0.067	0.076	<	<	0.018	0.059	<	0.026	0.016	0.075	0.022	0.052	0.120	0.002	0.392	1.982	0.311	0.070
	28/09/2000	old	n.d.	n.d.	0.15	n.d.	n.d.	n.d.	n.d.	n.d.	n.d.	0.043	0.063	<	<	0.004	0.047	<	0.032	0.024	0.084	0.025	0.061	0.116	0.002	0.413	1.940	0.326	0.052
	28/09/2000	new	brown	rotten	-	4.72	51	14.5	4.8	0.27	231	0.061	0.066	0.011	<	0.026	0.051	<	0.035	0.020	0.075	0.023	0.068	0.117	0.002	0.409	1.857	0.302	0.079
	05/10/2000	old	n.d.	n.d.	0.15	n.d.	n.d.	n.d.	n.d.	n.d.	n.d.	0.035	0.045	<	<	0.014	0.054	<	0.031	0.015	0.068	0.021	0.053	0.127	0.002	0.434	2.006	<	0.057
	12/10/2000	new	brown	n.d.	0.08	4.61	51	8.8	7.7	<	226	0.044	0.055	<	<	0.030	0.073	<	0.031	0.022	0.077	0.022	0.087	0.148	0.002	0.420	2.073	0.315	0.084
	26/10/2000	new	brown	like liquid manure	n.d.	5.12	51	8.9	28.4	<	230	0.060	0.084	<	<	0.010	0.066	<	0.027	0.019	0.085	0.024	0.074	0.113	0.003	0.381	1.590	<	0.054
	09/11/2000	new	light brown	like liquid manure	n.d.	4.83	55	6.5	8.0	<	281	0.070	0.081	<	<	0.026	0.086	<	0.027	0.016	0.080	0.023	0.076	0.151	0.002	0.360	1.657	<	0.091
	23/11/2000	new	slightly light brown	rotten	0.16	4.89	46	5	9.4	0.001	122	0.053	0.066	<	<	0.007	0.056	<	0.032	0.027	0.079	0.022	0.052	0.108	0.002	0.374	1.848	<	0.057
	30/11/2000	old	n.d.	n.d.	n.d.	n.d.	n.d.	n.d.	n.d.	n.d.	n.d.	0.038	0.051	<	<	<	0.036	<	0.038	0.023	0.070	0.020	0.039	0.087	0.002	0.374	1.948	<	0.039
GW IIIb	06/09/2000	old	brown	rotten	0.10	5.41	68	11.7	6.7	n.d.	n.d.	0.071	0.081	<	<	0.011	0.103	<	0.072	0.035	0.091	0.017	0.078	0.176	0.002	0.538	2.497	<	0.080
	14/09/2000	old	brown	rotten	0.10	n.d.	n.d.	n.d.	n.d.	n.d.	n.d.	0.060	0.068	<	<	<	0.047	<	0.073	0.031	0.048	0.015	0.056	0.125	0.002	0.481	2.062	<	0.058
	21/09/2000	old	n.d.	n.d.	0.06	n.d.	n.d.	n.d.	n.d.	n.d.	n.d.	0.078	0.087	<	<	0.011	0.043	<	0.030	0.016	0.077	0.019	0.036	0.098	0.002	0.381	1.690	0.255	0.057
	21/09/2000	new	light brown	rotten	-	4.3	41	7.8	1.8	<	233	0.080	0.088	<	<	<	0.036	<	0.028	0.016	0.078	0.020	0.031	0.124	0.002	0.381	1.632	0.292	0.043
	28/09/2000	old	n.d.	n.d.	0.12	n.d.	n.d.	n.d.	n.d.	n.d.	n.d.	0.075	0.090	<	<	0.004	0.036	<	0.033	0.018	0.081	0.020	0.032	0.094	0.002	0.374	1.748	<	0.051
	28/09/2000	new	brown	slightly rotten	-	4.61	43	12.6	1.4	<	266	0.076	0.093	0.010	<	0.011	0.033	<	0.064	0.022	0.081	0.023	0.042	0.092	0.002	0.420	1.807	<	0.062
	05/10/2000	old	n.d.	n.d.	n.d.	n.d.	n.d.	n.d.	n.d.	n.d.	n.d.	0.077	0.085	<	<	0.006	0.034	<	0.032	0.013	0.075	0.019	0.031	0.108	0.002	0.388	1.682	<	0.036
	12/10/2000	new	light brown	n.d.	0.04	4.43	44	8.6	7.2	<	256	0.067	0.077	<	<	0.006	0.049	<	0.038	0.019	0.069	0.017	0.045	0.099	0.002	0.363	1.848	<	0.047
	19/10/2000	old	n.d.	n.d.	0.05	n.d.	n.d.	n.d.	n.d.	n.d.	n.d.	0.069	0.078	<	<	<	0.032	<	0.036	0.014	0.076	0.019	0.023	0.087	0.002	0.360	1.857	<	0.034
	26/10/2000	new	brown	very slightly rotten	0.05	4.56	43	8.6	26.3	<	285	0.064	0.080	<	<	0.003	0.042	<	0.039	0.020	0.071	0.018	0.029	0.094	0.002	0.370	1.898	<	0.039
	02/11/2000	old	n.d.	n.d.	0.1	n.d.	n.d.	n.d.	n.d.	n.d.	n.d.	0.063	0.072	<	<	<	0.041	<	0.047	0.013	0.061	0.015	0.022	0.099	0.002	0.355	1.882	<	0.039
	09/11/2000	new	brown	very slightly rotten	0.1	4.1	42	6.6	8.1	<	315	0.060	0.074	<	<	0.003	0.035	<	0.044	0.018	0.064	0.016	0.026	0.087	0.002	0.347	1.973	<	0.040
	16/11/2000	old	n.d.	n.d.	0.12	n.d.	n.d.	n.d.	n.d.	n.d.	n.d.	0.069	0.080	<	<	<	0.034	<	0.044	0.016	0.055	0.014	0.018	0.147	0.002	0.353	1.982	<	0.039
	23/11/2000	new	grey-brown	slightly rotten	0.05	4.09	41	5.2	20.5	<	324	0.059	0.076	<	<	<	0.034	<	0.044	0.020	0.059	0.015	0.022	0.082	0.002	0.341	1.973	<	0.039
	30/11/2000	old	n.d.	n.d.	n.d.	n.d.	n.d.	n.d.	n.d.	n.d.	n.d.	0.058	0.073	<	<	<	0.030	<	0.049	0.017	0.055	0.013	0.018	0.083	0.002	0.337	1.990	<	0.036
GW IV	09/11/2000	old	whitish	neutral	2.52	5.22	101	6.5	72.4	<	284	0.212	0.212	0.065	<	0.018	0.117	<	0.013	<	0.144	0.029	0.089	0.189	0.001	0.381	0.247	<	<
	16/11/2000	old	n.d.	n.d.	2.58	n.d.	n.d.	n.d.	n.d.	n.d.	n.d.	0.238	0.251	0.066	<	0.005	0.107	<	0.013	<	0.166	0.032	0.076	0.217	0.002	0.381	0.210	<	0.080
	23/11/2000	old	whitish	neutral	2.89	n.d.	n.d.	6.8	83.3	<	n.d.	n.d.	0.250	n.d.	n.d.	n.d.	n.d.	n.d.	0.010	<	0.138	0.028	0.074	0.189	0.001	0.354	n.d.	n.d.	n.d.
Weir 2	12/10/2000	-	n.d.	n.d.	-	n.d.	n.d.	n.d.	n.d.	n.d.	n.d.	0.192	0.188	<	<	<	0.046	<	0.020	0.006	0.087	0.029	0.026	0.149	0.004	0.303	0.474	<	0.017
	26/10/2000	-	n.d.	n.d.	-	n.d.	n.d.	n.d.	n.d.	n.d.	n.d.	0.197	0.211	<	<	<	0.046	<	0.017	0.005	0.089	0.030	0.026	0.158	0.004	0.295	0.386	<	0.014
	09/11/2000	-	n.d.	n.d.	-	n.d.	n.d.	n.d.	n.d.	n.d.	n.d.	0.209	0.212	<	<	<	0.043	<	0.015	0.004	0.096	0.032	0.022	0.161	0.005	0.300	0.374	<	0.016
	23/11/2000	-	n.d.	n.d.	-	n.d.	n.d.	n.d.	n.d.	n.d.	n.d.	0.212	0.236	<	<	<	0.045	<	0.015	0.004	0.096	0.032	0.021	0.153	0.005	0.296	0.407	<	0.012
Stream near GW	28/09/2000	-	n.d.	n.d.	-	n.d.	n.d.	n.d.	n.d.	n.d.	n.d.	0.083	0.094	<	<	0.004	0.034	<	0.049	0.020	0.037	0.010	<	0.101	0.001	0.280	2.698	<	0.055
	12/10/2000	-	n.d.	n.d.	-	n.d.	n.d.	n.d.	n.d.	n.d.	n.d.	0.088	0.109	<	<	<	0.033	<	0.053	0.019	0.044	0.012	<	0.093	0.001	0.263	2.531	<	0.046
	26/10/2000	-	n.d.	n.d.	-	n.d.	n.d.	n.d.	n.d.	n.d.	n.d.	0.089	0.112	<	<	0.004	0.046	<	0.048	0.020	0.040	0.011	<	0.109	0.001	0.311	2.498	<	0.048
	09/11/2000	-	n.d.	n.d.	-	n.d.	n.d.	n.d.	n.d.	n.d.	n.d.	0.089	0.101	<	<	<	0.040	<	0.049	0.017	0.039	0.012	<	0.102	0.001	0.333	2.431	<	0.047
	23/11/2000	-	n.d.	n.d.	-	n.d.	n.d.	n.d.	n.d.	n.d.	n.d.	0.098	0.118	<	<	0.004	0.041	<	0.050	0.017	0.042	0.013	<	0.099	0.001	0.328	2.331	<	0.050
Lenka	12/10/2000	-	n.d.	n.d.	-	n.d.	n.d.	n.d.	n.d.	n.d.	n.d.	0.274	0.290	0.113	<	<	0.053	<	0.018	<	0.239	0.045	0.039	0.227	0.001	0.330	<	<	0.107
	26/10/2000	-	n.d.	n.d.	-	n.d.	n.d.	n.d.	n.d.	n.d.	n.d.	0.271	0.293	0.115	<	<	0.055	<	0.015	<	0.234	0.044	0.033	0.244	0.001	0.330	<	<	0.111
	09/11/2000	-	n.d.	n.d.	-	n.d.	n.d.	n.d.	n.d.	n.d.	n.d.	0.274	0.294	0.114	<	<	0.052	<	0.017	<	0.235	0.044	0.038	0.227	0.001	0.323	<	<	0.117
	23/11/2000	-	n.d.	n.d.	-	n.d.	n.d.	n.d.	n.d.	n.d.	n.d.	0.276	0.331	0.097	<	<	0.056	<	0.016	<	0.233	0.044	0.032	0.227	0.001	0.315	<	<	0.106

Appendix B:
Texture, Colour, and Depth of the Lysina Soil Samples

	Sample no.	Depth [m b.s.]	Soil texture*	Colour	Comments	Soil analyses
GW Ia	1	0.65 - 0.90	Sand Ss	brown	grus	x
	2	1.21 - 1.49	Loamy Sand Sl2	white-pink	grus	x
	3	2.27 - 2.50	Sand Ss	white-pink	grus	x
	4	2.72 - 2.95	Silty Sand Su4	beige	grus	x
	5	3.40 - 3.70	Silty Sand Su4	white	grus	x

	Sample no.	Depth [m b.s.]	Soil texture*	Colour	Comments	Soil analyses
GW Ib	1	0.37 - 0.48	Loamy Sand Sl2	black		
	2	0.48 - 0.71	Silty Sand Su3	brown	grus	
	3	0.71 - 0.85	Silty Sand Su3	brown	grus	
	4	1.40 - 1.70	Silty Sand Su2	white	grus	
	5	2.50 - 2.80	Sand Ss	brown	grus	
	6	3.40 - 3.70	Loamy Sand Sl2	white-black	grus	
	7	3.90 - 4.20	Silty Sand Su3	red-brown	black minerals grus	x

	Sample no.	Depth [m b.s.]	Soil texture*	Colour	Comments	Soil analyses
GW IIa	1	0.70 - 0.90	Sandy Clay Ts3	dark brown	much org. matter	
	2	1.20 - 1.40	Sandy Loam Ls3	brown	grus	x

	Sample no.	Depth [m b.s.]	Soil texture*	Colour	Comments	Soil analyses
GW IIb	1	0.95 - 1.20	Sandy Clay Ts3	dark brown	much org. matter	x
	2	2.35 - 2.65	Silty Sand Su2	grey	grus	x
	3	2.80 - 3.00	Silty Sand Su3	grey	grus	x

	Sample no.	Depth [m b.s.]	Soil texture*	Colour	Comments	Soil analyses
GW IIIa	1	0.36 - 0.53	Sandy Loam Ls4	black-grey	much org. matter	
	2	0.53 - 0.75	Silty Sand Su3	light brown		x
	3	0.75 - 1.00	Silty Sand Su3	grey	grus	
	4	1.00 - 1.30	Sandy Clay Ts3	grey-brown-black	grus	x
	5	1.50 - 1.80	Silty Sand Su3	brown	grus	x

	Sample no.	Depth [m b.s.]	Soil texture*	Colour	Comments	Soil analyses
GW IIIb	1	0.34 - 0.60	n.d.	black	much org. matter	
	2	0.60 - 0.78	Cleyey Loam Lt2	lgrey-brown		
	3	0.78 - 1.00	Silty Sand Su3	light beige	grus	
	4	1.25 - 1.50	Sand Ss	grey-brown	grus	x

	Sample no.	Depth [m b.s.]	Soil texture*	Colour	Comments	Soil analyses
GW IV	1	0.00 - 0.40	Silty Sand Su3	brown-black		
	2	0.40 - 0.70	Loamy Sand Sl3	brown	grus	x
	3	0.80 - 0.90	Silty Sand Su3	brown	grus	
	4	1.30 - 1.75	Silty Sand Su3	light beige-pink	grus	x
	5	1.55 - 1.65	Clayey Sand St2	pink	grus	
	6	1.90 - 2.07	Loamy Sand Sl3	white-brown	grus	x
	7	2.50 - 2.80	Clayey Sand St2	white-brown	grus	
	8	3.00 - 3.20	Loamy Sand Sl3	white beige	grus	x

*according to the German soil classification scheme (Finnern *et al.*, 1994)

Appendix C: Linear Isotherm Coefficients of the Lysina Soil Samples

	Sample no.	Distribution coefficient K_d [$cm^3\ g^{-1}$]	Pearson correlation coefficient*
GW Ia	1	0.279	0.993
	2	0.550	0.993
	3	0.280	0.979
	4	0.352	1.000
	5	0.447	0.961
GW Ib	7	0.584	0.988
GW IIa	2	0.536	0.999
GW IIb	1	1.618	0.992
	2	0.103	0.968
	3	0.616	0.992
GW IIIa	2	0.535	0.999
	4	0.406	0.987
	5	0.061	n.s.
GW IIIb	4	0.333	0.999
GW IV	2	0.475	0.988
	4	0.377	0.974
	6	0.129	n.s.
	8	0.531	0.998

* only given for significant correlations ($\alpha<0.05$)

Appendix D: Sulphate Deposition Scenario as Applied in the Model

Lehstenbach catchment: 1854 - 1978 Alewell (1995); 1988 - 1999 Moritz *et al*. (1994); Moritz (unpublished data)

Time [yrs]	Deposition flux [kmol ha^{-1} yr^{-1}]	Normalised input conc. [mmol l^{-1}]
1854	0.00	0.000
1896	0.41	0.087
1950	1.07	0.227
1970	1.96	0.417
1978	2.25	0.478
1988	1.80	0.384
1989	1.89	0.401
1990	1.17	0.248
1991	1.39	0.296
1992	1.34	0.285
1993	1.14	0.242
1994	1.15	0.246
1995	0.88	0.186
1996	1.09	0.232
1997	0.59	0.125
1998	0.59	0.126
1999	0.46	0.099

Lysina catchment: Hruška & Krám (unpublished data)

Time [yrs]	Main catchment		Side catchment and Lenka	
	Deposition flux [kmol ha^{-1} yr^{-1}]	Normalised input conc. [mmol l^{-1}]	Deposition flux [kmol ha^{-1} yr^{-1}]	Normalised input conc. [mmol l^{-1}]
1840	0.00	0.000	0.00	0.000
1851	0.03	0.008	0.03	0.008
1910	0.20	0.046	0.20	0.046
1945	0.22	0.051	0.22	0.051
1955	0.66	0.152	0.66	0.152
1979	1.32	0.305	1.32	0.305
1985	1.26	0.291	1.56	0.361
1991	0.89	0.206	1.02	0.237
1992	0.85	0.197	1.08	0.249
1993	0.93	0.214	1.19	0.276
1994	0.76	0.175	0.99	0.228
1995	0.75	0.174	0.93	0.216
1996	0.69	0.160	0.88	0.204
1997	0.52	0.121	0.66	0.152
1998	0.46	0.107	0.57	0.131
1999	0.31	0.071	0.38	0.089
2000	0.27	0.062	0.31	0.072

Acknowledgements

I am indebted to a number of people for their support during this study. I wish to take the opportunity to say thank you

to Prof. Dr. Michael Hauhs for enabling this study and for the pleasant atmosphere in the department.

to Dr. Gunnar Lischeid for the excellent supervision of this thesis.

to Dr. Jakub Hruška and Dr. Pavel Krám from the Czech Geological Survey for enabling the field sampling in the Lysina catchment, for providing their data, and for discussion.

to Andreas Kolb, Uwe Hell, and Vaclav Kmínek for their help during field sampling and drilling.

to Tobias Rötting for performing the main part of the laboratory analysis and for his advice during the initial stage of this study.

to the staff of the Central Analytical Department of BITÖK for sample processing.

to Dr. Wigand Rathmann for discussing the numerics of the model.

to Stefan Büttcher for answering numerous questions on C++ programming.

to Mathias Göckede, Christel Bihl, Christine Röckmann, Donald Hougard, Ann Cowan, and Andrew Jaye for proof-reading the manuscript.

to my friends and my family for their love, support, and encouragement in whatever situation occurred.

Erklärung

Hiermit erkläre ich, dass ich die vorliegende Arbeit selbständig verfasst und nur die angegebenen Quellen und Hilfsmittel verwendet habe.

Bayreuth, im Juni 2001

(Heike Büttcher)